Colloids from oppositely charged polymers; reversibility and surface activity

Promotor:

Prof. dr. M.A. Cohen Stuart

Hoogleraar fysische chemie en kolloïdkunde

Copromotor:

Dr. A. de Keizer

Universitair hoofddocent, Laboratorium voor fysische chemie en kolloïdkunde

Promotiecommissie:

Dr. C. Detrembleur (University de Liège, Belgium)

Prof. dr. ir. A.J.H. Janssen (Wageningen Universiteit)

Dr. ing. G.J.M. Koper (TU Delft)

Prof. dr. C.G. de Kruijf (NIZO food research, Ede)

Dit onderzoek is uitgevoerd binnen de onderzoekschool VLAG

Colloids from oppositely charged polymers; reversibility and surface activity

Peter Sebastiaan (Bas) Hofs

Proefschrift
ter verkrijging van de graad van doctor
op gezag van de rector magnificus
van Wageningen Universiteit
Prof. dr. M.J. Kropff,
in het openbaar te verdedigen
op dinsdag 20 januari 2009
des namiddags te vier uur in de Aula

ISBN: 978-90-8585-310-7

Table of contents

Chapter One – Introduction 1

Chapter Two - Comparison of complex coacervate core micelles from two diblock copolymers or a single diblock copolymer with a polyelectrolyte 15

Chapter Three – On the stability of (highly aggregated) polyelectrolyte complexes containing a charged-block-neutral diblock copolymer 39

Chapter Four – Complex coacervate core micro-emulsions 57

Chapter Five – Reduction of protein adsorption to a solid surface by a coating composed of polymeric micelles with a glass-like core 81

Chapter Six – General Discussion 101

Summary 115
Samenvatting 119
Commonly used abbreviations 123
Dankwoord 124
List of publications 126
Levensloop 127
Educational activities 128

Chapter One

Introduction

The general field

The term ‘polyelectrolyte complex’ (PEC) was introduced several decades ago[1] and there are several characteristics which can be used to subdivide this broad term. PECs can form in aqueous solution when oppositely charged polyelectrolytes are mixed together. Thus they can be electrically neutral (stoichiometric complexes) or charged (either positively or negatively, usually named non-stoichiometric PECs, NPECs). The PECs can have either a liquid-like (e.g., complex coacervate) or a frozen (solid-like, e.g., complex precipitate) structure, and, once formed, they can phase separate into a macroscopic phase (e.g., a complex coacervate phase) or stay dispersed in the medium (e.g., in the form of colloidal particles, stabilized by an electrical double layer, or as complex coacervate core micelles, C3Ms, stabilized by neutral hydrophilic chains). For a schematic summary of some of the more relevant terms used to describe sub-regions of the PEC area, see Fig. 1.1.

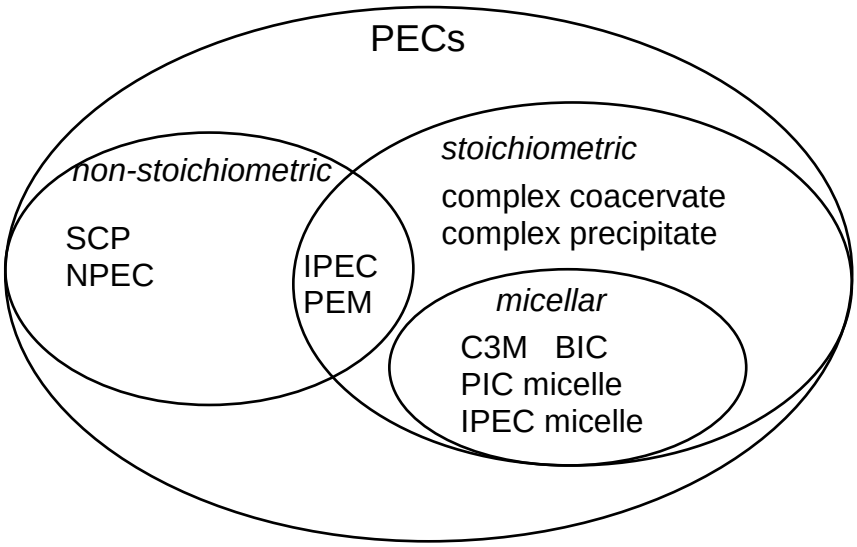

Figure 1.1: Overview of different terms used in the literature about PECs. C3M = complex coacervate core micelle[2], BIC = block ionomer complex[3], PIC = polyion complex[4,5], IPEC = inter-polyelectrolyte complex (IPEC micelle[6]), PEM = polyelectrolyte multilayer. SCP = soluble complex particle[2], NPEC = non-stoichiometric polyelectrolyte complex[7,8]. The terms complex coacervate and complex precipitate are from ref. 9 and references therein.

One of the earliest publications on complexation of oppositely charged hydrophilic colloids is almost a century old[10] and concerns the co-precipitation of gelatin and gum arabic. Initially an accidental discovery, this phenomenon became the main topic for H.G.

Bungenberg de Jong, with, according to H.R. Kruyt, his most important paper appearing in 1929[11]. Much of his work on coacervation is summarized in Colloid Science II by H.R. Kruyt[12], from which follows a quote: “If one starts from a sol, that is the solution of the colloids in an appropriate solvent, then according to the nature of the colloid, various changes (temperature, pH, addition of a substance) can bring about reduction of the solubility as a result of which a larger part of the colloid separates out into a new phase. (…) The separated colloid can either appear in a low dispersed state or in higher dispersed states. In the first case macroscopic or microscopic investigation allows one to distinguish by crystallization, when obviously *crystalline* individuals are formed and *coacervation* when amorphous liquid drops are formed (…).” (italics expressing emphasis by H.G. Bungenberg de Jong)[9].

Complex coacervation was defined by the same author[9]: in *complex coacervation* it are only the charges on the macromolecules which are concerned in the reduction of solubility and the associations deriving from it. The International Union of Pure and Applied Chemistry (IUPAC) gives the definition of complex coacervation as “coacervation caused by the interaction of two oppositely charged colloids”.

In the following paragraphs we will emphasize the most important properties of PECs, and shortly discuss various sub-regions, in order to give the reader a short overview of the field.

Main parameters

Whether complexation of oppositely charged polyelectrolytes occurs, and what type of complex results depends on the salt concentration, and the chemical structure and length of the polyelectrolytes used. If the two oppositely charged polyelectrolytes are both strong, the complexation takes place independent of the pH. If one is strong and one weak, there is a pH region where the weak polyelectrolyte will be uncharged and no PECs are formed. For the combination of two weak polyelectrolytes, e.g. poly(acrylic acid) (PAA) and poly(N,N-dimethylaminoethyl methacrylate) (PDMAEMA), there will be a pH optimum for complexation (Fig. 1.2). For a stoichiometric amount (in this case an equal number of charges of the reacting species) of PAA and PDMAEMA the optimum complexation pH coincides with the maximum in the product of the charge densities, which is at pH 6.7[2]. Deviation from this optimum, either by changing the pH or the charge ratio of the polyelectrolytes, leads to a decrease in the interaction strength and a lower stability of the PEC against addition of salt.

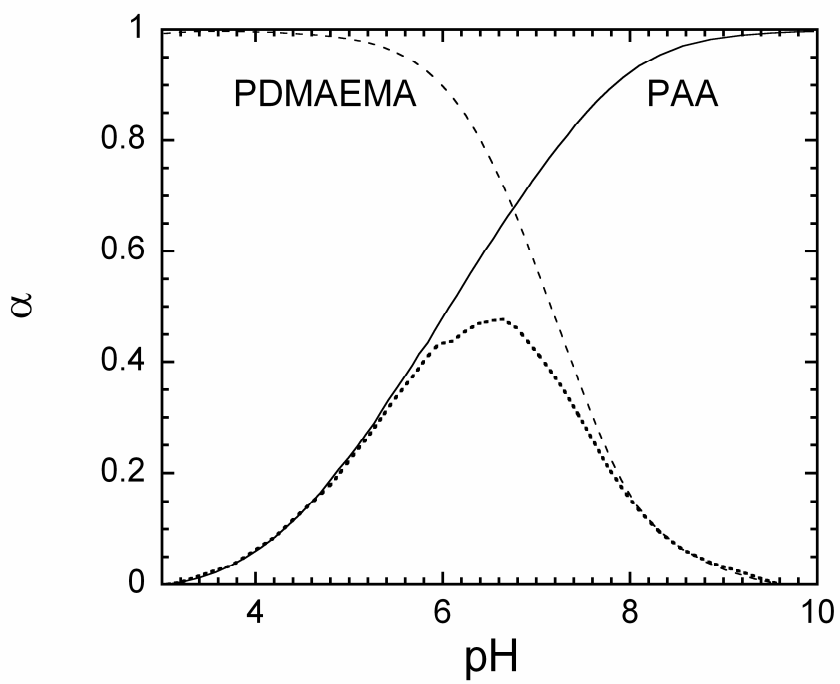

Figure 1.2: Charge density, α, of PAA (full line) and PDMAEMA (dashed line), both in 10 mM $NaNO_3$ (data from ref. 13). $\alpha_{PAA} \times \alpha_{PDMAEMA}$ (dotted line) is a measure for the strength of the attraction between the two oppositely charged weak polyelectrolytes, when mixed in a ratio of 1:1.

Because the attraction is electrostatic in nature, salt is expected to weaken the complexation. The salt resistance of a particular PEC depends on the polyelectrolyte pair in question. For NPECs composed of the synthethic polyelectrolytes poly(methacrylic acid) (PMAA) and poly(N-ethyl-4-vinylpyridinium bromide) (P4EVP) mixed in a ratio of about 3 to 1, it has been shown that the critical ionic strength varies in the range 0.2-0.4 M NaCl, depending on the length of the shortest polyelectrolyte[14]. The fact that the chain length matters tells us that chain entropy considerations are needed in order to fully understand this system. For the system of the natural polyelectrolytes gelatin and gum arabic the maximum critical salt concentration of KCl is about 50 mM[9]. The difference in the critical salt concentration between the two systems is at least partly due to the differences in the charge densities of the polyelectrolytes.

Driving forces

The main driving forces for the formation of PECs are; the decreases in free energy upon complexation, due to the close approach of the oppositely charged groups (enthalpic contribution), and counter-ion release (entropic contribution). Which of these two is dominant

depends on the system and circumstances (background electrolyte concentration, temperature). For some systems there is an increase in enthalpy upon complex formation[15] which makes these entropy-driven. Secondary driving forces are due to the nature of the used colloids (hydrophobic groups, hydrogen bonding, etc.) and the factors affecting them (temperature, pH, ionic strength, etc.)[16]. These can have large effects on the Coulombic interaction energy between oppositely charged groups, especially if the dielectric constant of the medium is lowered, as this can increase the interaction energy dramatically.

Theoretically speaking, the work of Voorn and Overbeek is usually seen as a starting point[17]. They derived that the gain in electrical free energy upon complexation is enough to drive complex coacervation, given that there are multiple charges on the complexing colloids [18,19]. Veis and Aranyi tested the theory of Voorn and Overbeek experimentally and found that in some cases experimental data (showing complex coacervation), could not be reconciled with the theory (which predicted there should be none). Therefore they adapted the theory, including solvent-solute parameters (Flory-Huggins) and ion-pair formation. Veis and Aranyi showed that complex coacervation can be represented as a two-step process[20]. First, aggregation of the oppositely charged colloids (driven by electrostatics) takes place, followed by rearrangement of these aggregates. This rearrangement is slow, is driven by a gain in conformational entropy[20], and has been observed in experiments for different systems[21-24].

Complex coacervates

Natural polyelectrolytes usually have many chemically different groups. Gum arabic is not a single chemical species, but a mixture of different ones, overall consisting of > 95 % polysaccharides with a small amount of protein. The isoelectric point (i.e.p.) is < 2, and the charge density is very low[25]. Gelatin is a protein which is produced by hydrolysis of collagen. The i.e.p. varies depending on the ionic strength and preparation procedure[26]; the one used by Bungenberg de Jong had an i.e.p. of 4.8. A fairly complete phase diagram of the complexation between these two weak polyelectrolytes was obtained by mixing isohydric (= with the same pH) sols. This figure shows some important features (Fig. 1.3), some of which have been mentioned here before for PECs. There is a critical salt concentration, and for each pH (as both gum arabic and gelatin are weak polyelectrolytes) there is an optimum mixing ratio, which is at stoichiometric amount of opposite charge. For a certain pH (about 3.6) the gum arabic and gelatin have an equal absolute charge density and here the complexation is strongest as can be seen by the high salt resistance, and, hence, the largest gain in the free energy upon complexation. This can also be deduced from the fact that the lowest water

content is found at the same point[9,27,28] which means that the charged groups are closest to each other and the electrical energy is lowest. Moving away from the optimum mixing ratio and/or pH lowers the salt resistance, and the points of charge reversal are always very close to the optimum mixing proportion. Also, the complexation takes place over a range of mixing ratios of the two oppositely charged components. The width of the complexation range decreases with increasing salt concentration and, as we are discussing weak polyelectrolytes here, on the pH as well.

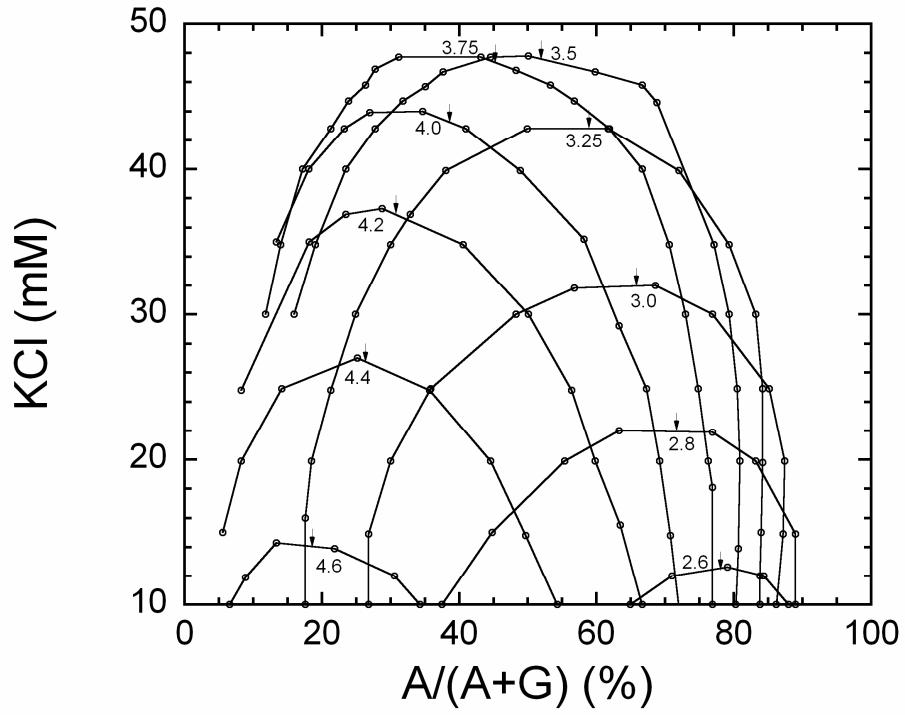

Figure 1.3: From ref. 9. Mixing fraction A/(A+G), expressed as gum arabic, A, over total colloid content (including gelatin, G), vs. KCl concentration. Obtained by mixing of two 0.05 % sols of A and G, respectively. The points are for solutions with 2 % turbidity and the region below the lines gives a higher turbidity. Numbers in the graph denote pH for the points on the line. Arrows indicate the point of charge reversal.

An important variable for complex coacervation is the charge density (or the distance between the charges) of the polyelectrolytes. At high charge densities more salt will be required to dissociate the complex than if the charge density is low. The charge densities of both gum arabic and gelatin are low and this leads to the earlier mentioned low maximum critical salt concentration (50 mM KCl). The extent to which a liquid character is displayed depends on the charge density, on the nature (presence of hydrophobic groups) of the polyelectrolytes, and on the concentration and nature of ions present in the solution, which all

influence the solubility of the components and the complex. The solubility can be influenced by other parameters as well, e.g. temperature. In the above example, the complex coacervation of gelatin and gum arabic was investigated above 33 °C as gelatin forms a gel below this temperature[29]. When the complex coacervate contains many charges, the complex coacervate drops can be destroyed by applying a strong enough DC electric field. Deformation of the drops can be observed in an AC electric field[9]. The water content of complex coacervates is generally high, e.g. for gelatin and gum arabic at 1:1 mixing ratio at pH 3.5, only about 18 % of the complex consists of polymer[9]. The water content can be increased by increasing the salt concentration. Even though the water content is high (> 80 %), rather hydrophobic materials, such as e.g. carbon particles, are taken up by the complex coacervate[9].

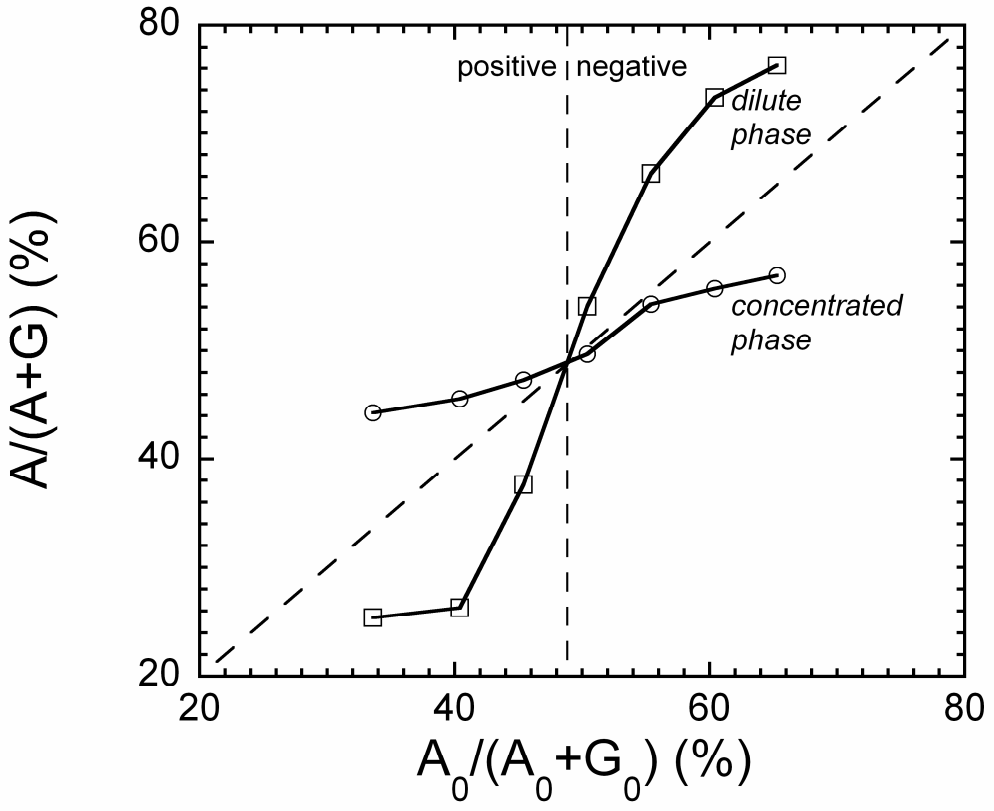

Figure 1.4: Composition A/(A+G) as a function of initial composition ($A_0/(A_0+G_0)$) of the complex coacervate (○) and the bulk phase (□), expressed as gum arabic, A, over total colloid content (including gelatin, G). The vertical dashed line denotes the transition from positively to negatively charged complex coacervate. The dashed diagonal line gives the composition if no changes would take place upon complexation. Experimental data from[30,31]. Lines to guide the eye.

Since complex coacervation is an associative phase separation, involving two solutes, composition is an important variable. Generally, the complex coacervate strives to be near an optimum composition, as was made clear by mixing the colloids at different ratio's and determining the composition of the complex coacervate and the equilibrium solution (Fig. 1.4). The complex coacervate is enriched in the minority component, while the bulk phase is enriched in the majority component.

PolyElectrolyte Multilayers

Polelectrolyte multilayers (PEMs) are built up by alternatingly applying solutions of a cationic and anionic polyelectrolyte. This can lead to a multilayer composed of alternating layers of cationic and anionic polyelectrolyte and is also known as layer-by-layer, LbL, assembly. Whether a multilayer can be grown in this way depends on the combination of polyelectrolytes used and the type of salt and ionic strength (and pH, for weak polyelectrolytes)[32]. For example, the total adsorbed amount does not continuously grow with alternatingly applying polyelectrolyte solutions of P4EVP and poly(methacrylic acid) (PMAA) when the solvent is 10 mM phosphate buffer, nor for (in the same buffer) the combination of PAA and PDMAEMA; with this salt type and concentration, the presence of an excess of one of the polyelectrolyte species brings the system to the edge of the PEC phase diagram and thus causes dissolution of the polymers[33]. Lowering the buffer concentration to a value where the polyelectrolyte complex is in a glass state prohibits dissolution and allows continuous multilayer growth in both cases. This, and other experiments, show that the complexing polyelectrolytes have to be kinetically frozen on the time scales of the deposition or exposure times in order for multilayer formation to occur[32].

Micelles

Obtaining micelles, i.e. objects, with a finite size, requires a driving force and a stop-mechanism which stops the growth of the core of the micelle in such a way that well defined spherical core-shell particles are obtained. Micelles are traditionally composed of amphiphilic molecules; in aqueous solution, the hydrophobic part forms the core and the hydrophilic part the shell. Micelles can be made from a variety of molecules, most common being surfactants and amphiphilic diblock copolymers. Their formation is driven by what has been called the hydrophobic effect[34]; water looses a lot of entropy around hydrophobic groups, and therefore, hydrophobic groups in water tend to aggregate in order to minimize the hydrophobic surface area in order to maximize the entropy of the water. For amphiphilic molecules this

aggregation only happens above a certain (usually low) concentration of the amphiphiles, which is called the critical micellar concentration (CMC). Above the CMC, micelles and molecularly dissolved amphiphiles coexist in solution. For surfactants, the hydrophilic head-groups (either neutral or charged) provide the stop-mechanism, whilst in the case of amphiphilic diblock copolymers it are the neutral hydrophilic chains that stop the growth of the hydrophobic core.

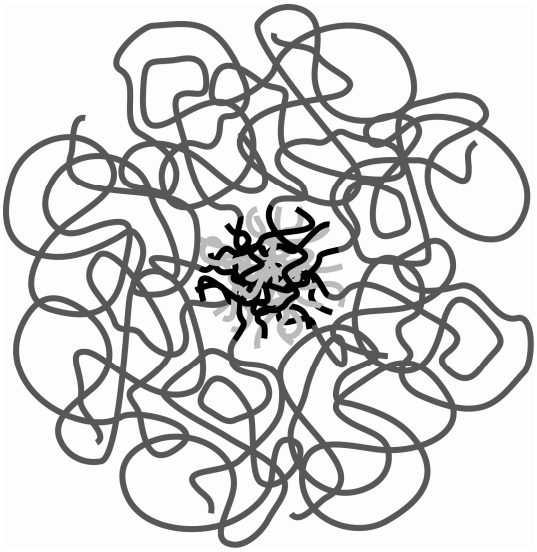

Figure 1.5: Schematic of a C3M, BIC, or PIC-micelle. The core is composed of the complexed oppositely charged polyelectrolytes and is surrounded by the neutral hydrophilic corona. Black = polycations, light grey = polyanions , dark grey = neutral hydrophilic polymers.

The initial aggregation of PECs is due to electrostatic forces and a gain in entropy due to counter-ion release. There are two ways to introduce a stop-mechanism in order to try and obtain small stabilized complexes. One, is to mix the oppositely charged polymers at non-stoichiometric amounts; than NPECs can be obtained and excess charge is their stabilizing factor. The second, is by mixing solutions of diblock copolymers with one polyelectrolyte block and one water-soluble neutral block with oppositely charged polyelectrolytes. If the size of the neutral block with respect to the that of the polyelectrolytes is large enough to prevent macroscopic phase separation, small (10-40 nm hydrodynamic radius) micelles can be obtained[2,22]. Several groups used this strategy successfully in the mid nineteen nineties and thus polyion complex micelles (PIC micelles)[4], block ionomer complexes (BICs)[3], and complex coacervate core micelles (C3Ms)[22] were born. The core of these micelles is formed

by the complexing polyelectrolytes, and the neutral hydrophilic blocks form the shell, or corona (Fig. 1.5).

The use of neutral blocks, especially the use of chemically different neutral blocks, gives rise to extra forces which can be exploited to obtain new structures. Using poly(ethylene oxide) (PEO) and poly(acrylamide) (PAAm) as neutral blocks, Janus C3Ms – with on one side of the complex coacervate core the PEO and on the other side the PAAm – were obtained[35].

This thesis

In this thesis we explore several aspects of C3Ms: effects of corona densities, core hydrophobicity, added polyelectrolyte homopolymer and C3M layers on solid substrates. In *chapter 2* we investigate the formation of C3Ms from either one or two diblock copolymer species, with the aid of light scattering. The used diblock copolymers are PAA-PAAm and PDMAEMA-poly(glyceryl methacrylate) (PGMA), which carry opposite charges in the used pH range. The homopolyelectrolyte PDMAEMA is also used and different mixtures of the two positively charged polymers (diblock and homopolyelectrolyte) are used to investigate the effect of incorporation of more diblock and hence more neutral blocks on the size and aggregation number of the formed C3Ms. As the neutral blocks act as a stopping force the size and aggregation number goes down with increasing neutral block (second diblock copolymer) content. A simple geometrical model is introduced which uses the measured hydrodynamic radius and light scattering intensity to interpret the light scattering results in terms of aggregation numbers.

In *chapter 3* the emphasis is on the formation and rearrangements of PECs formed from poly([4-(2-amino-ethylthio)-butylene] hydrochloride)-*block*-poly(ethylene oxide) (PAETB-PEO) and PAA. The PAETB polyelectrolyte has a rather hydrophobic backbone leading to complexes with a low mobility. This allows us to make observations on intermediate stages during C3M formation. The formation of the PEC upon mixing with PAA is investigated as a function of the mixing fraction f_- (the number of negatively chargeable groups divided by the total number of chargeable groups), with light scattering measurements. Cryogenic transmission electron microscopy is used to visualize the differences between the initially formed highly aggregated PEC (HAPEC) and the final (smaller) PEC. The rearrangement behaviour as a function of f_- is explained in terms of excess charge on the PECs and the amount of neutral block; excess charge increases the rearrangement rate and neutral blocks slow it down. Also, pH-cycles are performed on C3M solutions. In these, the pH is first

changed to an extreme region where one of the polyelectrolytes carries virtually no charge, in order to completely dissociate the C3Ms. Then, the pH is brought back to the region where C3Ms are formed, thereby allowing the polyelectrolytes to form complexes once again. It is shown that the pH cycle is a fast method to obtain small C3Ms (which are close to thermodynamic equilibrium) from large PECs, that were initially formed by direct mixing of the oppositely charged polymers.

A method to control the size and mass of the C3Ms is by effectively adding extra complex coacervate core material to the C3Ms. In *chapter 4* this is achieved by mixing solutions containing both PAA-PAAm and PAA (in varying amounts) with solutions containing PDMAEMA, in such a way that $f_+ = 0.5$. The geometrical model introduced in chapter 2 is extended, and used to interpret the experimental results. If the polymers are mixed in 10 mM $NaNO_3$ solutions, the formed non-relaxed C3Ms grow unrealistically strongly (as compared to the model) upon the addition of complex coacervate core forming material. Performing the experiment in phosphate buffer with a 10 mM ionic strength, however, yields particles of the expected sizes. Since these particles are probably equilibrium structures, we refer to them as complex coacervate core micro-emulsions (C3-μEs). Discrepancies between the growth as predicted by the geometrical model and the experimental data are explained with the help of self-consistent mean field calculations. These show that there is a transition from more ‘star-like’ to ‘crew-cut’ morphology caused by the increasing size of the core and the concomitant decrease in curvature that goes with the addition of core forming material to the C3-μEs.

In *chapter 5* the effect of a C3M coating on protein adsorption to the solid-liquid interface is investigated. The C3Ms used here have a rather hydrophobic, more glass-like core and their effect on reducing protein adsorption (using four proteins; lysozyme, bovine serum albumin, fibrinogen, and β-lactoglobulin) is compared to a previous study using C3Ms as a surface coating to prevent protein adsorption (lysozyme), which showed promising results (100 % reduction)[36]. The advantage of using C3Ms with a glass-like core for coating over normal C3Ms is the more irreversible nature of the former, as this is expected to result in a more stable coating. It is shown that the more hydrophobic C3Ms adsorb as particles without coalescing and that the amount of protein adsorption depends on the type of surface and solvent as well.

A *general discussion and summary* follows in which a comparison between C3Ms and conventional micelles from amphiphilic diblock copolymers is made.

Literature

(1) Reid, S. J.; Overbeek, J. T.; Vieth, W.; Fleming, S. M. *Journal of Colloid and Interface Science* **1968**, *26*, 222.
(2) van der Burgh, S.; de Keizer, A.; Cohen Stuart, M. A. *Langmuir* **2004**, *20*, 1073.
(3) Kabanov, A. V.; Bronich, T. K.; Kabanov, V. A.; Yu, K.; Eisenberg, A. *Macromolecules* **1996**, *29*, 6797.
(4) Harada, A.; Kataoka, K. *Macromolecules* **1995**, *28*, 5294.
(5) Harada, A.; Kataoka, K. *Macromolecules* **2003**, *36*, 4995.
(6) Gohy, J.-F.; Varshney, S. K.; Jerome, R. *Macromolecules* **2001**, *34*, 3361.
(7) Dautzenberg, H. *Macromolecules* **1997**, *30*, 7810.
(8) Izumrudov, V. A.; Bronich, T. K.; Zezin, A. B.; Kabanov, V. A. *Journal of Polymer Science Part C-Polymer Letters* **1985**, *23*, 439.
(9) Bungenberg de Jong, H. G. In *Colloid Science*; Kruyt, H. R., Ed.; Elsevier: Amsterdam, 1949; Vol. II.
(10) Tiebackx, F. W. *Zeitschrift für Chemie und Industrie der Kolloide* **1911**, *8*, 198.
(11) Bungenberg de Jong, H. G.; Kruyt, H. R. *Proceedings of the Koninklijke Nederlandse Akademie der Wetenschappen* **1929**, *32*, 849.
(12) Kruyt, H. R. *Colloid Science*; Elsevier: Amsterdam, 1949; Vol. II.
(13) van der Burgh, S. Complex Coacervate Core Micelles in Solution and at Interfaces. PhD-thesis, Wageningen Universiteit, 2004.
(14) Pergushov, D. V.; Izumrudov, V. A.; Zezin, A. B.; Kabanov, V. A. *Vysokomolekulyarnye Soedineniya Seriya A & Seriya B* **1995**, *37*, 1739.
(15) Ball, V.; Winterhalter, M.; Schwinte, P.; Lavalle, P.; Voegel, J. C.; Schaaf, P. *Journal of Physical Chemistry B* **2002**, *106*, 2357.
(16) Turgeon, S. L.; Beaulieu, M.; Schmitt, C.; Sanchez, C. *Current Opinion in Colloid & Interface Science* **2003**, *8*, 401.
(17) Burgess, D. J. *Journal of Colloid and Interface Science* **1990**, *140*, 227.
(18) Michaeli, I.; Overbeek, J. T. G.; Voorn, M. J. *Journal Of Polymer Science* **1957**, *23*, 443.
(19) Overbeek, J. T. G.; Voorn, M. J. *Journal of Cellular and Comparitive Physiology* **1957**, *49*, 7.
(20) Veis, A.; Aranyi, C. *Journal of Physical Chemistry* **1960**, *64*, 1203.
(21) Bakeev, K. N.; Izumrudov, V. A.; Kuchanov, S. I.; Zezin, A. B.; Kabanov, V. A. *Macromolecules* **1992**, *25*, 4249.
(22) Cohen Stuart, M. A.; Besseling, N. A. M.; Fokkink, R. G. *Langmuir* **1998**, *14*, 6846.
(23) Okubo, T.; Hongyo, K.; Enokida, A. *Journal of the Chemical Society-Faraday Transactions I* **1984**, *80*, 2087.
(24) Zintchenko, A.; Rother, G.; Dautzenberg, H. *Langmuir* **2003**, *19*, 2507.
(25) Jayme, M. L.; Dunstan, D. E.; Gee, M. L. *Food Hydrocolloids* **1999**, *13*, 459.
(26) Jackson, D. S.; Neuberger, A. *Biochimica et Biophysica Acta* **1957**, *26*, 638.
(27) Koets, P. *Journal of Physical Chemistry* **1936**, *40*, 1191.
(28) Koets, P. *Progress Reports in Physics* **1944**, *4*, 129.
(29) Tosh, S. M.; Marangoni, A. G. *Applied Physics Letters* **2004**, *84*, 4242.
(30) Bungenberg de Jong, H. G. *Proceedings of the Koninklijke Nederlandse Akademie der Wetenschappen* **1947**, *50*, 707.
(31) Bungenberg de Jong, H. G.; Dekker, W. A. L. *Kolloid Beihefte* **1936**, *43*, 213.

(32) Sukhishvili, S. A.; Kharlampieva, E.; Izumrudov, V. *Macromolecules* **2006**, *39*, 8873.
(33) Kovacevic, D.; van der Burgh, S.; de Keizer, A.; Cohen Stuart, M. A. *Langmuir* **2002**, *18*, 5607.
(34) Tanford, C. *The hydrophobic effect: formation of micelles and biological membranes*; Wiley, 1973.
(35) Voets, I. K.; de Keizer, A.; de Waard, P.; Frederik, P. M.; Bomans, P. H. H.; Schmalz, H.; Walther, A.; King, S. M.; Leermakers, F. A. M.; Cohen Stuart, M. A. *Angewandte Chemie-International Edition* **2006**, *45*, 6673.
(36) van der Burgh, S.; Fokkink, R.; de Keizer, A.; Cohen Stuart, M. A. *Colloids and Surfaces A: Physicochemical and Engineering Aspects* **2004**, *242*, 167.

Chapter Two

Comparison of complex coacervate core micelles from two diblock copolymers or a single diblock copolymer with a polyelectrolyte

Abstract

With light-scattering titrations, we show that complex coacervate core micelles (C3Ms) form from a diblock copolymer with a polyelectrolyte block and either an oppositely charged polyelectrolyte, a diblock copolymer with an oppositely charged polyelectrolyte block or a mixture of the two. The effect of added salt and pH on both types of C3Ms is investigated. The hydrodynamic radius of mixed C3Ms can be controlled by varying the percentage of oppositely charged polyelectrolyte or diblock copolymer. A simple core-shell model is used to interpret the results from light scattering, giving the same trends as the experiments for both the hydrodynamic radius and the relative scattering intensities. Temperature has only a small effect on the C3Ms. Isothermal titration calorimetry shows that the complexation is mainly driven by Coulombic attraction and by the entropy gain due to counterion release.

Published as: Hofs, B., Voets, I.K., de Keizer, A. and Cohen Stuart M.A., Physical Chemistry Chemical Physics, 2006, 8, 4242

Introduction

Complex coacervation is the associative phase separation into a liquid like phase that occurs when two oppositely charged polyions are mixed[1]. The highest density of the resulting complex coacervate is reached when the mixing ratio is optimal[1], i.e. when the charge density on the oppositely charged polyelectrolytes is high and the total number of anionic and cationic charges is equal. The pH influences the charge density of many polyions, e.g. proteins and weak polyelectrolytes, and thus changes the optimal composition. Added salt weakens the complexation; above a critical ionic strength complex coacervation is suppressed.

The phase separation becomes microscopic when one or both of the polyions are attached to a water-soluble neutral block[2]. One then obtains colloidal (nano-)objects, for which the terms Block Ionomer Complexes (BICs)[3], poly-ion complex micelles (PIC micelles)[4], InterPolyElectrolyte Complexes (IPECs)[5] and Complex Coacervate Core Micelles (C3Ms)[6] have all been used. These complexes or micelles share the following properties; (i) the aggregation is largely driven by Coulombic attraction of the oppositely charged polyelectrolytes and counter-ion release, (ii) a core of micro-phase-separated complexed polyelectrolytes is surrounded by a neutral water soluble corona, (iii) the complexes or micelles are responsive to the surrounding medium, for example, they fall apart above a certain critical ionic strength[3,5,7].

Investigation of their responsiveness to additions of extra polyelectrolyte has been performed by Light Scattering Titrations (LS-T)[6]. The aim of our study is to compare the formation of complexes from a diblock copolymer with either oppositely charged polyelectrolyte, oppositely charged diblock copolymer, or a mixture of these two. This will help to elucidate the effect of the neutral block on the hydrodynamic radius and aggregation number of C3Ms. The effects of ionic strength, pH and temperature on the size, responsiveness and stability of the formed complexes are also investigated.

Materials and methods

Chemicals

Poly(N,N-dimethyl aminoethyl methacrylate)-*block*-poly(glyceryl methacrylate) (PDMAEMA-b-PGMA) diblock copolymer was synthesized by anionic polymerization[8]. Characterization of this diblock copolymer with matrix-assisted laser desorption/ionisation-time of flight mass spectrometry (MALDI-TOF MS) with an α-cyano-4-hydroxy-cinnamic-acid (ACHCA) matrix, prepared with the sandwich method[9], showed the expected peaks

around a molecular weight of 20 kDa. Also a low molecular weight peak at 3000 Da with a peak spacing of 157 Da, the molecular weight of a DMAEMA unit, was observed. Using ^{1}H-NMR, which gives a constant peak height per proton if one takes the MALDI-TOF MS data into account, we conclude that the polymer is a mixture of 89 wt% $PDMAEMA_{30}PGMA_{90}$ and 11 wt% $PDMAEMA_{19}$. This mixture was used as such. For notational simplicity and since PDMAEMA homopolymer will be taken up in the core of the C3Ms as if it were part of a charged block, we consider $PDMAEMA_{19}$ as a part of the main diblock polyelectrolyte chain, denoting the sample as $PDMAEMA_{45}PGMA_{90}$.

Poly(acrylic acid)-*block*-poly(acryl amide) (PAA-b-PAAm) diblock copolymer was synthesized with the MADIX process[10] and was a gift from Rhodia, Aubervilliers, France. The PDMAEMA homopolymer and PAA homopolymer were obtained from Polymer Source Inc., Canada and used as received. Properties of all polymers are summarized in Table 2.1. Polymer concentrations given are in monomeric units of the charged block. Numbers following the abbreviation of a polymer are the number of monomeric units. $NaNO_3$ (>99%) and Na_2HPO_4 (>99.8%) obtained from J.T.Baker, Deventer, The Netherlands were used as received.

Polymer	no. of ionic monomers	no. of neutral monomers	M_w/M_n
PAA-b-PAAm	42	417	1.2 / 1.4[a]
PAA	139	-	1.15
PDMAEMA-b-PGMA	45	90	1.08[b]
PDMAEMA	150	-	1.04

Table 2.1: Polymer characteristics.

[a] First M_w/M_n is for the PAA, second for the total diblock copolymer.

[b] M_w/M_n of the neutral block in the diblock copolymer. With 11 wt% of $PDMAEMA_{19}$ included in the polyelectrolyte block of the diblock copolymer.

Light Scattering Titrations

Light Scattering (LS) at a scattering angle of 90 degrees was performed with an ALV5000 multiple tau digital correlator and an argon laser operating at a wavelength of 514.5 nm with 0.20 W power. All LS measurements were performed at 298 K (temperature controlled by a thermostat, ±0.01 K), unless noted otherwise. In the experiments with varying

temperature a Haake C35 thermostat was used at a scan rate of 0.6 ºC/minute. Typically, solutions were filtered (0.2 μm Acrodisk, Pall, Ann Arbor, MI) and degassed before titration.

Light Scattering Titrations (LS-T) were performed with a Schott-Geräte computer controlled titration set-up, communicating with the LS computer, which allowed to control added volumes, stirring times and pH measurement[6]. In most of the LS-T a polyelectrolyte or diblock copolymer solution was titrated into an oppositely charged diblock copolymer solution (typical volume 10 ml) in a glass sample cell equipped with a pH electrode.

The composition of the system is defined in terms of f_+, the fraction of positively chargeable polymer groups with respect to the total number of chargeable polymer groups:

$$f_+ = 1 - f_- = \frac{[c_+]}{[c_+]+[c_-]} \qquad (2.1)$$

Here $[c_+]$ and $[c_-]$ are, respectively, the molar concentrations of the positively and negatively chargeable monomers in the polyelectrolytes. For each point in the LS-T curve five dynamic light scattering measurements were performed, only averages of these are shown. The titration typically took about 3 hours. Prior to measurements the pH of the sample and titrant were adjusted to within 0.1 pH unit of a chosen value with 0.1 or 1 M NaOH or HNO_3 solutions. To compare the different titrations qualitatively, the intensity of scattered light at f_+, $I(f_+)$, was normalized by the total concentration of polymer (in g/l) at f_+, $C_p(f_+)$.

The diffusion coefficient of the scattering objects was obtained with the cumulant method[11] and expressed in hydrodynamic radius, R_h, using the Stokes-Einstein equation. Corrections to the radii for changes in temperature, and for changes in refractive index and viscosity due to changes in temperature were taken into account using tabulated data[12].

Isothermal titration calorimetry

The heat of mixing of a solution of polyelectrolyte or diblock copolymer with a polyelectrolyte solution was determined with the Thermal Activity Monitor (TAM), an isothermal titration calorimeter (Thermometric LKB 2277, Sweden). Enthalpies of dilution of PDMAEMA were also determined. Experiments were performed in two 4 ml stirred cells (sample and reference) positioned in a 25 l thermostatted water bath. This bath is connected to a pre-thermostat resulting in a temperature control of ±0.01 K in the operating range of 278-353 K.

The titration was controlled by a PC with DigiTAM software (v.4.1.0.32, ThermoMetric AB, Sweden), which collects the data and integrates the output signal. Electrical calibration was performed at the end of each measurement.

Results and discussion

Simple geometrical core-shell model for C3Ms

LS-T as a function of f_+ for a diblock copolymer consisting of a polyelectrolyte block and a water soluble neutral block with an oppositely charged polyelectrolyte, have already been reported in literature[6]. The following aggregation mechanism was proposed (Fig. 2.1). At low f_+ so called soluble complex particles (SCPs) are formed which are stabilized by an excess anionic charge. With increasing f_+, the excess anionic charge decreases until at a critical excess anionic charge (CEAC), complex coacervate core micelles (C3Ms) appear. At the preferred micellar composition (PMC) there is an equal amount of positive and negative charges on the polyelectrolytes (f_+ = 0.5) and all polymeric components are present in the form of micelles. Upon further increase of f_+ beyond a critical excess cationic charge (CECC), the C3Ms dissociate into positively charged SCPs.

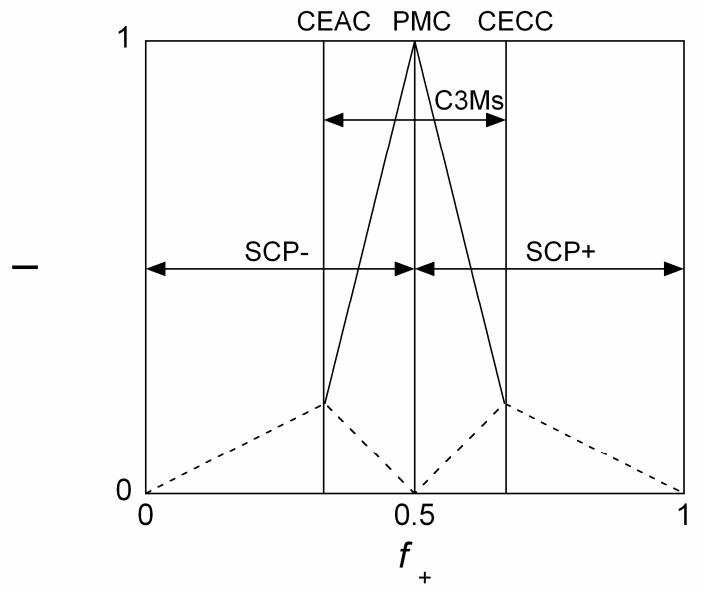

Figure 2.1: Aggregation diagram for C3Ms. Intensity I vs. f_+ is shown. The dashed line shows the changes in the scattering intensity due to SCPs, the solid line shows the changes in the scattering intensity due to C3Ms.

Here, we study how the aggregation of two oppositely charged diblock copolymers into double diblock C3Ms (D-C3Ms) differs from to the aggregation of one diblock copolymer plus oppositely charged homopolyelectrolyte into single diblock C3Ms (S-C3Ms). A simple model can be derived for the radius of such C3Ms based on the area A of the interface between the core and the corona, equation (2.2), the volume of the core V_{core}, eq. (2.3), and the volume of the corona V_{corona}. For a spherical micelle, we have

$$A = 4\pi R_{core}^2 = n_1 a_1 + n_2 a_2 \tag{2.2}$$

where R_{core} is the radius of the core, n_1 and n_2 are the number of diblocks 1 and 2 in a single micelle and a_1 and a_2 are the (effective) areas they occupy in the interface. For S-C3Ms, a_2 obviously vanishes. The volume of the core is

$$V_{core} = \frac{4}{3}\pi R_{core}^3 = \frac{\left(n_1 v_1^p p_1^p + n_2 v_2^p p_2^p\right)}{\varphi} \tag{2.3}$$

Here v_1^p and v_2^p are the volumes occupied by a monomer of the polyelectrolyte of the (diblock co)polymers 1 and 2 respectively, p_1^p and p_2^p are the respective degrees of polymerization of these polyelectrolyte blocks and φ is the total volume fraction of polyelectrolyte in the core. At the PMC, charge neutrality imposes

$$\alpha_1 n_1 p_1^p = \alpha_2 n_2 p_2^p \tag{2.4}$$

where α_1 and α_2 are the effective charge per monomer of polyelectrolyte 1 and 2 respectively. From (2.2), (2.3) and (2.4) R_{core} follows as:

$$R_{core} = \frac{3 p_1^p p_2^p (\alpha_2 v_1^p + \alpha_1 v_2^p)}{(\alpha_2 p_2^p a_1 + \alpha_1 p_1^p a_2)\varphi} \tag{2.5}$$

Then, n_1 and n_2 follow from equations (2.2), (2.3), and (2.5). The corona volume fraction profile is described by a step function. This is a simplification; more precise profile shapes have been discussed[13]. However, the scaling properties of brushes are known to be the same for step function and more refined models. The height of the corona can now be derived. The volume of the corona, V_{corona}, can be calculated and should be equal to

$$V_{corona} = \frac{n_1 v_1^n p_1^n}{\varphi_1} + \frac{n_2 v_2^n p_2^n}{\varphi_2} \tag{2.6}$$

where the first and second term are the effective occupied volumes of neutral blocks of polymer 1 and 2 respectively. v_1^n/φ_1 and v_2^n/φ_2 are the effective volumes of a monomer of

the neutral blocks and p_1^n and p_2^n are the degrees of polymerization of the neutral blocks. The radius of the C3M is then calculated from the total micellar volume ($V = V_{core} + V_{corona} = 4\pi R^3/3$). The height of the corona, *H*, is equal to $R - R_{core}$. The intensity of scattered light can also be estimated from the aggregation numbers obtained with this model, since the micelles are Rayleigh scatterers for which the intensity is proportional to NM^2, where *N* is the number of particles and *M* their mass.

In comparing the model to the experiments, subindex 1 indicates $PAA_{42}PAAm_{417}$ and subindex 2 indicates either $PDMAEMA_{150}$ or $PDMAEMA_{45}PGMA_{90}$ (or a mixture of these two). Used input: a_1 = 15 nm^2, a_2 = 11 nm^2 (a_2 = 0, in case of a polyelectrolyte instead of a diblock). For our system $a_1 > a2$ since water is a better solvent for PAAm than for PGMA. The areas used here are comparable to areas for PEO chains in PIC micelles derived in a different study[14]. The monomer volumes are calculated from the molecular weight and density (assumed to be 1 kg/l) and are v_1^p = 0.12 nm^3, v_1^n = 0.12 nm^3, v_2^p = 0.26 nm^3 and v_2^n = 0.27 nm^3. φ = 0.4, which is a reasonable value for the density of the complex coacervate core[15]. φ_1 = 0.04, a reasonable value for a polymer brush and φ_2 is larger than φ_1 since the density of the corona (a polymer brush) is expected to be higher for shorter chains[13,16,17] and because it is not in an equally good solvent.

Although this model simplifies and neglects many aspects of the micelles like, e.g., the density profile of the neutral polymers and the variation in the area of the neutral blocks with varying core density, it can be used to interpret the effect of varying block length on the radii and the aggregation numbers of C3Ms.

Thermodynamics of formation of C3Ms

Complexation of oppositely charged polyelectrolytes can be followed by measuring the heat of mixing with isothermal titration calorimetry (ITC). The heat of mixing of $PAA_{42}PAAm_{417}$ with $PDMAEMA_{150}$ is exothermic up to f_+ = 0.5 and decreases with increasing salt concentration (Fig. 2.2a). Above f_+ = 0.5 ΔH approaches zero. Initially, at low f_+, the ΔH of complexation of $PAA_{42}PAAm_{417}$ with $PDMAEMA_{150}$ in 50 mM $NaNO_3$ is nearly the same as that of PAA_{139} complexing with $PDMAEMA_{150}$ (in buffer with a comparable ionic strength). However, just before the PMC the ΔH of mixing PAA_{139} with $PDMAEMA_{150}$ shows a pronounced exothermic peak, probably because of compensation of charges that were present in the soluble complexes, due to phase separation into a high-

density complex coacervate. In the formation of S-C3Ms at 50 mM $NaNO_3$ there is a small endothermic peak around $f_+ = 0.5$. Apparently, some Coulombic bonds are broken in the last step of the C3M formation.

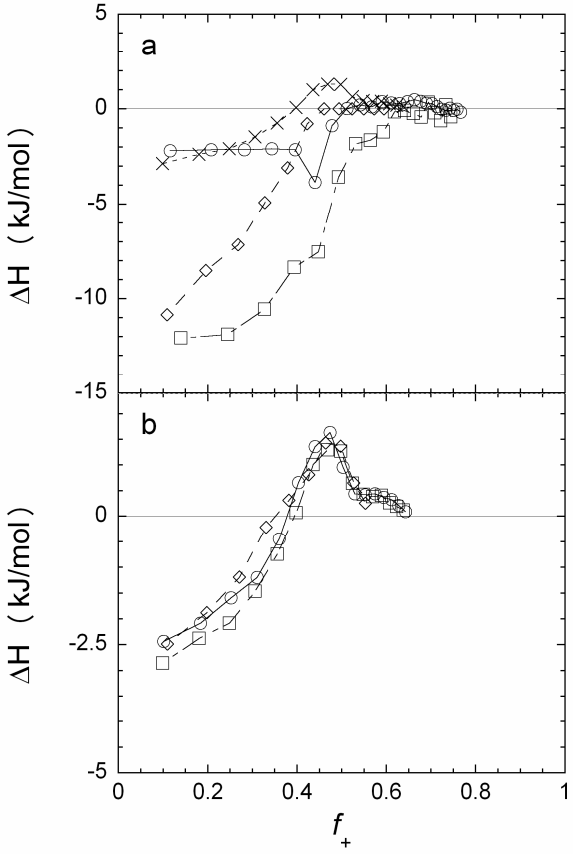

Figure 2.2: a) The effect of salt on the heat of mixing of $PAA_{42}PAAm_{417}$ with $PDMAEMA_{150}$ as a function of f_+, at 1 (□), 10 (◊) and 50 (×) mM $NaNO_3$. For comparison, ΔH (kJ mol^{-1}) of titrating 2.7 mM PAA_{139} with 37 mM $PDMAEMA_{150}$, both in 20 mM phosphate buffer (ionic strength 54 mM) is also shown (○). Initial pH of the solutions was 6.7 and the experiments were performed at 298 K. b) Effect of temperature on the heat of mixing of $PAA_{42}PAAm_{417}$ with $PDMAEMA_{150}$ in 50 mM $NaNO_3$, starting pH of all solutions was 6.7. T = 284 K (◊), 298 K (□) or 318 (○).

In calorimetric studies, variation of temperature often helps to identify a hydrophobic effect[18]. Here, there is no change in ΔH with temperature (Fig. 2.2b), e.g. $\Delta C_p = 0$. Hydrophobic interactions and dehydration of polar groups result in a significant temperature dependence with opposite sign[19], whereas the temperature dependence of Coulombic

interactions is (almost) absent. From the absence of temperature dependence of ΔH in the formation of C3Ms we conclude that the enthalpy of formation of C3Ms must be predominantly attributed to Coulombic interactions. Alternatively, the contributions to ΔC_p of the hydrophobic interactions and dehydration of polar groups cancel each other out, but this seems unlikely. It follows that the complexation is mainly driven by Coulombic attraction and the gain in entropy due to the release of counterions.

Polymer 2	Model					Experiment	
	R_{core} [nm]	R_{total} [nm]	n_1	n_2	I/I_{150}	R_h [nm]	I/I_{150}
45-90	5	16	11	11	0.28	17	0.26
82-90	6	19	21	11	0.43	21	0.39
195-90	7	22	35	8	0.65	23	0.58
150-0	8	25	54	15	1	24	1

Table 2.2: Comparison of model and experiment for single, mixed and double diblock C3Ms Comparison of model and experiment at the PMC for LS-T of 1 g/l $PAA_{42}PAAm_{417}$ (polymer 1) with $PDMAEMA_{45}PGMA_{90}$ and $PDMAEMA_{150}$ and mixtures thereof ('polymer' 2). The mixture was described as a single diblock copolymer species with the polyelectrolyte length divided by the number of diblocks as added polyelectrolyte length, where the 45-90, 82-90, 195-90 and 150-0 polymers correspond to a $PDMAEMA_{45}PGMA_{90}$ percentage of 100, 80, 50 and 0 % respectively. R_h are as measured from LS-T (Fig. 2.2 and 2.4). R_{total}, R_{core}, n_1 and n_2 were obtained from the model described by equations (2.2-2.6).

Comparison of single and double diblock C3Ms

In figure 2.3 we compare the results of titrations of $PAA_{42}PAAm_{417}$ with $PDMAEMA_{150}$, or with $PDMAEMA_{45}PGMA_{90}$, respectively. The intensity of scattered light normalized by the total polymer weight concentration in g/l, R_h and pH are presented as a function of f_+. The intensity of scattered light, I, gives a sharp peak around $f_+ = 0.5$ with a maximum intensity I_{max}, and the derivative of the pH vs. f_+ curve, $\delta pH/\delta f_+$ has a maximum at the same f_+ value, both indicating the formation of C3Ms[6].

The result of the titration of D-C3Ms is very similar to that of the S-C3Ms, although I and R_h of the S-C3Ms are higher and larger. In both cases the estimated radii from the simple model correspond well with the experimental data (Table 2.2). Using the aggregation numbers and assuming $I \sim NM^2$, one can also calculate the expected relative intensities (relative to I_{max}

for the S-C3Ms, I_{150}, all divided by the polymer concentration (g/l) at I_{max}) for both systems. The relative intensities agree well with the data indicating that our model is at least giving reliable estimates for the relative aggregation numbers.

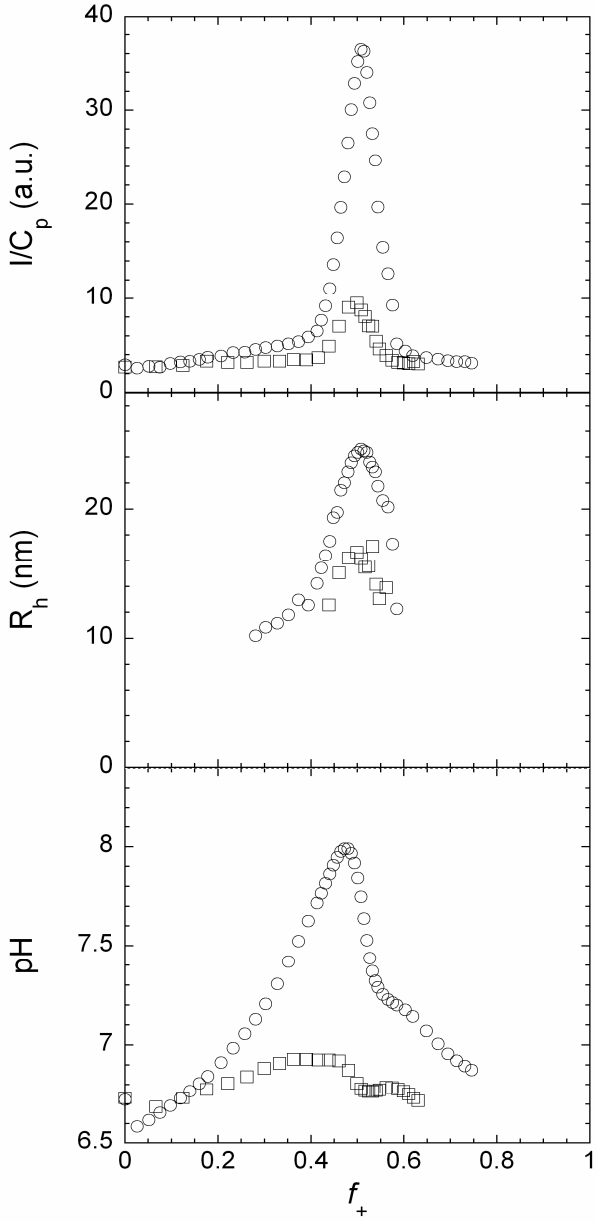

Figure 2.3: LS-T of 1 g/l of $PAA_{42}PAAm_{417}$ with 2 g/l $PDMAEMA_{150}$ (○) or with 8 g/l $PDMAEMA_{45}PGMA_{90}$ (□). All solutions were prepared in 1 mM $NaNO_3$ and their pH was adjusted to 6.7 prior to titration. The scattering intensity, I, normalized by the polymer concentration, C_p in g/l (to correct for the rise in intensity due to the increase in polymer concentration), hydrodynamic radius, R_h, and pH are all shown as a function of f_+. Only radii that could be determined with a reasonably low error are shown.

Start pH	Model						Experiment		
	Predicted position of I_{max} [f_+]	R_{core} [nm]	R_{total} [nm]	n_1	n_2	I/I$_{150}$	Position of I_{max} [f_+]	R_h [nm]	I/I_{150}
5.1	0.28	5	17	17	2	0.30	0.29	20	0.41
6.2	0.42	6	22	34	7	0.67	0.44	23	0.62
6.7	0.48	8	24	47	12	1	0.48	26	1
7.5	0.62	12	33	113	52	3.04	0.62	57	1.34

Table 2.3: Comparison of model and experiment; effect of pH.

Start pH of both solutions of $PAA_{42}PAAm_{417}$ and $PDMAEMA_{150}$, the predicted position of I_{max} (calculated from charge densities at start pH[15]), experimental position of I_{max} and R_h at I_{max} for the LS-T shown in figure 2.7. R_{total}, R_{core}, n_1 and n_2 were obtained from the model described by equations (2.2-2.6). Input: a_1 = 15 nm^2, a_2 = 0 nm^2, v_1^p = 0.12 nm^3, v_1^n = 0.12 nm^3, v_2^p = 0.26 nm3 and v_2^n = 0.27 nm^3, φ = 0.4[15], φ_1 = 0.04 and φ_2 = 0.08.

The pH changes for the S-C3Ms system are more pronounced than for the D-C3Ms system. This may be attributed to a slightly different starting pH. At low concentrations of added salt, the pH varies strongly with a small deviation from the ideal starting pH because Coulombic attractions are stronger and the driving force for proton uptake or release is accordingly greater.

Both systems show the expected pattern in $I(f_+)$ as a function of f_+[6]. At first, only $PAA_{42}PAAm_{417}$ is in solution but upon adding the oppositely charged polyelectrolyte or diblock copolymer, $I(f_+)$ slowly increases as SCPs are formed. The complexation between PAA and PDMAEMA can also be seen from the change in the pH. Since there is an approximately equal fraction of charges on the PAA and PDMAEMA, but there is far more PAA then PDMAEMA, maximum complexation requires an increase in the charge density of PDMAEMA. H^+ can be taken up by the PDMAEMA, thus increasing its charge density as well as the pH of the solution.

Once one passes the CEAC, $I(f_+)$ increases sharply as heavier objects (C3Ms) are formed. For both systems, the pH decreases prior to reaching I_{max}, where a maximum number of micelles and maximum core-density is reached. The decrease in pH must now be due to an increase in the charge density of PAA with respect to PDMAEMA. This occurs since the PDMAEMA is slightly overcharged at lower f_+ compared to the PAA.

The highest number of the particles with highest density (C3Ms) should be present at approximately the f_+ value where there is an equal amount of positive and negative charged polymer groups (Fig. 2.1, 2.3). Hence, for these systems the PMC is expected to occur at f_+ = 0.5 and pH 6.7 as deduced from the charge densities of the polyelectrolytes in bulk solution[15]. Indeed, for the D-C3Ms system I_{max}, is located close to f_+ = 0.50 and the pH at I_{max} is close to 6.7. Beyond the maximum in $\delta pH/\delta f_+$, the intensity decreases as the C3Ms fall apart into SCPs. The pH continues to decrease as the PAA tries to compensate for the total amount of charges on the PDMAEMA. Upon further increasing f_+, the pH further decreases due to addition of the titrant (which has pH 6.7).

Effect of the mixing ratio of the cationic diblock and polyelectrolyte

Another way to vary the number of neutral blocks (and by this the size of the C3Ms) is by titration with a mixture of diblock copolymer and polyelectrolyte. The percentage of diblock copolymer in the titrant was varied to investigate the effect on C3M formation (Fig. 2.4).

From the start of the LS-T up to the PMC, the LS-T with the mixtures of polyelectrolyte and diblock as titrant show the same trend in the intensity, pH and R_h as seen previously (Fig. 2.2). First, there is the slow increase in the intensity, accompanied by an increase in the pH, due to formation of SCPs. Then, at $f_+ \approx 0.38$, all LS-T show a faster increase in the intensity, the pH starts to drop around this f_+ and the R_h increases. All these features are characteristic of the formation of C3Ms. The maxima in intensity, $\delta pH/\delta f_+$ and R_h coincide well at $f_+ \approx 0.48$ for all mixtures. The R_h at this point (the PMC) and I_{max} decrease with increasing percentage of $PDMAEMA_{45}PGMA_{90}$ in the titrant. Good agreement is found between the hydrodynamic radius and the calculated radius and the relative intensities (Fig. 2.5). The latter is a strong indication that the relative aggregation numbers (Table 2.2) are reliable.

Upon increasing f_+ beyond the PMC, the intensity decreases as usual. However, one also observes a shoulder in the $I(f_+)$ curve for the 50 and 80 percent diblock, coinciding with a small second peak in the R_h. The C3Ms formed in this shoulder have a lower density than those at the PMC as their scattering intensity is much lower than I_{max} while the R_h is similar in both cases. A similar shoulder has also been observed in LS-T of $PAA_{42}PAAm_{417}$ and $PDMAEMA_{150}$ (data not shown). This shoulder in the intensity could be due to the increase of pH with increasing f_+ around the shoulder, which changes the charge densities of the

polyelectrolytes and the charge balance of the system. Thus, instead of further dissociation of C3Ms into SCPs, more C3M-like objects are formed.

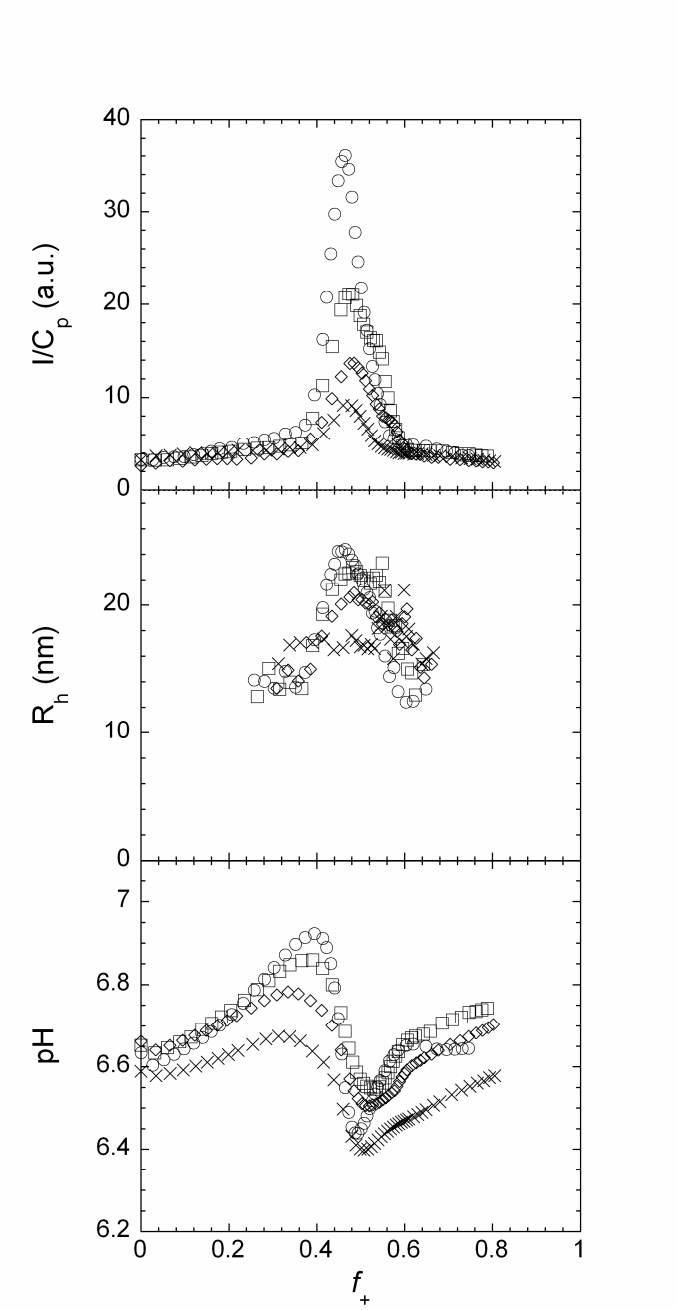

Figure 2.4: LS-T of 1 g/l of $PAA_{42}PAAm_{417}$ with mixtures of $PDMAEMA_{150}$ and $PDMAEMA_{45}PGMA_{90}$: 0 (○), 50 (□), 80 (◊), and 100 (×) % $PDMAEMA_{45}PGMA_{90}$. All solutions were prepared in 10 mM $NaNO_3$ and their pH was adjusted to 6.7 prior to titration. The scattering intensity, I, normalized by the polymer concentration, C_p in g/l, hydrodynamic radius, R_h, and pH are all shown as a function of f_+. Only radii that could be determined with a reasonably low error are shown.

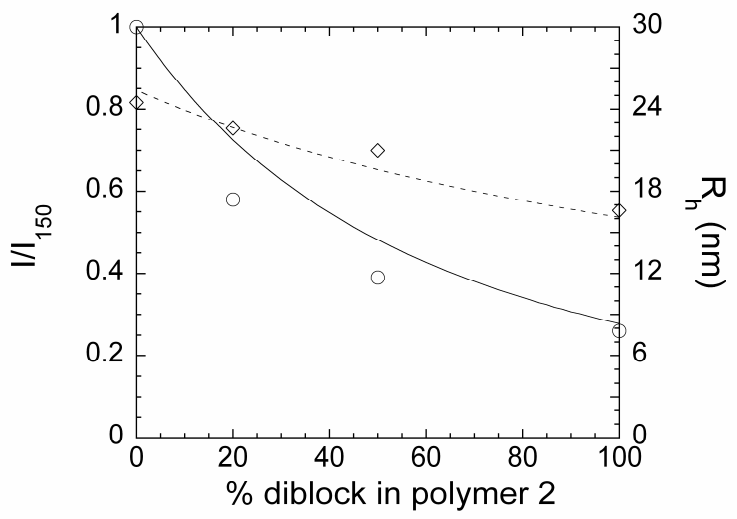

Figure 2.5: Comparison of relative intensities at I_{max}, I/I_{150}, and hydrodynamic radii, R_h, obtained with the model and experiments. I/I_{150} (– and ○) and R_h (-- and ◊) are given as a function of the percentage of diblock copolymer ($PDMAEMA_{45}PGMA_{90}$) in polymer 2. Lines are from the model, symbols are from experiments (Fig. 2.4).

Effect of ionic strength

The ionic strength is an important parameter in complex coacervation. Above a certain salt concentration, no complexation will occur as all charges are screened[3,5,7]. We investigated the effect of salt on the complexation of our systems. LS-T at 1, 10 and 50 mM $NaNO_3$ for the S-C3Ms system and the D-C3Ms system (Fig. 2.6) show that at 50 mM $NaNO_3$, the scattering intensity of D-C3Ms is much lower than at lower salt concentrations. In contrast, for the S-C3Ms there is almost no difference in intensity *I* between the different salt concentrations. Apparently, the D-C3Ms are more sensitive to salt than the S-C3Ms. The critical salt concentration for the D-C3Ms will thus also be lower.

Differences in the effect of salt on the formation of S-C3Ms and D-C3Ms can be attributed to: (i) The decreased length of the polyelectrolyte, being 150 in the polyelectrolyte and 30 or 19 monomeric units in the second diblock copolymer, decreases the strength of complex coacervation. It has been seen for non-stoichiometric polyelectrolyte complexes that decreasing the length of the polyelectrolytes lowers the critical salt concentration[20]. In earlier work, no micelles were formed when combinations with short polyelectrolyte blocks were used[6], indicating that a minimum block length is required for C3M formation. This minimum block length most likely is a function of the ionic strength and in the case of the D-C3Ms in 50 mM $NaNO_3$, this minimum length is probably of order 30 units. (ii) The interactions between both neutral water soluble blocks may be unfavorable, thereby decreasing the

stability of the C3Ms. From 2D ^{1}H-NMR NOESY experiments it was concluded that the neutral blocks are mixed[21]. (iii) There is an entropic penalty since all polyelectrolyte block-neutral block junctions should be at the interface between core and corona. This might be the reason for the so-called chain length recognition[14] found for micelles from two types of diblock copolymers, although others find micelles with unmatched polyelectrolyte blocks[5].

For both systems the width of the intensity peak at half height, $W_{1/2}$, increases with increasing salt concentration. In contrast, in most macroscopic cases of complex coacervation the width of the region of phase separation decreases with increasing salt concentration, until at a certain critical salt concentration the complex coacervation does not take place anymore[1,22]. The increase in the width observed here may be due to; (i) pH changes during the LS-T. The amplitude of the changes in pH decreases with increasing ionic strength (data not shown). The larger changes in pH as a function of f_+ with decreasing salt concentration are logical, not only because salt decreases the strength of the Coulombic attraction that causes the complexation, but also because a higher fraction of the charges can form a pair with a small counterion rather than with a charge from the oppositely charged polyelectrolyte. As the pH of the solvent determines the charge densities of weak polyelectrolytes in solution and the charge densities of the (oppositely charged) polyelectrolytes together with their concentrations determine the point where the number of charges on both polyelectrolytes is equal, one expects the pH to shift the f_+ value where complex coacervation occurs. In our case the pH first rises with addition of $PDMAEMA_{150}$, due to an increase in the charge density of the complexing PDMAEMA. The charge densities of the non-complexed parts of the PDMAEMA however, should decrease as the pH increases, resulting in a reduced driving force for complex coacervation due to electrostatic repulsion. (ii) screening effects. C3Ms are formed when the charge on the SCPs drops below the CEAC (or CECC)[6]. With increasing salt concentration, electrostatic effects are increasingly screened and thus the formation of C3Ms may well occur at higher excess charge. It is known that some phase diagrams of oppositely charged polyelectrolytes show (iii) a non-monotonic change in the width of the phase separation with increasing salt concentration[23,24] indicating that the repulsive interaction between complexes responds more strongly to added salt than the attractive (correlation) contribution. This might also be the case for our system, explaining why the width of the peak (which is a measure for the width of C3M formation and thus complex coacervation) increases, rather than decreases, with increasing salt concentration.

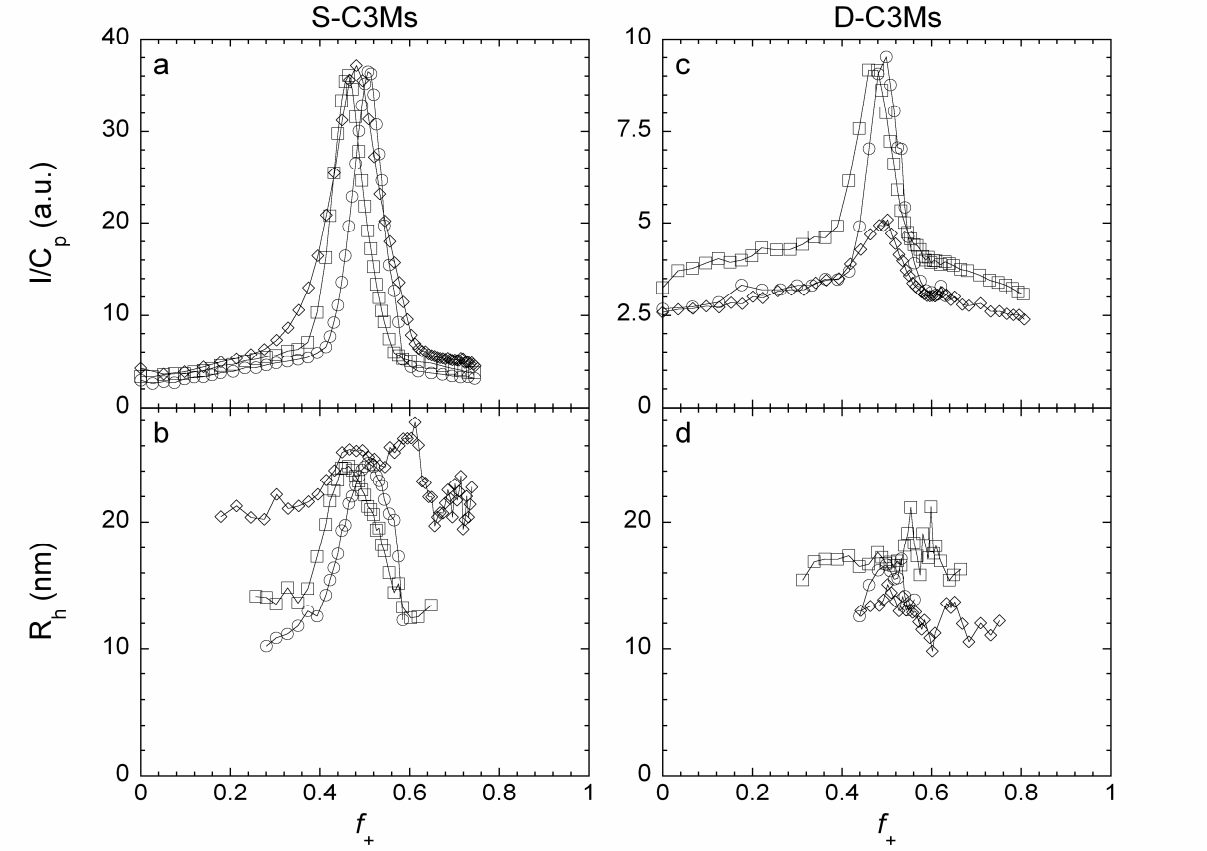

Figure 2.6: Influence of concentration of $NaNO_3$ on LS-T of 1 g/l $PAA_{42}PAAm_{417}$ with 2 g/l $PDMAEMA_{150}$ (2.6a, 2.6b) or with 8 g/l $PDMAEMA_{45}PGMA_{90}$ (2.6c, 2.6d), initial pH of all solutions 6.7. Three different salt concentrations have been used, 1(○), 10 (□) and 50 mM $NaNO_3$ (◊). Intensity, pH and R_h as a function of f_+ are shown. Note that the LS-T for 1 mM $NaNO_3$ was already shown in figure 2.3 and the LS-T for 10 mM $NaNO_3$ in figure 2.4, both are reproduced here. Intensity is normalized by the concentration of total polymer in g/l. Only radii which could be determined with a reasonably low error are shown.

For all salt concentrations and for both S-C3Ms and D-C3Ms the intensity follows the same pattern as a function of f_+. The intensity in the peak is virtually the same for the S-C3Ms, as is the R_h, indicating that the S-C3Ms that are formed are identical in size and density. Theoretical work on complex coacervation shows that the density of the complex does not vary much with ionic strength as long as the ionic strength is below the critical value[22], presumably because salt is almost entirely excluded from the complex coacervate. Moreover, the increase in salt concentration does not have a significant effect on the solubility or conformation of the PAAm block in water[25]. Hence, the shape and size do not change since

neither the core (consisting of the complex coacervate) nor the corona (consisting of PAAm blocks) are affected by the salt concentrations used.

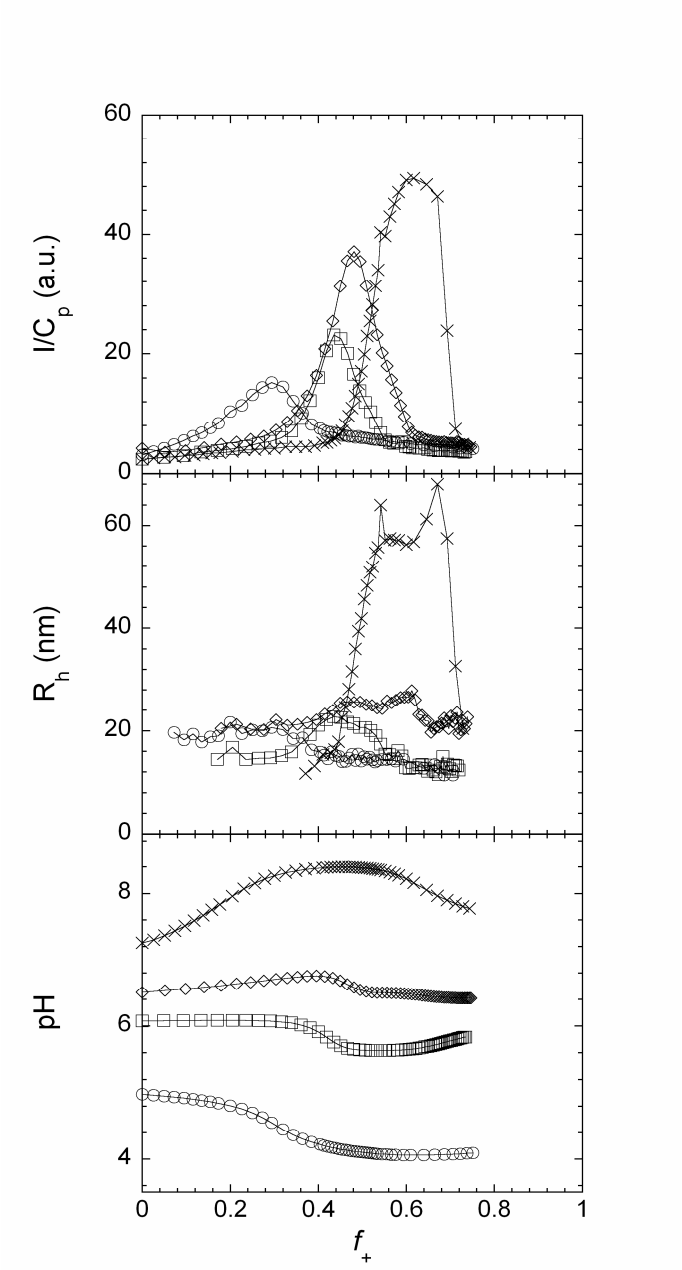

Figure 2.7: Influence of starting pH on a titration of 1 g/l $PAA_{42}PAAm_{417}$ with 2 g/l $PDMAEMA_{150}$, both solutions in 50 mM $NaNO_3$ and at equal starting pH, being 5.1 (○), 6.2 (□), 6.7 (◊) and 7.5 (×). Intensity, pH and R_h as a function of f_+ are shown. Intensity is normalized by the concentration of total polymer in g/l. Note that the LS-T at start pH 6.7 was already shown in figure 2.6 and is reproduced here. Only radii which could be determined with a reasonably low error are shown.

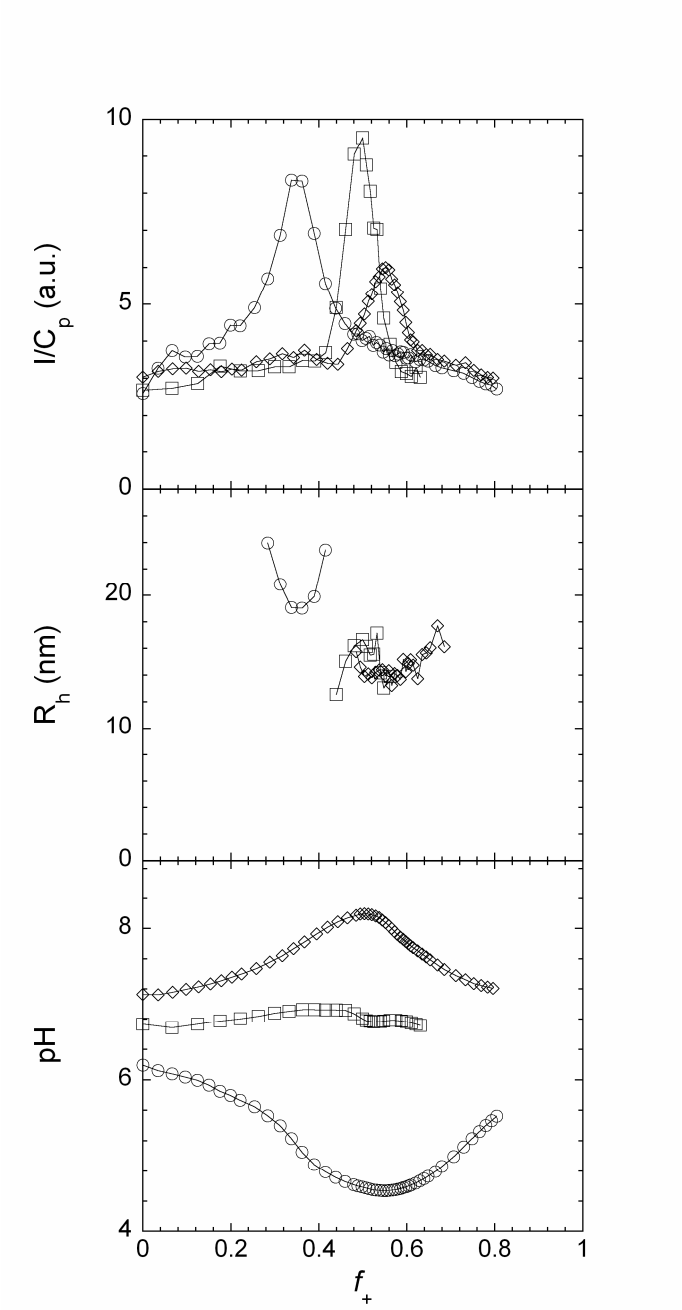

Figure 2.8: Influence of starting pH on a titration of 1 g/l $PAA_{42}PAAm_{417}$ with 8 g/l $PDMAEMA_{45}PGMA_{90}$, both solutions in 1 mM $NaNO_3$ and at equal starting pH, being 6.2 (○), 6.7 (□) and 7.2 (◊). Intensity, pH and R_h as a function of f_+ are shown. Intensity is divided by the concentration of total polymer in g/l. Note that the LS-T at starting pH 6.7 was already shown in figure 2.3 and is reproduced here. Only radii which could be determined with a reasonably low error are shown.

Effect of pH

The pH of the solution has a pronounced effect on the complex coacervation as the charge densities of weak polyelectrolytes like PAA and PDMAEMA strongly depend on pH and the stability of the complex coacervate depends on the charge densities[1,22]. LS-T of the S-C3M ($PAA_{42}PAAm_{417}$ with $PDMAEMA_{150}$ in 50mM $NaNO_3$) and the D-C3M ($PAA_{42}PAAm_{417}$ with $PDMAEMA_{45}PGMA_{90}$ in 1mM $NaNO_3$) system were performed to investigate the effect of varying starting pH and ionic strength on formation of C3Ms (Fig. 2.7 and 2.8) as a function of f_+.

I_{max} appears at different f_+ with different starting pH for both systems. Recall that f_+ is defined in terms of the amount of chargeable groups, not the actual amount of charges present. For both systems the shift is to lower f_+ for lower starting pH (compared to the optimum pH 6.7), and to higher f_+ for higher starting pH. This due to changes in the charge densities of the weak polyelectrolytes, PAA and PDMAEMA. For the S-C3M system the LS-T were performed in 50 mM $NaNO_3$, while for the D-C3M system the LS-T were in 1 mM $NaNO_3$. With decreasing salt concentration, the shifts in pH and f_+ at the PMC are larger (Fig. 2.7 and 2.8), indicating a higher driving force for complex coacervation at lower ionic strength. Charge densities for uncomplexed PAA and PDMAEMA in aqueous solution were obtained from potentiometric titrations[15]. Using these charge densities, the changes in pH in the LS-Ts and assuming that the complexation induces an increase in charge density[26] for both polyelectrolytes, we can predict the position of I_{max} (as $\alpha_+[c+]/(\alpha_+[c+]+\alpha_-[c-]) \equiv 0.5$, where α_+ and α_- are the effective charge per monomer of the positively and negatively charged polyelectrolyte, respectively). For S-C3Ms, the predicted positions of the I_{max} agree well with the observed location of the maxima (within experimental error, table 3). Note that at a pH of 4.6 and 50 mM $NaNO_3$ the effective charge density of PAA in the complex coacervate is about twice as high as it would be in the corresponding bulk solution.

For the S-C3M system I_{max} increases with increasing pH and increasing f_+, while for the D-C3Ms I_{max} decreases when one deviates from the optimal mixing proportions (pH 6.7 and $f_+ = 0.5$). Estimations from the simple model for the S-C3Ms show an increase in size at the PMC with increasing pH (table 3), corresponding well with experimental values (Fig. 2.7), except at pH 7.5. With increasing start pH from 6.7 to 7.5 the density of the complex coacervate core decreases (which can be seen from the relatively small increase in intensity with a more than two-fold increase in R_h) and this probably changes the area the neutral blocks occupy at the core-corona interface. For the objects formed at the highest pH, to reach

the experimental value of R_h with the structure for C3Ms as proposed[6], the PAAm block would have to be stretched about 5 times its radius of gyration (a fully stretched PAA_{42} polyelectrolyte block is about 17 nm, leaving 30 nm for the $PAAm_{417}$ blocks to fill). Probably the objects formed here are no longer spherical, but we did not investigate this further.

For D-C3Ms the estimates from the model show a constant size (15 nm), in contrast to a decrease in size with increasing pH as seen experimentally (Fig. 2.8). This is probably due to changes in the density of the core, which are not taken into account in our model.

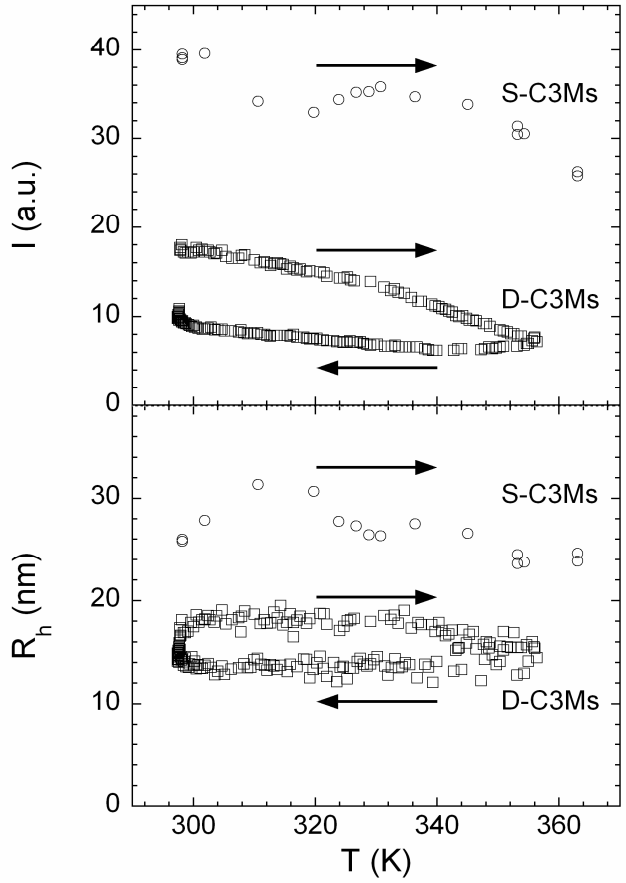

Figure 2.9: Effect of temperature, T, on C3Ms at the PMC, pH 6.7 and $f_+ = 0.48$. I and R_h as a function of f_+ are shown for C3Ms composed of $PAA_{42}PAAm_{417}$ and $PDMAEMA_{150}$ in 50 mM $NaNO_3$ (○) and C3Ms composed of $PAA_{42}PAAm_{417}$ and $PDMAEMA_{45}PGMA_{90}$ in 1 mM $NaNO_3$ (□). R_h was corrected for changes in viscosity and temperature. The arrow indicates the direction of the temperature-scan, the experiments were started with an upscan (arrow pointing towards the right).

Effect of temperature

For many possible applications, for instance in drug delivery, the stability of C3Ms with temperature is of interest. A temperature scan between 298 and 363 K was performed for both S-, and D-C3Ms. In this temperature range, S- C3Ms and D-C3Ms vary in size by about 20 % (Fig. 2.9). The R_h has a maximum around 313 K and the intensity decreases slightly with increasing temperature over the whole range. From the decrease in intensity it appears that the aggregation number of the C3Ms decreases weakly with increasing temperature. The decrease in size might be due to the decrease in the solubility of PDMAEMA, which has a cloud point at approximately 313 K[27]. Interestingly, there is some hysteresis in the temperature scan of the D-C3Ms. Probably, the core density of the C3Ms increases with increasing temperature as one passes the cloud point of the PDMAEMA. Upon decreasing the temperature, the complex coacervate core does not rearrange quickly, although R_h upon returning to 298 K is nearly identical to R_h at the start of the experiment.

Conclusions

Calorimetry shows that the driving force for complexation of S-C3Ms composed of $PAA_{42}PAAm_{417}$ and $PDMAEMA_{150}$ is Coulombic attraction between the oppositely charged polyelectrolytes and the release of counterions, with no contribution from hydrophobic interactions. Light scattering titrations of S-C3Ms and D-C3Ms show the expected differences: the radii of D-C3Ms are smaller than that of S-C3Ms. Partially ‘replacing’ the second diblock in D-C3Ms with the polyelectrolyte (by titration with a mixture) does not seem to change the formation of C3Ms, but does change the size. Hence, size can be controlled in a limited range by choosing the percentage of diblock copolymer in the mixture. Alternatively, the starting pH, together with f_+, can be used to control the size of the C3Ms.

A geometrical core-shell model estimates the variations in size and aggregation number. By considering the areas occupied by the neutral blocks one can explain the effects of the second diblock architecture, as well as the mixtures of second diblock with polyelectrolyte. The simple model cannot be used however, to estimate the changes in the size of the D-C3Ms with the variation in pH as the density of the core is not known.

The concentration of $NaNO_3$ above which no complexes are formed is about 50 mM for the D-C3Ms which is lower than for S-C3Ms, because the polyelectrolyte part of the diblock is shorter for the D-C3Ms and because of the unfavorable interactions between the two different kind of neutral blocks. In the range investigated here the salt concentration has no

effect on the size of the S-C3Ms. Interestingly, the width of the micellar peak, $W_{1/2}$, increases with increasing salt concentration for both systems. This seems to indicate a subtle interplay between electrostatic repulsion and attraction for f_+ = CEAC or CECC.

Increasing temperature from 298 to 363 K has almost no effect on the size of both types of C3Ms.

Literature

(1) Bungenberg de Jong, H. G. In *Colloid Science*; Kruyt, H. R., Ed.; Elsevier: Amsterdam, 1949; Vol. II.
(2) Cohen Stuart, M. A.; Hofs, B.; Voets, I. K.; de Keizer, A. *Current Opinion in Colloid & Interface Science* **2005**, *10*, 30.
(3) Kabanov, A. V.; Bronich, T. K.; Kabanov, V. A.; Yu, K.; Eisenberg, A. *Macromolecules* **1996**, *29*, 6797.
(4) Harada, A.; Kataoka, K. *Macromolecules* **1995**, *28*, 5294.
(5) Gohy, J.-F.; Varshney, S. K.; Jerome, R. *Macromolecules* **2001**, *34*, 3361.
(6) van der Burgh, S.; de Keizer, A.; Cohen Stuart, M. A. *Langmuir* **2004**, *20*, 1073.
(7) Cohen Stuart, M. A.; Besseling, N. A. M.; Fokkink, R. G. *Langmuir* **1998**, *14*, 6846.
(8) Hoogeveen, N. G.; Cohen Stuart, M. A.; Fleer, G. J.; Frank, W.; Arnold, M. *Macromolecular Chemistry and Physics* **1996**, *197*, 2553.
(9) Fraering, P.; Imhof, I.; Meyer, U.; Strub, J. M.; van Dorsselaer, A.; Vionnet, C.; Conzelmann, A. *Molecular Biology of the Cell* **2001**, *12*, 3295.
(10) Taton, D.; Wilczewska, A. Z.; Destarac, M. *Macromolecular Rapid Communications* **2001**, *22*, 1497.
(11) Koppel, D. E. *Journal of Chemical Physics* **1972**, *57*, 4814.
(12) Lide, D. R. *CRC Handbook of Chemistry and Physics*, 82 ed., 2001-2002.
(13) Wijmans, C. M.; Zhulina, E. B. *Macromolecules* **1993**, *26*, 7214.
(14) Harada, A.; Kataoka, K. *Macromolecules* **2003**, *36*, 4995.
(15) van der Burgh, S. Complex Coacervate Core Micelles in Solution and at Interfaces. PhD-thesis, Wageningen Universiteit, 2004.
(16) Birshtein, T. M.; Liatskaya, Y. V.; Zhulina, E. B. *Polymer* **1990**, *31*, 2185.
(17) Skvortsov, A. M.; Klushin, L. I.; Gorbunov, A. A. *Macromolecules* **1997**, *30*, 1818.
(18) Mehrian, T.; de Keizer, A.; Korteweg, A. J.; Lyklema, J. *Colloids and Surfaces A-Physicochemical and Engineering Aspects* **1993**, *71*, 255.
(19) Murphy, K. P. *Medicinal Research Reviews* **1999**, *19*, 333.
(20) Pergushov, D. V.; Izumrudov, V. A.; Zezin, A. B.; Kabanov, V. A. *Vysokomolekulyarnye Soedineniya Seriya A & Seriya B* **1995**, *37*, 1739.
(21) Voets, I. K.; de Keizer, A.; Cohen Stuart, M. A.; de Waard, P. *Macromolecules* **2006**, *39*, 5952.
(22) Biesheuvel, P. M.; Cohen Stuart, M. A. *Langmuir* **2004**, *20*, 4764.
(23) Izumrudov, V.; Kharlampieva, E.; Sukhishvili, S. A. *Macromolecules* **2004**, *37*, 8400.
(24) Pergushov, D. V.; Izumrudov, V. A.; Zezin, A. B.; Kabanov, V. A. *Vysokomolekulyarnye Soedineniya Seriya A & Seriya B* **1993**, *35*, A844.
(25) Molyneux, P. *Water-soluble synthetic polymers: properties and behavior*; CRC Press, Boca Raton, Florida, US, 1983/84; Vol. I en II.
(26) Biesheuvel, P. M.; Cohen Stuart, M. A. *Langmuir* **2004**, *20*, 2785.
(27) Lowe, A. B.; Billingham, N. C.; Armes, S. P. *Macromolecules* **1998**, *31*, 5991

Chapter Three

On the stability of (highly aggregated) polyelectrolyte complexes containing a charged-*block*-neutral diblock copolymer

Abstract

Using light scattering and cryogenic transmission electron microscopy, we show that highly aggregated polyelectrolyte complexes (HAPECs) composed of poly([4-(2-amino-ethylthio)-butylene] hydrochloride)$_{49}$-*block*-poly(ethylene oxide)$_{212}$ and poly(acrylic acid) (PAA) of varying lengths (140, 160 and 2000 monomeric units) are metastable or unstable if the method of preparation is direct mixing of two solutions containing the oppositely charged components. The stability of the resulting HAPECs decreases with decreasing neutral block content and with increasing deviation from 1:1 mixing (expressed in number of chargeable groups) of the oppositely charged polyelectrolytes, most probably due to electrostatic reasons. The difference between the metastable state and stable state, obtained with pH cycles, increases with increasing PAA length and increasing pH mismatch between the two solutions with the oppositely charged components.

Published in modified form as: Hofs, B., de Keizer, A. and Cohen Stuart M.A., Journal of Physical Chemistry B, 2007, 111, 5621

Introduction

A fair number of articles have been published on complexation between oppositely charged polyelectrolytes[1-4], either with a phase-separation arresting neutral-polyelectrolyte diblock copolymer (forming micelles, named Complex Coacervate Core Micelles (C3Ms), Block Ionomer Complexes (BICs), PolyIon Complex (PIC) micelles or InterPolyelectrolyte Complexes (IPECs))[5-10] or with even more complicated polymers (e.g. triblocks)[11]. The most important parameters in these systems are the ionic strength and the mixing ratio of the oppositely charged polyelectrolytes. Complex coacervation can also be accomplished with different, more natural components. The large number of different systems under study – combinations of proteins and polysaccharides[12-14], proteins and polyelectrolytes[11,12,15], polyelectrolytes and nanoparticles[11,16], multivalent counterions, surfactants[11], coordination polymers[17] or DNA[18] – and possible applications in gene delivery, as anti-fouling agent, as emulsion stabilizer and in wastewater treatment[11,18] show the importance of complex coacervation as a tool for building functional nanoparticles.

The kinetics of the formation and especially the rearrangement of polyelectrolyte complexes (PECs) without neutral polymer blocks have been investigated rather well[19-22]. The rate constant of the exchange reaction depends on the salt concentration, the length of the shortest polyelectrolyte species, the polyelectrolyte concentration and the charge density of the polyelectrolytes. For highly aggregated polyelectrolyte complexes (HAPECs) containing copolymers with multiple neutral blocks, a transition to soluble complexes has been reported, unfortunately the used polymer seems to have had a rather high polydispersity[23].

To the best of our knowledge only two papers have been published touching on the effect of time in the formation of micelles with a polyelectrolyte and an oppositely charged neutral-charged diblock copolymer with low polydispersity[24,25]. Cohen Stuart and co-workers showed that initially there is an excess scattering, indicating initial formation of larger complexes, which reorganize into smaller aggregates. The time during which the reorganization process occurs depends strongly on the ionic strength of the solvent. Without added salt or buffer, the process takes about 10^3 s, whereas in 0.3 M NaCl, it takes only 10^{-1} s.

In this chapter we examine the stability of aggregates composed of a polyelectrolyte and a diblock copolymer with an oppositely charged polyelectrolyte block and a neutral water-soluble block. The effect of the mixing ratio of the polyelectrolytes on the stability is of special interest. A possible way to quickly reach what might be the stable state is introduced as well.

Experimental methods

Chemicals

Poly(acrylic acid)$_{140}$ (PAA_{140}, number denotes the degree of polymerization, M_n = 10.0 kg/mol), PAA_{160}, M_n = 11.7 kg/mol) and PAA_{2000} (M_n = 145 kg/mol), polydispersity index (PDI) 1.15, 1.07 and 1.13, respectively, were purchased from Polymer Source Inc. (Canada) and used as received. Poly([4-(2-aminoethylthio)-butylene] hydrochloride)$_{49}$-*block*-PEO_{212} ($PAETB_{49}PEO_{212}$, M_w = 16.6 kg/mol), PDI 1.1, was prepared by modification with a mercaptan from poly(butadiene)$_{65}$-*block*-PEO_{212} - which was prepared by sequential anionic polymerization of 1,3-butadiene and ethylene oxide - and was a kind gift from Helmut Schlaad (MPI Golm). The synthesis and analysis of this polymer has been described in great detail elsewhere[26]. Structures of the used polymers are shown in figure 3.1. All salts used were of analytical grade and were used as received. Aqueous solutions of polymers were prepared by dissolution of known amounts of polymer into deionized water (Milli-Q) to which known amounts of $NaNO_3$ had been added.

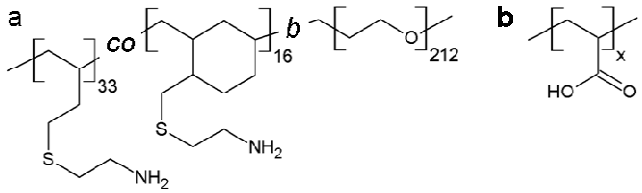

Figure 3.1: Chemical structures of the neutral forms of the polymers used, being a) $PAETB_{49}PEO_{212}$ and b) PAA_x (x = 140, 160 or 2000).

Cryogenic Transmission Electron Microscopy (Cryo-TEM)

Cryo-TEM images were obtained with a Technai Sphera (FEI Company) TEM operating at a voltage of 120 kV. Samples were prepared on 200 mesh copper grids containing a carbon coated holey support film (Agar Scientific, UK and Ted Pella Inc. USA). A small drop of sample was placed on the grid and the excess fluid was blotted off using Whatmann #4 filter paper, in a high humidity chamber to prevent drying . The grids with the thin aqueous films were vitrified by dropping into liquid ethane and transferred under liquid nitrogen into a Gatan CT3500 cryo-holder and, subsequently, into the TEM. Images were taken under low dose conditions.

Light Scattering

Light Scattering (LS) at a scattering angle of 90 degrees was performed with an argon laser operating at a wavelength of 514.5 nm with 0.20 W power as light source. The intensity autocorrelation function was determined with an ALV5000 multiple tau digital correlator. All LS measurements were performed at room temperature (around 293 K). The samples were prepared by direct mixing of two aqueous solutions, of which pH and background electrolyte concentration were matched, and which contained the separate polymers needed for complexation (in one $PAETB_{49}PEO_{212}$ and in the other PAA). After mixing, LS data were recorded as a function of time.

Light Scattering Titrations (LS-T) were performed with a Schott-Geräte computer controlled titration set-up, communicating with the LS computer, which allowed to control added volumes, stirring times and pH measurement. In most of the LS-T a polyelectrolyte solution was titrated into an oppositely charged diblock copolymer solution (typical volume 10 ml) in a glass sample cell equipped with a pH electrode. Typically, the separate solutions, containing just one of the two polyelectrolyte species, were filtered (0.2 μm Acrodisk, Pall, Ann Arbor, MI) before titration.

The composition of the system is defined in terms of f_+, the fraction of positively chargeable polymer groups with respect to the total number of chargeable polymer groups:

$$f_+ = 1 - f_- = \frac{c_+}{c_+ + c_-} \qquad (3.1)$$

Here c_+ and c_- are, respectively, the molar concentrations of the positively and negatively chargeable monomers in the polyelectrolytes. For each point in the LS-T curve five dynamic light scattering (DLS) measurements were performed. The titrations took either 3 or 60 hours, in order to probe different timescales. Prior to measurement, the pH of the sample and titrant were adjusted to within 0.1 pH unit of a chosen value with 0.1 or 1 M NaOH or HNO_3 solutions. To compare the different titrations qualitatively, the intensity of scattered light at f_-, $I(f_-)$, was normalized by the total concentration of polymer (in g/l) at f_-, $c(f_-)$.

The diffusion coefficient of the scattering objects was obtained with the cumulant method[27] and expressed as hydrodynamic radius, R_h, using the Stokes-Einstein equation.

Results and discussion

Light scattering

Effect of f_- on the stability of polyelectrolyte complexes

Mixing two oppositely charged polyelectrolytes results in polyelectrolyte complexes (PECs), at least when there is not too much salt present. Mixing a polyelectrolyte with an oppositely charged diblock copolymer (with a neutral block) also gives PECs over a wide range of mixing ratios or fractions.

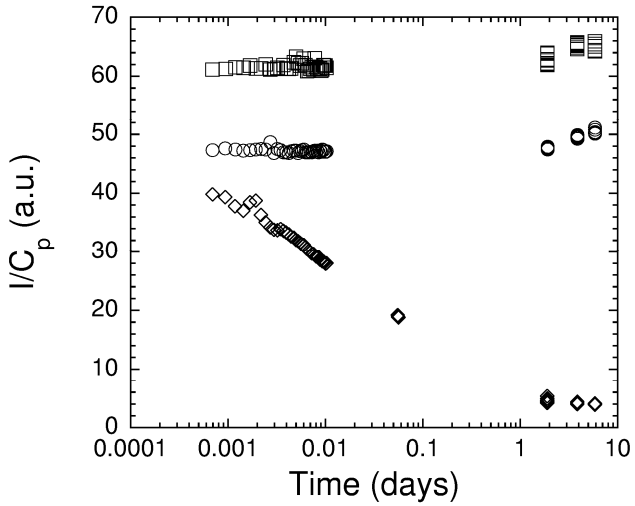

Figure 3.2: Reorganization after direct mixing of $PAETB_{49}PEO_{212}$ and PAA_{160} (both in 10 mM $NaNO_3$, pH 7) followed with light scattering. Three different mixing fractions are shown, being f_- = 0.35 (○), 0.52 (□) and 0.69 (◊), with total polymer concentrations being 1.04, 1.04 and 1.03 g/l respectively. Shown is the light scattering intensity, I, divided by the total polymer concentration, C_p, vs. time.

To investigate the effect of the mixing ratio of the polyelectrolytes on the changes of the HAPECs with time after mixing of the polyelectrolyte and a diblock copolymer, solutions containing 1 g/l $PAETB_{49}PEO_{212}$ and 1 g/l PAA_{160} were made by direct mixing (both in 10 mM $NaNO_3$, pH 7). Note that the PAETB part of the diblock copolymer is potentially hydrophobic, as it has been reported that the diblock copolymer forms micelles by itself at pH > 9[25]. Three f_- values (0.35, 0.52 and 0.69) were created, and the light scattering intensity (Fig. 3.2) and hydrodynamic radius R_h were followed with light scattering in time. Note that, for this system, the isoelectric point of the PECs is expected to be at f_- = 0.50, as the polyelectrolytes have an equal charge density at pH 7 (determined from potentiometric

titrations, data not shown). This point is called the preferred micellar composition (PMC)[5]. Interestingly, the intensity of the $f_- = 0.69$ sample decreased rapidly, whereas those of the other two samples were constant. There was no change in R_h for these aggregates in time ($R_h = 20 \pm 2$ nm). This shows that the complexes with the lowest fraction of neutral blocks and a high amount of excess charge show the fastest reorganization (i.o.w., they are unstable).

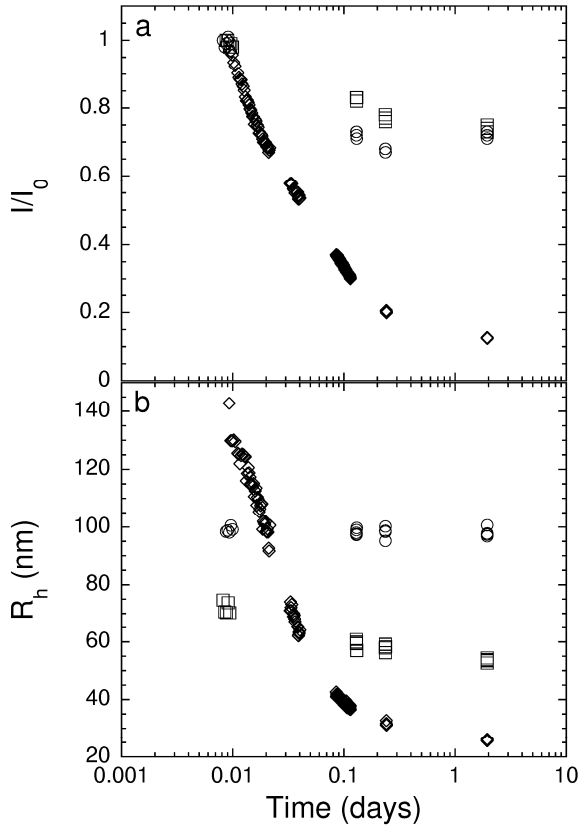

Figure 3.3: Reorganization after direct mixing of $PAETB_{49}PEO_{212}$ and PAA_{2000} (both in 10 mM $NaNO_3$, pH 7) followed with light scattering. Three different fractions are used, being $f_- = 0.32$ (□), 0.53 (○) and 0.72 (◊), with total polymer concentrations being 1.08, 1.14 and 1.27 g/l respectively. a) The normalized light scattering intensity I/I_0 vs. time and b) hydrodynamic radius R_h vs. time.

For HAPECs with a longer PAA component, PAA_{2000}, the picture is similar. Initially, HAPECs are formed that rearrange to smaller PECs (Fig. 3.3). Apparently, the stability of the PECs decreases upon deviating from the PMC as the amount of charges on the complexes increases, and with decreasing neutral block content. The latter could be due to the neutral blocks stabilizing the HAPECs, as the neutral blocks are a steric barrier that has to be overcome for rearrangements to occur. The formation of transient large aggregates upon deep

quenching (for amphiphilic micelles) has already been predicted in literature[28]. Apparently, this effect is easily reached with the complexation of a polyelectrolyte and an oppositely charged diblock copolymer.

Effect of polyelectrolyte chain length

With increasing polyelectrolyte length, the reorganization process could be slower as initially larger aggregates can be formed. Therefore, experiments with a much longer PAA, PAA_{2000}, were performed to investigate the effect of the length of the polyelectrolyte on the rate of the rearrangements (Fig. 3.3). At $f_- = 0.72$, the rearrangements of the HAPECs to smaller PECs are clearly visible as the intensity decreases with time, while for $f_- = 0.32$ and 0.53 there is a relatively small decrease in intensity. The R_h of the $f_- = 0.72$ sample decreased quickly as well, whereas for $f_- = 0.53$ is constant, and that for $f_- = 0.32$ decreases. There does not seem to be a marked decrease in the total time needed to reach a stable state however, as both for the short and long PAA, the decreases in I/I_0 are equally slow.

Effect of the concentration

In kinetics, the effect of the concentration of the 'reacting' species is of special interest. In the case of HAPECs, investigating the effect of concentration on the rate of rearrangements may help to distinguish between inter- and intracomplex processes. Rearrangements can be due to either reordering of the polycation and polyanion within a single complex, or due to two HAPECs colliding and exchanging material. Alternatively, single-chain diffusion may play a role, but at low salt concentration this does not seem very likely. Three different concentrations of HAPECs at $f_- = 0.69$ were created by direct mixing of 1 g/l $PAETB_{49}PEO_{212}$ with 10 g/l, 1 g/l, and 0.1 g/l PAA_{160} (all at pH 7 and in 10 mM $NaNO_3$) and their light scattering intensity was followed in time (Fig. 3.4). As the complexes obtained initially seem to be of equal size ($R_h = 18 \pm 1$ nm) and the intensity (not shown) is proportional to the concentration, it seems that the initial situation is largely independent of the polymer concentration. From the change in the normalized intensity with time, we can see that with increasing total polymer concentration, the reorganization of the HAPECs is faster. Note that the pH of the three different concentrations is slightly different, which might be a reason for the increased speed of rearrangements. However, upon increasing bulk pH from 7.2 to 7.8, the excess negative charge on the $f_- = 0.69$ complexes actually decreases (as H^+ is taken up by the HAPECs, the charge becomes less negative). This decrease in excess charge, if it has any

measurable effect at all, will probably decrease the rate of rearrangements. Hence, we conclude that the rate of rearrangement increases with increasing polymer concentration.

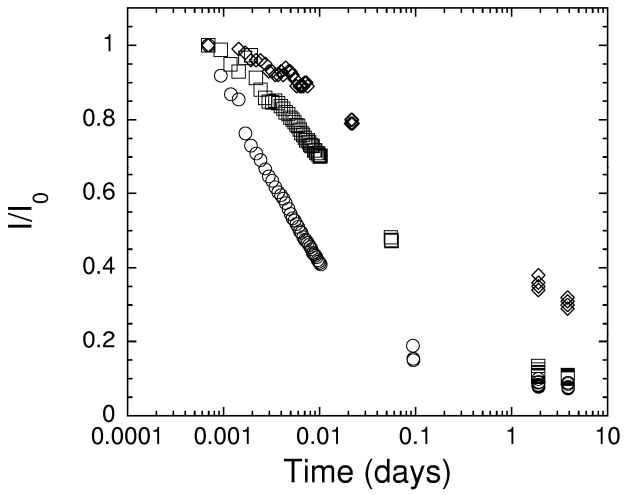

Figure 3.4**:** Reorganization after direct mixing of $PAETB_{49}PEO_{212}$ and PAA_{160} (both in 10 mM $NaNO_3$, pH 7.0 followed with light scattering. Three different concentrations of $f_- = 0.69$, with total polymer concentrations being 0.26 g/l (◊), 1.03 (□) and 1.45 (○) respectively. Shown is the normalized light scattering intensity, I/I_0 vs. time.

Effect of pH variation

As the radii and intensities of the samples created with direct mixing decrease in time (or are constant but rather large, considering the small size of the used polymers), the question arises as to whether the (HA)PECs obtained by direct mixing are in the metastable or stable state. In order to allow a more controlled complexation to occur, pH cycles of mixtures of 1 g/l $PAETB_{49}PEO_{212}$ and 2.3 g/l PAA_{160} (both in 1 mM $NaNO_3$) at $f_- = 0.52$ were performed. The pH`s of the polymer solutions before mixing of the two polymer species were however, **not** adjusted prior to mixing. Initially (top left, figure 3.5), increasing the pH leads to a fast decrease in intensity and R_h. At pH 6 this changes to a slow decrease in intensity and R_h. Note that the HAPECs formed here, during the first pH sweep upwards around pH 7, are far (in R_h) from expected for these kind of small polymers. Normally, upon mixing of similar polymers with matched pH`s, C3Ms with a R_h of about 20 nm are obtained[5,7,8,29,30] instead of the 100 nm obtained here.

From pH 9 up to 11.3 the decrease in intensity and R_h is again fast, reaching a minimum of about 12 kHz and 13 nm, respectively. At this point the initial aggregates have been

completely broken down, as the $PAETB_{49}PEO_{212}$ is fully uncharged at this pH (potentiometric titrations show that it is uncharged at pH 10 in 10 mM $NaNO_3$, data not shown) and the PAA is completely charged[29]. Decreasing the pH from this point on to pH 2.7 (arrow 2), gives formation of PECs as the charge density on PAETB increases. It seems that in the pH range 6-9 stable micelles in equilibrium are obtained, as there is only little hysteresis upon increasing the pH from 2.7 to 11 again (arrow 3). The stability of the intensity (around 40 kHz) and R_h (around 15 nm) in the pH 5-9 range for the second and third pH shift, show that rearrangements are either very slow or absent when there is no excess charge on the complexes.

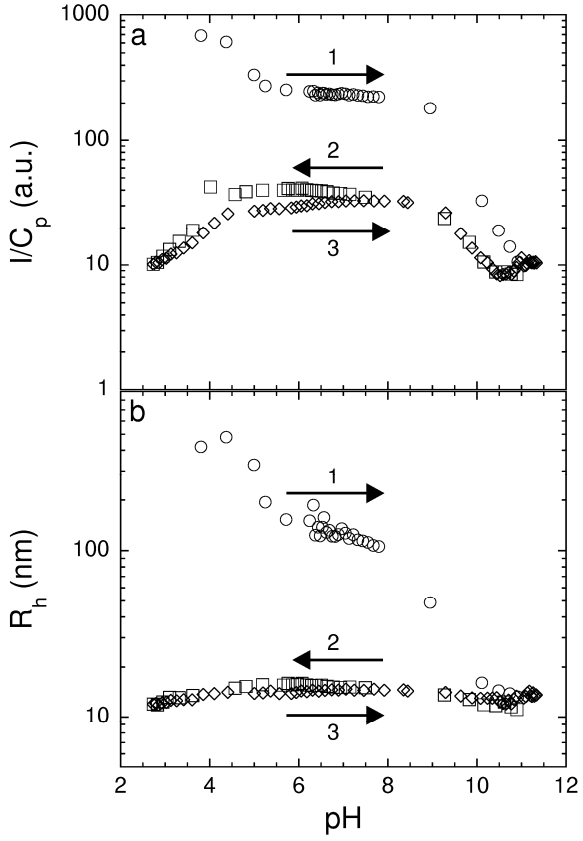

Figure 3.5: pH cycle of a mixture 1 g/l $PAETB_{49}PEO_{212}$ and 2.3 g/l PAA_{160} (1 mM $NaNO_3$), mixed such that f_- = 0.52. The pH`s of the polymer solutions were **not** adjusted prior to mixing. a) The light scattering intensity, I, divided by the total polymer concentration, C_p vs. pH and b) R_h vs. pH. The arrows in a) and b) show the direction of the pH shift due to addition of 0.1 M HNO_3 / 0.1 M NaOH – being up (○, arrow 1), down (□, arrow 2) and up (◊, arrow 3). The ionic strength increase due to acid/base addition was about 12 mM.

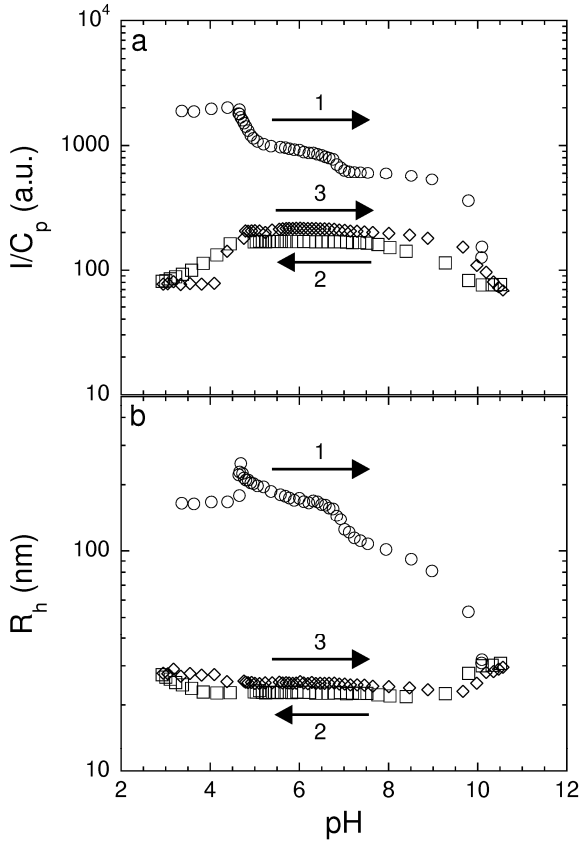

Figure 3.6: pH cycle of a mixture 1 g/l $PAETB_{49}PEO_{212}$ and 2.3 g/l PAA_{2000} (10 mM $NaNO_3$), mixed such that f_- = 0.50. The pH`s of the polymer solutions were **not** adjusted prior to mixing. a) The light scattering intensity, I, divided by the total polymer concentration, C_p vs. pH and b) R_h vs. pH. The arrows in a) and b) show the direction of the pH shift due to addition of 0.1 M HNO_3 / 0.1 M NaOH – being up (○, arrow 1), down (□, arrow 2) and up (◊, arrow 3). The ionic strength increase due to acid/base addition was about 12 mM.

For the aggregates from $PAETB_{49}PEO_{212}$ + PAA_{2000}, a pH cycle shows a picture (Fig. 3.6) highly similar to the one just discussed (Fig. 3.5). Initially, HAPECs with high scattering intensity and size are formed, which decrease in size and intensity with increasing pH up to 11. Decreasing the pH gives an increase in intensity, but a slight decrease in R_h down to about 24 nm. This shows that the HAPECs obtained by direct mixing (Fig. 3.3) can be considered to be metastable on the timescale probed, as their R_h is constant and a factor 4 higher (approximately 100 nm) than the small C3Ms formed in a pH cycle. Also, one would expect the most favourable distribution (minimum free energy) to be the one with a maximum number of C3Ms, with a corresponding small R_h.

Stability effects in Light Scattering Titrations

Several articles have been published in which light scattering titrations (LS-Ts) were employed as the main method to investigate the formation of C3Ms[5,8,15,17,25,29]. Note that LS-Ts for polymeric systems have been discussed in great detail elsewhere[5,8,25] and the general picture is similar for various other systems employing proteins[31,32] or nanoparticles[16] as 'polyelectrolyte'. However, the effect of the total duration time of these titrations may have played a role in the observed phenomena, especially when the reorganization towards the stable state is slow. Two titrations at different speeds were performed to investigate the effect of time on LS-Ts of 1 g/l $PAETB_{49}PEO_{212}$ with a short PAA (Fig. 3.7). In the intensity vs. f_- plot there are clear similarities, but also differences: the intensity increases with increasing f_- (starting from 0) in both plots, until f_- is approximately 0.5. From there on the intensity decreases, but it decreases much more steeply in the 60 hrs titration (Fig. 3.7d). The R_h in the 3 hrs titration (Fig. 3.7b) is nearly constant, around 25 nm, whereas the R_h varies more in the 60 hrs titration (Fig. 3.7e). Most interesting however, is the difference in the normalized change in intensity vs. f_- (Fig. 3.7c and 3.7f), as this gives information on the stability of the complexes as a function of f_- over a large part (about 75%) of the possible range. The changes for the 3 hrs titration are around zero, while for the 60 hrs titration it is clear that at $f_- > 0.53$ the intensity drops significantly with time. There are two pronounced maxima in the normalized change in intensity vs. $f_- > 0.5$; one at $f_- = 0.54$ and one at 0.70. Why this occurs is not clear, but perhaps the first maximum is connected to dissociation of C3Ms and the second to dissociation of soluble complex particles (SCPs, as defined previously[5,8]) as these two types of particles are expected to fall apart and appear as a function of f_-. At $f_- < 0.5$ there seems to be no change in intensity, even at this timescale. Part of the differences between the 3 and 60 hours titration may be due to the difference in salt concentration, being 1 and 10 mM $NaNO_3$ respectively.

Again, the same overall picture is obtained in comparing a 3 hours and 60 hours titration of $PAETB_{49}PEO_{212}$ with PAA_{2000} (all solution in 10 mM $NaNO_3$, pH 7, figure 3.8). The intensity vs. f_- plots (Fig. 3.8a) shows the same pattern, being slightly lower in intensity for the 60 hrs titration. Given that rearrangement to smaller particles occurs over the course of time, and the light scattering intensity is mainly dependent on the size of the scattering object, also a slightly lower R_h is obtained for the 60 hrs titration. As with the shorter PAA, the normalized change in the intensity is zero for $f_- = 0.50$. Around $f_- = 0.6$ change in the intensity with time is fastest and most clearly visible, while at low f_- there is also a clear (but slower) decrease in intensity with time.

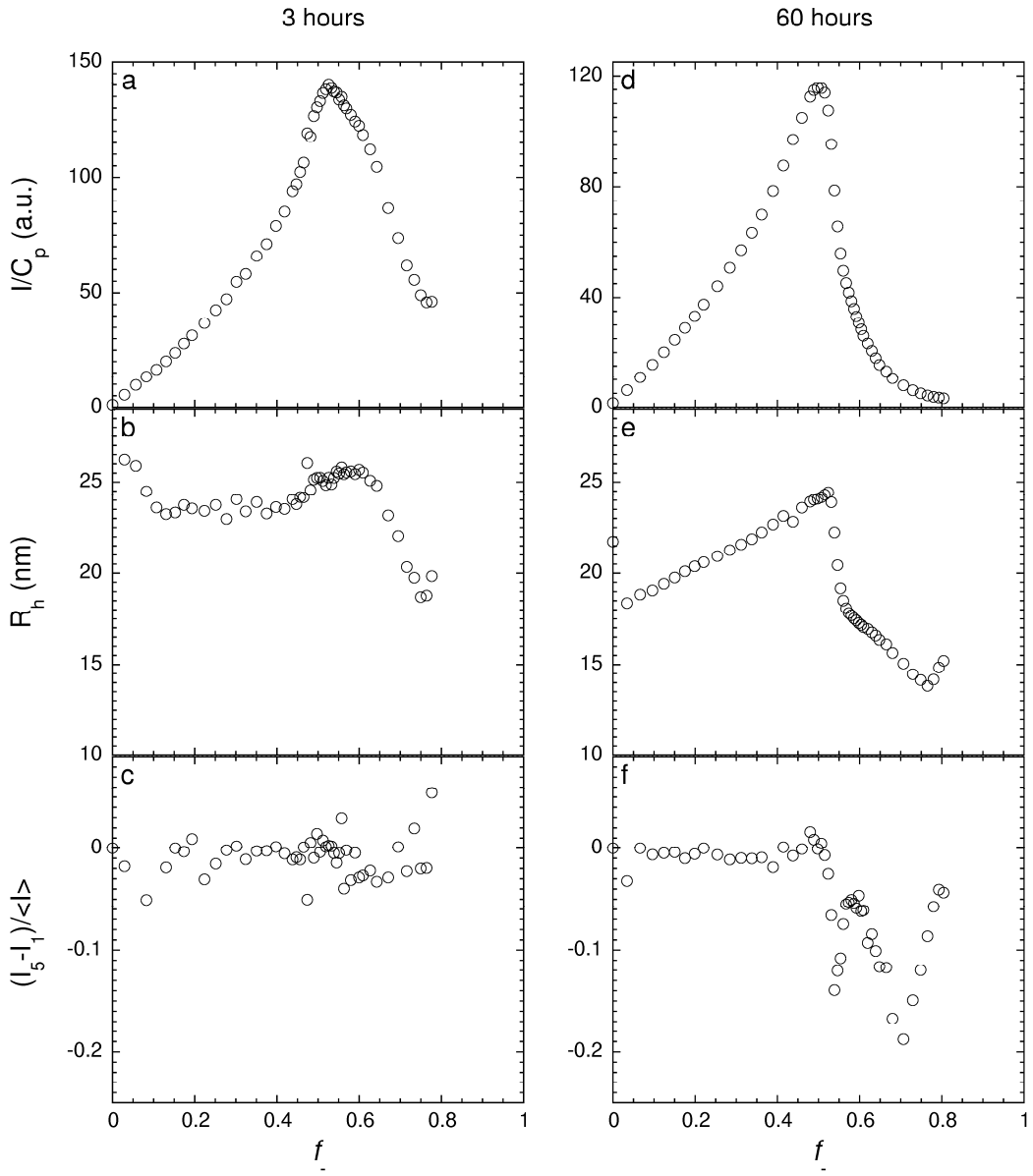

Figure 3.7: a,b,c) LS-T of 1 g/l $PAETB_{49}PEO_{212}$ with 2.3 g/l PAA_{160}, both in 1 mM $NaNO_3$, pH 7.1. Total titration time is approximately 3 hrs. d,e,f) LS-T of 1 g/l $PAETB_{49}PEO_{212}$ with 2.3 g/l PAA_{140}, both in 10 mM $NaNO_3$, pH 7.1. Total titration time is approximately 60 hrs. Shown are the light scattering intensity, I, divided by the total polymer concentration, C_p, the R_h and the normalized change in the intensity vs. f_-. Per point in the graphs a) and d), five LS measurements, I_1,I_2,..I_5, were made of which the average intensity, $\langle I \rangle$, is shown. The normalized change in the intensity is calculated per titration point as $(I_5-I_1)/\langle I \rangle$, where I_5 and I_1 are the fifth and first intensity measured, of the displayed average $\langle I \rangle$ of 5. The pH-variations (always within 2 pH units, with a minimum of 6.1 and a maximum of 8.5, data not shown) only have a very minor influence on the results.

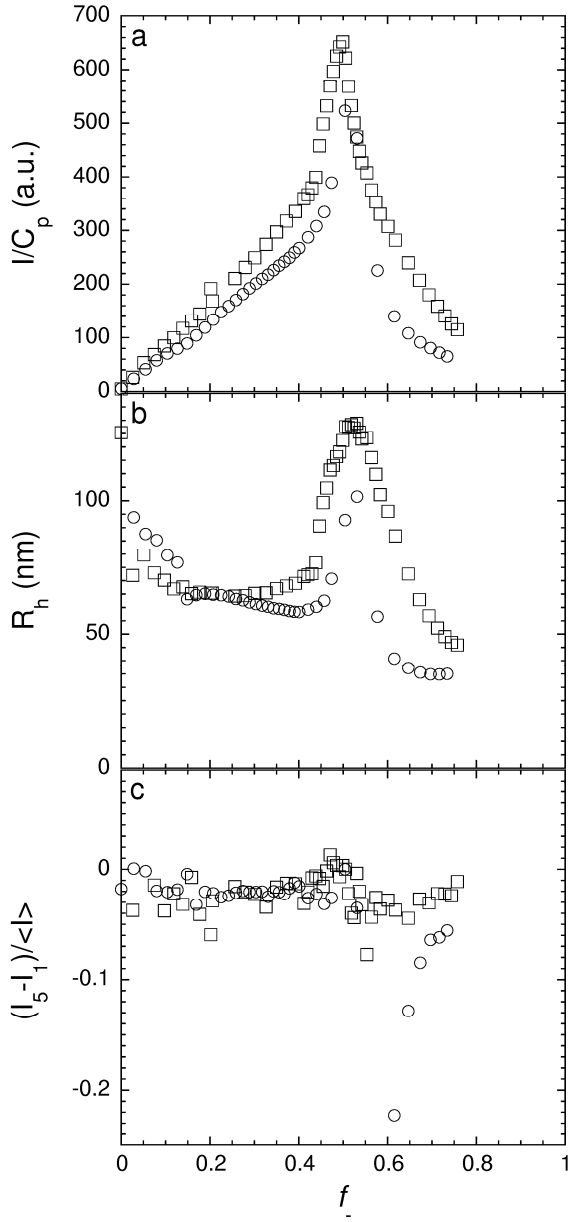

Figure 3.8: a,b,c) LS-T of 1 g/l $PAETB_{49}PEO_{212}$ with 2.3 g/l PAA_{2000}, both in 10 mM $NaNO_3$, pH 7. Total titration time is approximately 3 hrs (□) or 60 hrs (○). Shown are the light scattering intensity, I, divided by the total polymer concentration, C_p, the R_h and the normalized change in the intensity vs. f_-. Per point in the graph a) five LS measurements, I_1,I_2,..I_5, were made of which the average intensity, $\langle I \rangle$, is shown. The normalized change in the intensity is calculated per titration point as $(I_5-I_1)/\langle I \rangle$, where I_5 and I_1 are the fifth and first intensity measured, of the displayed average $\langle I \rangle$ of 5. The pH-variations (always within 1 pH unit, with a minimum of 6.6 and a maximum of 7.7, data not shown) only have a very minor influence on the results.

To determine whether equilibrium is reached in the LS-Ts, one can compare the radii obtained to those obtained via pH cycles. The R_h obtained at f_- =0.50 with LS-Ts (Fig. 3.7 and 3.8) is about 25 nm for the HAPECs with a short PAA, while it is about 110 nm for the longer PAA_{2000}. The R_h obtained via pH cycles (Fig. 3.5 and 3.6) however, are clearly smaller –15 and 24 nm respectively. This shows that metastable states are obtained with LS-Ts, as was found to be the case for direct mixing.

Factors influencing stability

This brings us to stress the following factors for rearrangements in polyelectrolyte complexes comprising a diblock copolymer with a charged and a neutral block. Four factors influence the stability of (HA)PECs, namely (i) salt, the addition of which has been shown to enhance the rate of rearrangements by a factor of 10^4 [24], (ii) high diblock copolymer content, since a larger fraction of neutral chains increases the stability by hampering reordering (Fig. 3.2, 3.3, 3.7 and 3.8), (iii) excess charge; around the PMC there is no excess charge and hence the complexes are very stable, whereas deviating from f_- = 0.5 increases the net charge of the complexes and thus increases the rearrangement rate (Fig. 3.2, 3.3, 3.7 and 3.8), (iv) the chemistry of the polyelectrolytes, as the more hydrophobic backbones used in this study give rise to very slow rates of rearrangements.

Cryo-TEM

To visualize the difference between the initial stage of complexation (i.o.w. HAPECs) and a situation close to the stable state (i.o.w. PECs), cryo-TEM images were obtained of mixtures of $PAETB_{49}PEO_{212}$ and PAA_{2000} in 10 mM $NaNO_3$ with f_- = 0.69. For one sample, two stock solutions of the oppositely charged polymers were mixed 30 s before vitrification and imaged (Fig. 3.9a). A second sample, mixed 30 days earlier was also vitrified and imaged (Fig. 3.9b). The differences between the two samples are clear: initially, transient large networks are formed which appear to rearrange to smaller, more spherical particles. It seems that the cores which rearrange into smaller particles are already present in the initial stage. The average diameter of the smaller objects after 30 days is 16 ± 4 nm, while the average distance between them is about 25 ± 6 nm. This is in good agreement with the R_h obtained with light scattering after 30 days (23 nm, data not shown). The transient large aggregates found here have already been predicted in literature for quenching of micelles composed of amphiphilic components[28] and observed experimentally[23]. However, for micelles composed of amphiphilic molecules, the first step of association is intramolecular compaction of the

hydrophobic component. Then, rearrangement to micelles takes place by association of multiple amphiphiles. For the formation of HAPECs the quenching depends on two oppositely charged polyelectrolytes meeting in solution. Thus, the initial complexes formed here are more network-like, as no initial intramolecular compaction occurs.

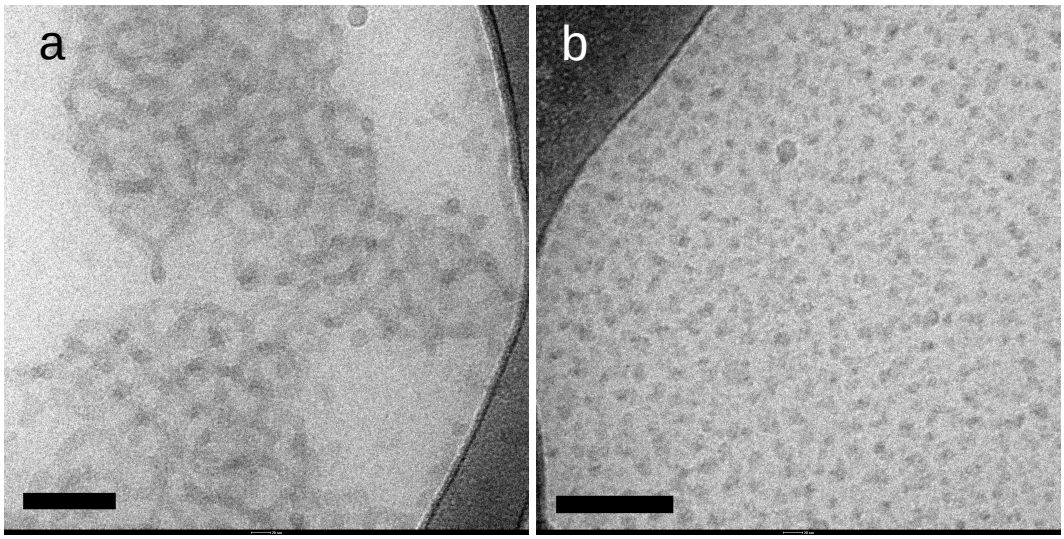

Figure 3.9: Cryo-TEM images a) $PAETB_{49}PEO_{212}$ + PAA_{2000}, f_- = 0.69, 10 mM $NaNO_3$, vitrified 30 s after mixing of $PAETB_{49}PEO_{212}$ (10 mM $NaNO_3$, pH 7) and PAA_{2000} (10 mM $NaNO_3$, pH 7) solutions. Bar is 100 nm. b) $PAETB_{49}PEO_{212}$ + PAA_{2000}, f_- = 0.69, 10 mM $NaNO_3$, vitrified 30 days after mixing of $PAETB_{49}PEO_{212}$ (10 mM $NaNO_3$, pH 7) and PAA_{2000} (10 mM $NaNO_3$, pH 7) solutions. Bar represents 100 nm.

Conclusions

Light scattering and Cryo-TEM show that upon mixing $PAETB_{49}PEO_{212}$ with PAA (at fixed pH around 7), polyelectrolyte complexes are obtained which are either metastable or unstable, on the time scales investigated. Initially, large clusters – named HAPECs – are obtained which eventually rearrange into small presumably micellar particles. Light scattering and Light Scattering Titrations show that with increasing deviation from the PMC, the rate of the rearrangement process increases, as is also the case with decreasing neutral polymer content. The light scattering intensity and R_h of complexes of $PAETB_{49}PEO_{212}$ with PAA around f_- = 0.5 are constant in time, but a pH cycle can show whether the obtained complexes are in a metastable or in a stable state.

Finally, it is shown that mixing of oppositely charged polyelectrolyte solutions whose pH values are not matched and increasing the chain length of the longest polyelectrolyte, increases the differences between the metastable and the stable states.

Literature

(1) Bungenberg de Jong, H. G. In *Colloid Science*; Kruyt, H. R., Ed.; Elsevier: Amsterdam, 1949; Vol. II.
(2) Izumrudov, V. A.; Lim, S. K. *Vysokomolekulyarnye Soedineniya Seriya A & Seriya B* **1998**, *40*, 459.
(3) Pergushov, D. V.; Izumrudov, V. A.; Zezin, A. B.; Kabanov, V. A. *Vysokomolekulyarnye Soedineniya Seriya A & Seriya B* **1993**, *35*, A844.
(4) Pergushov, D. V.; Izumrudov, V. A.; Zezin, A. B.; Kabanov, V. A. *Vysokomolekulyarnye Soedineniya Seriya A & Seriya B* **1995**, *37*, 1739.
(5) van der Burgh, S.; de Keizer, A.; Cohen Stuart, M. A. *Langmuir* **2004**, *20*, 1073.
(6) Gohy, J.-F.; Varshney, S. K.; Jerome, R. *Macromolecules* **2001**, *34*, 3361.
(7) Harada, A.; Kataoka, K. *Macromolecules* **1995**, *28*, 5294.
(8) Hofs, B.; Voets, I. K.; de Keizer, A.; Cohen Stuart, M. A. *Physical Chemistry Chemical Physics* **2006**, *8*, 4242.
(9) Kabanov, A. V.; Bronich, T. K.; Kabanov, V. A.; Yu, K.; Eisenberg, A. *Macromolecules* **1996**, *29*, 6797.
(10) Voets, I. K.; de Keizer, A.; de Waard, P.; Frederik, P. M.; Bomans, P. H. H.; Schmalz, H.; Walther, A.; King, S. M.; Leermakers, F. A. M.; Cohen Stuart, M. A. *Angewandte Chemie-International Edition* **2006**, *45*, 6673.
(11) Cohen Stuart, M. A.; Hofs, B.; Voets, I. K.; de Keizer, A. *Current Opinion in Colloid & Interface Science* **2005**, *10*, 30.
(12) Doublier, J. L.; Garnier, C.; Renard, D.; Sanchez, C. *Current Opinion in Colloid & Interface Science* **2000**, *5*, 202.
(13) de Kruif, C. G.; Weinbreck, F.; de Vries, R. *Current Opinion in Colloid & Interface Science* **2004**, *9*, 340.
(14) Turgeon, S. L.; Beaulieu, M.; Schmitt, C.; Sanchez, C. *Current Opinion in Colloid & Interface Science* **2003**, *8*, 401.
(15) Lindhoud, S.; de Vries, R.; Norde, W.; Cohen Stuart, M. A. *Biomacromolecules* **2007**, *8*, 2219.
(16) Berret, J. F.; Schonbeck, N.; Gazeau, F.; El Kharrat, D.; Sandre, O.; Vacher, A.; Airiau, M. *Journal of the American Chemical Society* **2006**, *128*, 1755.
(17) Yan, Y.; Besseling, N. A. M.; de Keizer, A.; Marcelis, A. T. M.; Drechsler, M.; Cohen Stuart, M. A. *Angewandte Chemie International Edition* **2007**, *46*, 1807.
(18) Kabanov, A. V.; Kabanov, V. A. *Advanced Drug Delivery Reviews* **1998**, *30*, 49.
(19) Bakeev, K. N.; Izumrudov, V. A.; Kuchanov, S. I.; Zezin, A. B.; Kabanov, V. A. *Macromolecules* **1992**, *25*, 4249.
(20) Izumrudov, V. A.; Bronich, T. K.; Zezin, A. B.; Kabanov, V. A. *Journal of Polymer Science Part C-Polymer Letters* **1985**, *23*, 439.
(21) Okubo, T.; Hongyo, K.; Enokida, A. *Journal of the Chemical Society-Faraday Transactions I* **1984**, *80*, 2087.
(22) Pogodina, N. V.; Tsvetkov, N. V. *Macromolecules* **1997**, *30*, 4897.
(23) Zintchenko, A.; Rother, G.; Dautzenberg, H. *Langmuir* **2003**, *19*, 2507.
(24) Cohen Stuart, M. A.; Besseling, N. A. M.; Fokkink, R. G. *Langmuir* **1998**, *14*, 6846.
(25) Voets, I. K.; de Keizer, A.; Cohen Stuart, M. A.; Justynska, J.; Schlaad, H. *Macromolecules* **2007**, *40*, 2158.
(26) Justynska, J.; Hordyjewicz, Z.; Schlaad, H. *Polymer* **2005**, *46*, 12057.

(27) Koppel, D. E. *Journal of Chemical Physics* **1972**, *57*, 4814.
(28) Besseling, N. A. M.; Cohen Stuart, M. A. *Journal of Chemical Physics* **1999**, *110*, 5432.
(29) van der Burgh, S. Complex Coacervate Core Micelles in Solution and at Interfaces. PhD-thesis, Wageningen Universiteit, 2004.
(30) Harada, A.; Kataoka, K. *Macromolecules* **2003**, *36*, 4995.
(31) Ball, V.; Winterhalter, M.; Schwinte, P.; Lavalle, P.; Voegel, J. C.; Schaaf, P. *Journal of Physical Chemistry B* **2002**, *106*, 2357.
(32) Tsuboi, A.; Izumi, T.; Hirata, M.; Xia, J. L.; Dubin, P. L.; Kokufuta, E. *Langmuir* **1996**, *12*, 6295.

Chapter Four

Complex coacervate core micro-emulsions

Abstract

Complex coacervate core micelles form in aqueous solutions from poly(acrylic acid)-*block*-poly(acrylamide) (PAA_xPAAm_y, x and y denote degree of polymerization) and poly(*N*,*N*-dimethyl aminoethyl methacrylate) ($PDMAEMA_{150}$) around the stoichiometric charge ratio of the two components. The hydrodynamic radius, R_h, can be increased by adding oppositely charged homopolyelectrolytes, PAA_{140} and $PDMAEMA_{150}$, at stoichiometric charge ratio. Mixing the components in $NaNO_3$ gives particles in highly aggregated metastable states, whose R_h remain unchanged (less than 5% deviation) for at least 1 month. The R_h increases more strongly with increasing added oppositely charged homopolyelectrolytes than is predicted by a geometrical packing model, which relates surface and volume of the particles. Preparation in a phosphate buffer – known to weaken the electrostatic interactions between PAA and PDMAEMA – yields swollen particles called complex coacervate core micro-emulsions (C3-μEs) whose R_h increase is close to that predicted by the model. These are believed to be in the stable state (lowest free energy). A two-regime increase in R_h is observed, which is attributed to a transition from more star-like to crew-cut-like, as shown by self-consistent field calculations. Varying the length of the neutral and polyelectrolyte block in electrophoretic mobility measurements shows that for long neutral blocks ($PAA_{26}PAAm_{405}$ and $PAA_{39}PAAm_{381}$) the ζ-potential is nearly zero. For shorter neutral blocks the ζ-potential is around -10 mV. This shows that the C3-μEs have excess charge, which can be almost completely screened by long enough neutral blocks.

Published as: Hofs, B., de Keizer, A., van der Burgh, S., Leermakers, F.A.M., Cohen Stuart, M.A., Millard, P.-E. and Müller, A.H.E., Soft Matter, 2008, 4, 1473

Introduction

A micro-emulsion can be defined as a spontaneously formed thermodynamically stable sub-micron sized dispersion of liquid (or liquid crystal) in another liquid. Usually, micro-emulsions are made of oil and water, and stabilized by surfactants (often with a co-surfactant) that favor the oil-water interface[1]. Their thermodynamic stability is due to the fact that the surfactant lowers the interfacial tension to values low enough to permit translational entropy to drive – together with spontaneous curvature – the formation of the dispersed state. The question we address here is whether micro-emulsions can form when we replace the oil by a different liquid that is immiscible with water, namely complex coacervate. A complex coacervate is the polymer-rich fluid phase that can form upon mixing aqueous solutions of oppositely charged polyions[2]. In this chapter we consider a new kind of micro-emulsion consisting of complex coacervate core micelles (C3Ms), into which an extra amount of complex coacervate has been introduced. C3Ms are composed of diblock copolymers with a neutral water-soluble block and a polyelectrolyte block, and an oppositely charged homopolyelectrolyte[3-6]. Due to addition of a (charge) stoichiometric mixture of oppositely charged homopolyeletrolytes, we obtain a new kind of particle, which can be called – in analogy to conventional amphiphile-based micro-emulsions – complex coacervate core micro-emulsion (C3-μE).

One of the potential applications of C3Ms is drug delivery[7-9]. The size of these C3Ms is an important parameter, as it may influence the biodistribution, efficacy, and safety[10]. Multiple strategies can be used to control the size of complex coacervate core micelles (C3Ms, also known as polyion complexes (PICs), interpolyelectrolyte complexes (IPECs), or block ionomer complexes (BICs)[5,6,11,12]). The most obvious way is to select block copolymers with core and/or corona blocks with different lengths[12-14]; however, to increase the micellar size over a large range, rather long polymers are needed. Synthesis of well-defined block copolymers with long blocks and low polydispersity is notoriously difficult. Some complexes composed of a polyelectrolyte and a diblock copolymer obtain an increased hydrodynamic radius due to kinetic trapping of irreversibly complexing polyions[15]. Disadvantages here, are that the structure is not well-controlled and reproducibility may be low. A straightforward procedure to control the size is by mixing extra amount of anionic polyelectrolytes with diblock copolymers with an anionic block to a stoichiometric amount of cationic polyelectrolyte. The oppositely charged polyelectrolytes will form a complex coacervate and

are expected to form the cores of the C3Ms, just as the hydrophobic core of polymeric micelle is formed by the non-polar molecules[16,17].

We have studied the formation and stability of systems that are expected to be C3-μEs. The obtained sizes of the C3-μEs will be interpreted in terms of a geometrical packing model, in which the radius is related to a compositional parameter, β (defined below). C3Ms form at a preferred micellar composition (PMC)[12] when the negative charge of the diblock copolymer is fully compensated by the positive charge of the homopolymer. C3-μEs are formed by mixing anionic polyelectrolytes and diblock copolymers with a neutral and anionic block, and than adding a stoichiometric amount of cationic polyelectrolyte. The size can be controlled by the ratio of anionic polyelectrolyte and anionic-neutral diblock copolymer. The radius and the aggregation number can be related to the composition of the C3Ms in way similar to that derived earlier for C3Ms with one or two diblock copolymers[18]. The total radius, R_{total}, for C3-μEs composed of one charged diblock copolymer species and two oppositely charged polyelectrolyte species can be written as (see the appendix for the derivation):

$$R_{total} = R_{corona} + R_{core}^{0}\left(1+\frac{N_{hp}^{-}}{N_{db}^{-}}\right) = R_{corona} + R_{core}^{0}\beta \qquad (4.1)$$

Here, N_{db}^{-} and N_{hp}^{-} are the total number of anionic monomers, present in solution, namely in the charged blocks of the diblock copolymer (db) and the anionic homopolyelectrolytes (hp), respectively. The compositional parameter is defined as $\beta = 1+N_{hp}^{-}/N_{db}^{-}$. One sees that the increase in the size of the C3-μEs with added polyelectrolytes is expected to be proportional to the ratio of added free homopolyelectrolyte with respect to the polyelectrolyte in the diblock copolymers, multiplied by R_{core}^{0}, the core radius without added additional homopolyelectrolytes.

In addition to the geometrical packing model, self-consistent field (SCF) theory[19-21] will be used to mimic the experiments. So far, calculations of this type have focused on the case of amphiphiles in selective solvents (see e.g. [22] and references therein). From such a model one typically finds (consistent with the surfactant packing parameter approach) that the area per molecule in the micelle is only a weak function of the micelle geometry. More specifically, we model the molecular co-assembly that underlies the formation of C3Ms. An associative driving force is combined with a stopping force, leading to a first-order model of C3Ms. Details of this theory have been published elsewhere[23]. The thermodynamic analysis of

micelles generated in an SCF approach is based on the thermodynamics of small systems first used for micellisation problems by Hall and Pethica[24].

Materials and methods

Materials

Acrylic acid (AA), acrylamide (AAm), and other chemicals where purchased from Sigma-Aldrich at the highest available purity. AAm was purified by two recrystallizations in acetone. AA was distilled under vacuum and used freshly. The synthesis of the RAFT agent 3-benzylsulfanyl thiocarbonylsulfanyl propionic acid (BPATT) has been described elsewhere[25]. Poly(*N*,*N*-dimethyl aminoethyl methacrylate), denoted as $PDMAEMA_{150}$, the index denotes the degree of polymerization, with M_n = 23.5 kg/mol, M_w/M_n = 1.04, and poly(acrylic acid), PAA_{140}, M_n = 10.0 kg/mol, M_w/M_n = 1.15, were obtained from Polymer Source Inc. (Montreal, Canada) and used as received. For the molecular structures of the polymers, see Fig. 4.1. All salts used were of analytical grade and used as received. All solutions were prepared in deionized water (Milli-Q).

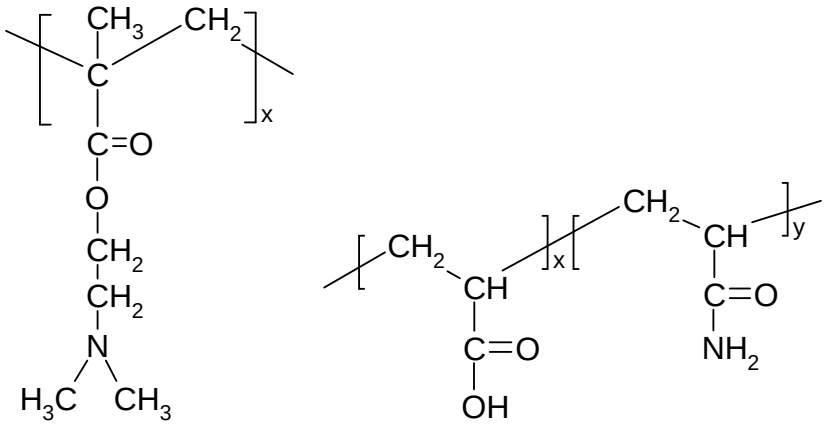

Figure 4.1: The molecular structure of $PDMAEMA_x$ (left) and PAA_x-$PAAm_y$ (right).

Methods

PAA_x and PAA_xPAAm_y (Fig. 4.1) were synthesized by RAFT polymerization in aqueous solution under γ-irradiation. The process details have been reported earlier[26]. Here the synthesis is described briefly. For PAA_x, in a round-bottom flask, AA (3 M) and BPATT (71.4 mM) are dissolved in a mixture of water/acetone 1/1. The vials were capped with rubber septa and deoxygenated by purging with nitrogen gas for 15 min. each. Then polymerization solutions were placed in an insulated room with a ^{60}Co source at ambient temperature

(typically close to 20°C) at a dose rate of 21 Gy h^{-1}. The flasks were taken after pre-selected time to obtain two different monomer conversions. The solvent mixture was removed by evaporation under vacuum followed by freeze-drying. PAA_x was purified by precipitation from an ethanol solution into a 20-fold excess of dichloromethane and dried under vacuum at 40°C before the block-copolymerizations. Degrees of polymerization were determined by ^1H NMR recorded on a Bruker Avance (250 MHz) spectrometer in D_2O by comparing the residual benzyl group of the RAFT agent to those associated with the polymer backbone. A similar procedure was carried out to obtain the different PAA_xPAAm_y. AAm (1.5 M) and the selected PAA_x macroRAFT agents (15, 7.5, and 3.75 mM respectively) were dissolved in a mixture of water/ethanol 3/2. The different solutions were sealed, degassed by nitrogen gas bubbling, and placed to receive a dose rate of 21 Gy h^{-1}. After a predetermined time flasks were removed, ethanol was evaporated under vacuum, and the residual aqueous solutions were freeze-dried. The different PAA_xPAAm_y were subsequently purified from residual monomers by 3 days of dialysis against deionized water. Degrees of polymerization of PAA_xPAAm_y were also determined by ^1H NMR in D_2O by comparing the residual benzyl group of the RAFT agent to those associated with the polymer backbone[27]. The molar mass and polydispersity index of the different polymers are listed in Table 4.1.

Polymer	x	y	M_n (kg/mol)	PDI
PAA_xPAAm_y	26	100	9.3	1.1
		200	16.4	1.2
		405	30.9	1.2
	39	97	10.0	1.2
		191	16.7	1.2
		381	30.1	1.2
PAA_x	140		10.0	1.15
$PDMAEMA_x$	150		23.5	1.04

Table 4.1: Used polymers, with number averaged molecular weight M_n and polydispersity index (PDI).

All solutions were prepared as follows: to a mixture of PAA_xPAAm_y and PAA_{140} a solution of $PDMAEMA_{150}$ was added. The polymers were dissolved to give a concentration of 3 mM positively and negatively chargeable groups. This method of creating the sample

will be referred to as 'direct mixing'. The pH was adjusted to the desired value with 0.1 M HNO_3 and/or 0.1 M NaOH, if necessary. Typically, only minor adjustments were needed (up to 1 pH unit). The phosphate buffer has an ionic strength of 10 mM, pH 7.1 (i.e. about 5 mM of phosphate ions).

Light scattering (LS) was performed at a scattering angle of 90 degrees, unless mentioned otherwise, with an argon laser operating at a wavelength of 514.5 nm with 0.20 W power as light source. The intensity autocorrelation function was determined with an ALV5000 multiple tau digital correlator. All LS measurements were performed at room temperature (around 293 K).

Light scattering titrations (LS-T) were performed with a Schott-Geräte computer controlled titration set-up, communicating with the LS computer, which allowed to control added volumes, stirring times, and pH measurement. In the pH LS-T a premixed solution containing all polymers in a glass sample cell equipped with a pH electrode, was titrated with 0.1 M NaOH or 0.1 M HNO_3.

As the C3Ms and C3-μEs are formed from oppositely charged components, the composition of the system with respect to the charged, or chargeable groups is a central parameter, and we express the charge composition as f_+, defined as

$$f_+ = 1 - f_- = \frac{[+]}{[+]+[-]} \qquad (4.2)$$

where [+] and [–] denote the total molar concentration of chargeable groups of the positively and negatively charged species forming the micellar core, respectively. Note that in C3-μEs the composition is not only determined by f_+ but also by β.

For each point in the LS-T curve five light scattering measurements were performed. Prior to measurement, the pH of the samples was adjusted to within 0.1 pH unit of a chosen value with 0.1 or 1 M NaOH or HNO_3 solutions. To compare the different titrations quantitatively, the intensity of scattered light, $I(f_-)$, was normalized by the total concentration of polymer $C_p(f_-)$ (in g/l).

The diffusion coefficient of the scattering objects was obtained with the cumulant method[28] and from which the hydrodynamic radius, R_h, was calculated using the Stokes-Einstein equation.

The electrophoretic mobility of the particles was determined with a Zetasizer 2000 (Malvern Instruments) with an attached PC running the accompanying software (PCS v1.51), operating at 25 °C with a 15 mW laser operating at a wavelength of 635 nm. The ζ-potential

of the particles was calculated from the electrophoretic mobility with the Smoluchowski equation.

Results and discussion

Effect of block copolymer architecture on C3Ms

Before discussing the formation of C3-μEs, we will first discuss the formation of regular, non-swollen, C3Ms for block copolymers with varying block length at a fixed f_+ and as a function of pH. With increasing pH the charge on the PAA will increase, while the charge on the PDMAEMA will decrease. From potentiometric titrations we expect that around pH 7 both polyelectrolytes are highly charged (and to a similar degree)[29]. Thus, at pH 7 and $f_+ = 0.50$, a maximum in the light scattering intensity will be obtained. For lower values of f_+, a neutral complex will be obtained at lower pH values.

pH titrations of mixtures of PDMAEMA and PAA_xPAAm_y show the above effects (Fig. 4.2). The maximum intensity is found for $f_+ = 0.5$ at pH 7. With decreasing f_+ the maximum in light scattering intensity and R_h shifts to lower pH. The decrease in intensity and R_h with decreasing f_+ can be attributed to the lower charge of the PAA block at lower pH. Thus, less PDMAEMA is required to compensate the charges and a smaller core with correspondingly lower aggregation number results. These effects are quite pronounced for C3Ms with $PAA_{26}PAAm_{200}$ (Fig. 4.2a,b) but are much less clear for those with $PAA_{39}PAAm_{381}$ (Fig. 4.2c,d), partly because f_+ is varied over a smaller range.

The effect of pH at fixed f_+ is highly similar for all mixtures of PDMAEMA and PAA_xPAAm_y (Fig. 4.3). The maximum scattering intensity and R_h are found at pH 7 ($f_+ = 0.45$ for $PAA_{39}PAAm_y$ and $f_+ = 0.50$ for $PAA_{26}PAAm_y$). One anomaly is observed; for C3Ms with $PAA_{39}PAAm_{97}$ (Fig. 4.3c,d) there are two peaks in intensity and R_h. The origin of the peak around pH 5.5 (not shown) is unclear. However, this peak is outside the region which we will investigate for C3-μEs, therefore we did not expand our study.

Increasing the neutral block length whilst keeping the polyelectrolyte block length constant leads to larger (in terms of R_h) C3Ms (Fig. 4.3). With increasing length of the neutral block, its area at the core-corona interface increases and, according to the geometrical packing model, the core radius decreases. The larger corona blocks increase the radius, and this effect obviously dominates.

The scattering intensity (normalized by polymer concentration) changes only slightly within each diblock copolymer series, being C3Ms with $PAA_{26}PAAm_x$ or $PAA_{39}PAAm_x$ (Fig.

4.3 a,b and c,d). As the normalized scattering intensity depends mainly on the mass of the particles this indicates that although R_h increases with increasing neutral block length, the total weight of the particles remains constant, because the dense complex coacervate core becomes smaller (this view is supported by small angle neutron scattering measurements on similar C3Ms, which shows that the mass of the C3Ms is similar regardless of neutral block length[30]). C3Ms with different length of the polyelectrolyte block but similar neutral block length of the diblock copolymers show a small increase in intensity and R_h (Fig. 4.3) with increasing polyelectrolyte block length. The core size increases with increasing polyelectrolyte block length and thus larger C3Ms are obtained.

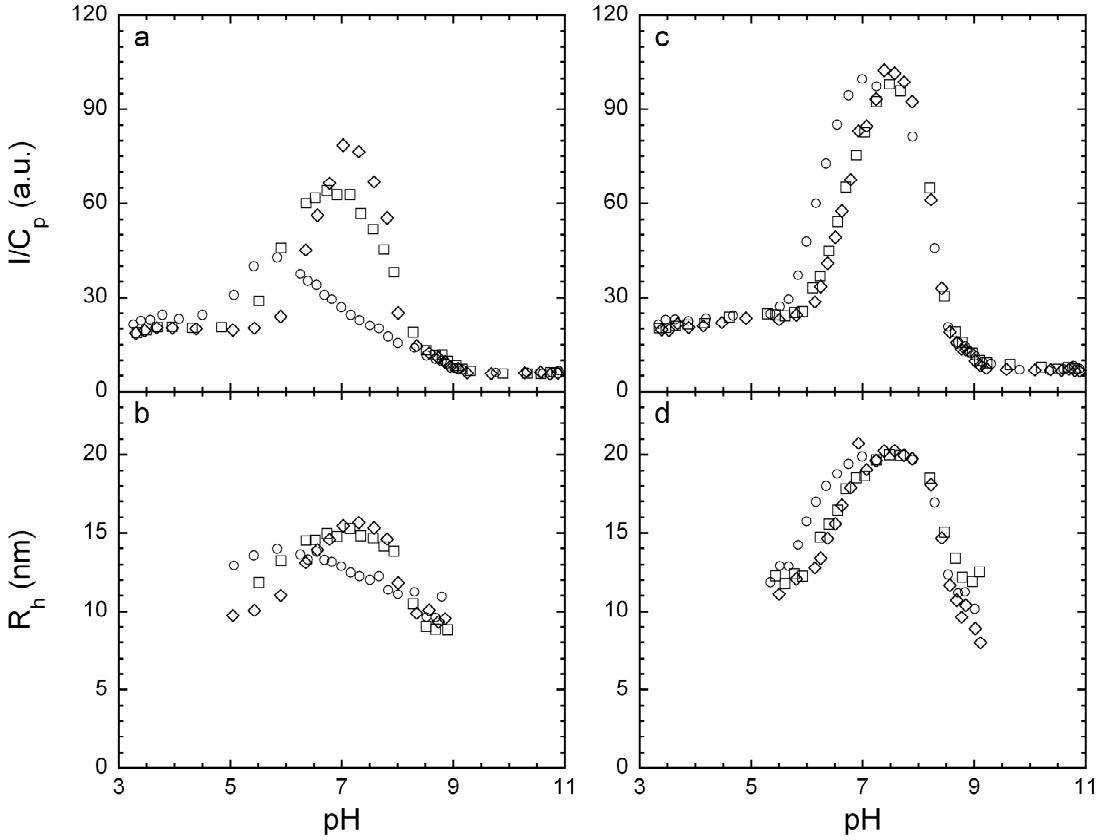

Figure 4.2: Light scattering intensity I (divided by total polymer concentration, C_p) and hydrodynamic radius R_h vs. pH for a,b) $PDMAEMA_{150}$ and $PAA_{26}PAAm_{200}$, $f_+ = 0.40$ (○), $f_+ = 0.45$ (□), and $f_+ = 0.50$ (◊), and c,d) $PDMAEMA_{150}$ and $PAA_{39}PAAm_{381}$, $f_+ = 0.45$ (○), $f_+ = 0.48$ (□) and $f_+ = 0.50$ (◊). Starting background electrolyte for all experiments: 10 mM $NaNO_3$. The solutions were titrated with 0.1 M NaOH from pH 3 to 11.

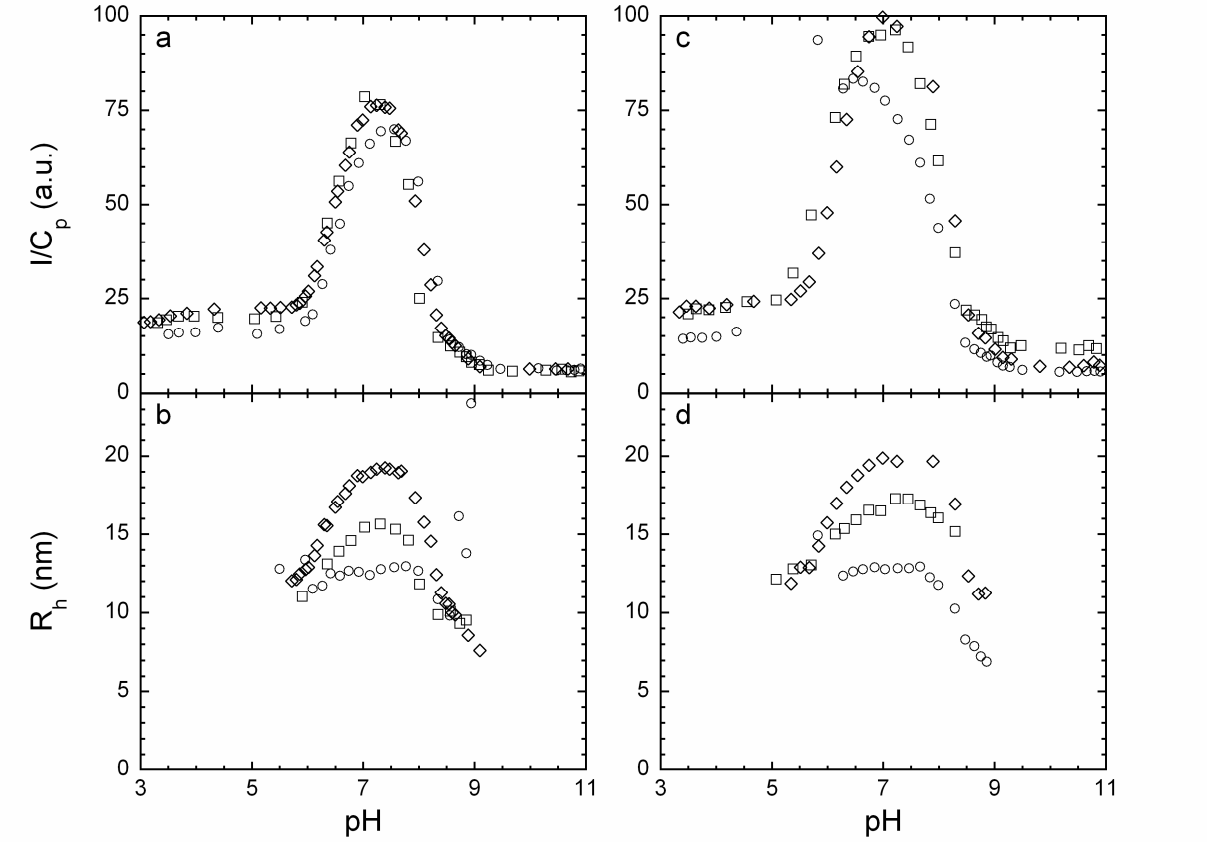

Figure 4.3: Light scattering intensity I (divided by total polymer concentration, C_p) and hydrodynamic radius R_h vs. pH of a,b) $PDMAEMA_{150}$ and $PAA_{26}PAAm_x$ at $f_+ = 0.50$, x =100 (○), x = 200 (□), and x = 405 (◊), and c,d) $PDMAEMA_{150}$ and $PAA_{39}PAAm_x$ at $f_+ = 0.45$, x = 97 (○), x = 191 (□), and x = 381 (◊). R_h measured for $PAA_{39}PAAm_{97}$ at pH 5 and 5.5 is about 200 nm, I/C_p at pH 5.5 is around 420 (not shown). Starting background electrolyte for all experiments: 10 mM $NaNO_3$. The solutions were titrated with 0.1 M NaOH from pH 3 to 11.

Formation of C3-μEs; effect of type of salt and added homopolyelectrolytes

We performed light scattering experiments to determine the increase in the hydrodynamic size and light scattering intensity with the increase in β. First, a set of experiments in 10 mM $NaNO_3$ was performed. With increasing β, both the intensity and R_h increases (Fig. 4.4); the increase is stronger for complexes with smaller neutral blocks. Analysing the results with the geometrical packing model leads to unrealistic values of R_{corona} of about -4 nm and R^0_{core} of about 25 nm. Previously, it was found that the formation of

C3Ms with longer polyelectrolytes gives rise to metastable states, so-called highly aggregated polyelectrolyte complexes (HAPECs)[15]. Here, similar non-relaxed aggregates also form when extra homopolyelectrolytes are added. Interestingly, ultra-sonication nor heating (30 minutes, 80 °C) have effect on the R_h of the non-relaxed C3-μEs (data not shown) and they are stable for at least one month (radii remain within 5% of the original values). Furthermore, pH cycling, which has previously been used to find the stable state[15], does work for C3Ms (Fig. 4.2 and 4.3) but not for the non-relaxed C3-μEs in 10 mM $NaNO_3$; the size and scattering intensity are highly path-dependent – that is, for the latter case, data collected along the first upwards, second downwards, and third upwards pH sweeps do not overlap (data not shown). As for simple C3Ms composed of the diblocks and $PDMAEMA_{150}$ in 10 mM $NaNO_3$ the stable state is easily found by applying a pH sweep, we infer that it is the added polyelectrolytes that cause the complication. Probably, the homopolyelectrolytes are able to form large networks[3,31-33] (as they have no covalently attached neutral block which can stop the growth of these networks), which – because at charge neutrality, any rearrangements in these kind of systems are very slow[15] – results in the formation of a metastable state. The mechanism behind the formation of the large networks is most probably spinodal decomposition (as upon mixing of the solutions of the polymers, the polyelectrolytes will complex everywhere in solution). As the diblock copolymers are also mixed throughout the solution and participate in the complexation, this should lead to the formation of particles with a fairly narrow size distribution (u_2/Γ^2, as determined from cumulant analysis[28], is fairly low (approximately 0.2) indicating that the size distribution is fairly narrow). Once the particles are formed, the relaxation is very slow as the randomly complexed polyelectrolytes have to either completely detach (a highly unlikely occurrence at this salt concentration) and then reattach, or a kind of reptation has to occur.

In order to form true C3-μEs (complexes in the stable state, this being the state with lowest free energy) we performed the same set of experiments in a phosphate buffer with the same ionic strength as the $NaNO_3$ solution. Phosphate ions are known to weaken the interactions between the used polyelectrolytes to a greater extent than NO_3^- ions[34,35]. This should allow for much faster relaxation. The increases in I and R_h with β are indeed much lower when phosphate buffer is used (Fig. 4.5) instead of $NaNO_3$. The difference between the highly aggregated species formed in $NaNO_3$ and the smaller species formed in phosphate buffer, is most likely caused because of this specific ionic effect. The C3-μEs formed in

phosphate buffer are probably in the stable state (lowest free energy). For an overview of the complexes obtained with different type of salt and β, see scheme 4.1.

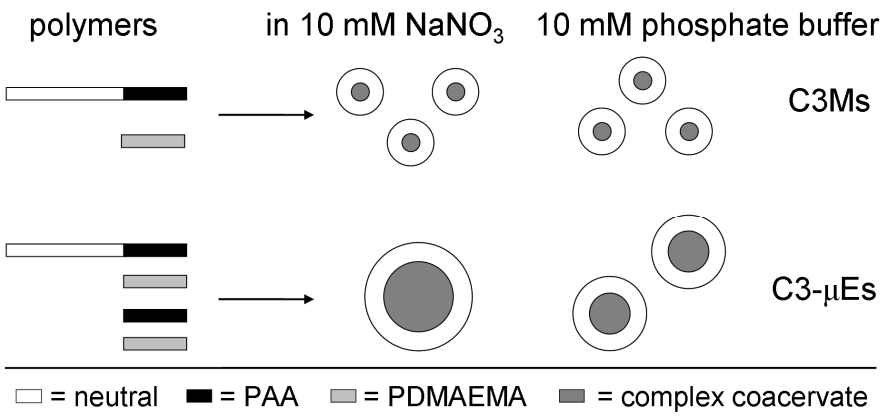

Scheme 4.1: Illustration of the formation of C3Ms and C3-μEs. If only PAA-PAAm and PDMAEMA are mixed (top), C3Ms with the same size are obtained. If a mixture of PAA-PAAm and PAA is mixed with PDMAEMA (bottom), however, in 10 mM $NaNO_3$ large, non-relaxed C3-μEs in a metastable state are obtained (middle) and in 10 mM phosphate buffer small, relaxed C3-μEs in the stable state (lowest free energy) are obtained (right). Legend shown below the full line.

For C3-μEs the experimental increase in I with increasing β can, to a first order approximation, be attributed to an increase in the particle size and mass, and the accompanying decrease in the number of particles, N, according to $I \propto Nv^2$, where v is the particle volume (Rayleigh scattering). The C3-μEs density is assumed to be constant, although it is expected to increase slightly with increasing β. At a fixed concentration, c, $c \sim Nv$, and $N \sim v^{-1}$; thus $I/c \propto R^3$. The increase in I with β is semi-quantitatively as expected for the C3-μEs with the medium and large sized neutral blocks in phosphate buffer (deviation of the thus calculated intensity increases with increasing β and goes up to a factor of 2). The intensity data can also be used to estimate the molar mass of the C3-μEs, as static light scattering measurements performed elsewhere, show that C3Ms composed of $PAA_{39}PAAm_{381}$ and $PDMAEMA_{150}$ have a micellar mass of 120 kg mol^{-1} [36]. For the corresponding C3-μEs with β = 8, I/c is 30 times that of the C3Ms. Following the analysis described above leads to a particle mass of the C3-μEs (with β = 8) of about 4×10^3 kg mol^{-1}.

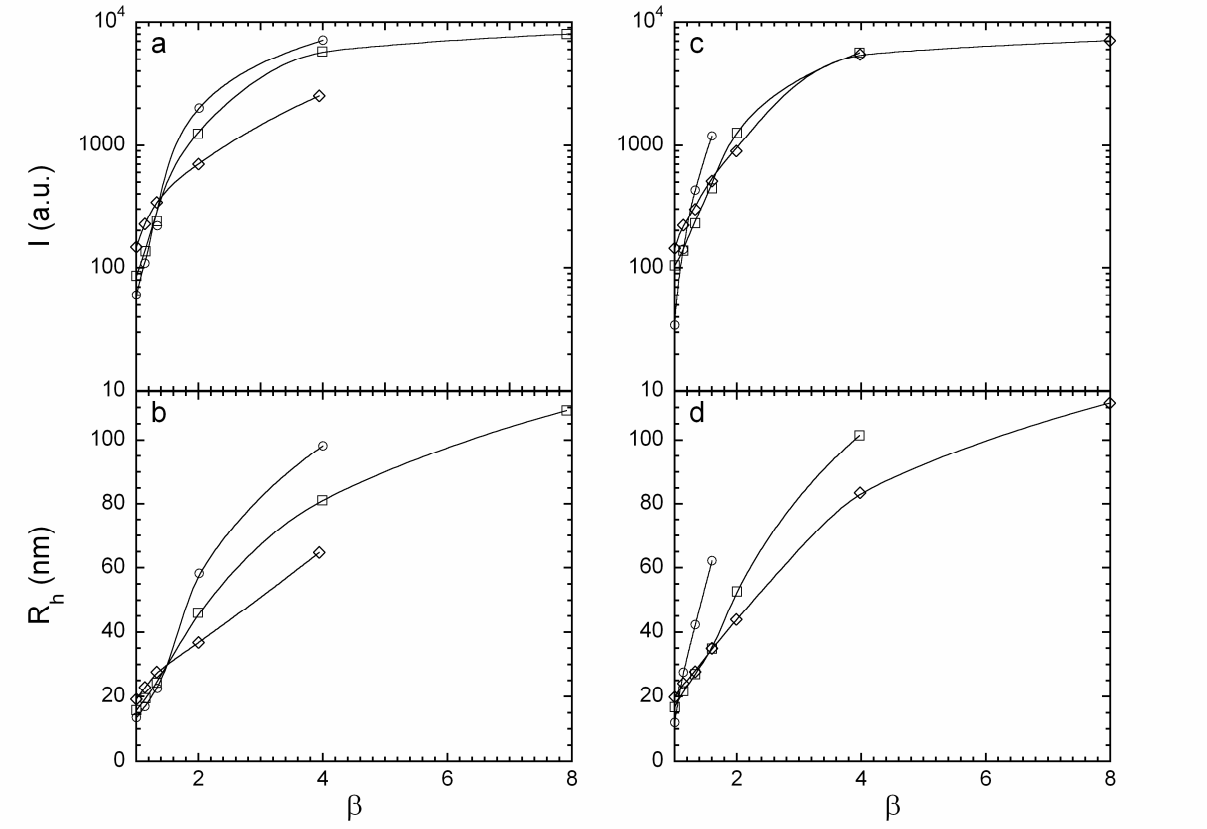

Figure 4.4: Light scattering intensity I and R_h vs. β of non-relaxed C3Ms composed of PAA_{140}, $PDMAEMA_{150}$ and PAA_xPAAm_y, a,b) at f_+ = 0.50, x-y = 26-100 (○), 26-200 (□) or 26-405 (◊), c,d) at f_+ = 0.45, x-y = 39-97 (○), 39-191 (□) or 39-381 (◊). Solvent is 10 mM $NaNO_3$, pH 7.1. Lines are to guide the eye.

The increase in R_h and I for C3-μEs with β (Fig. 4.5) is qualitatively as expected. That is, the increase in R_h and I is strongest for C3-μEs with the shortest neutral blocks and weakest for those with the longest neutral blocks. Also, the difference in increase in R_h and I between the $PAA_{26}PAAm_y$ and $PAA_{39}PAAm_y$ series (with approximately the same neutral block lengths) is as expected: the $PAA_{39}PAAm_y$ C3-μEs grow a slightly more with increasing β than the $PAA_{26}PAAm_y$, as about 1.5 times more oppositely charged homopolyelectrolytes are added to reach the same β for the former series.

For the two systems with the shortest neutral blocks, around 100 units, the micelles grow more quickly with increasing β than can be expected from the model (similar to that observed for non-relaxed C3-μEs in $NaNO_3$, resulting in negative values for R_{corona}). There are two possible explanations for this: (i) The complexes are only partly stabilized by the

neutral blocks – another stabilizing mechanism could be excess charge, however, there is little excess charge, as the mixing ratio is close to the point where there is an equal amount of negative and positive charges and this combination of factors causes the rapid growth in size with increasing β. (ii) The decrease in the size of the neutral blocks may allow the primary random complex[37] to be more network-like and larger, similar to what was seen here for the non-relaxed C3-μEs in $NaNO_3$.

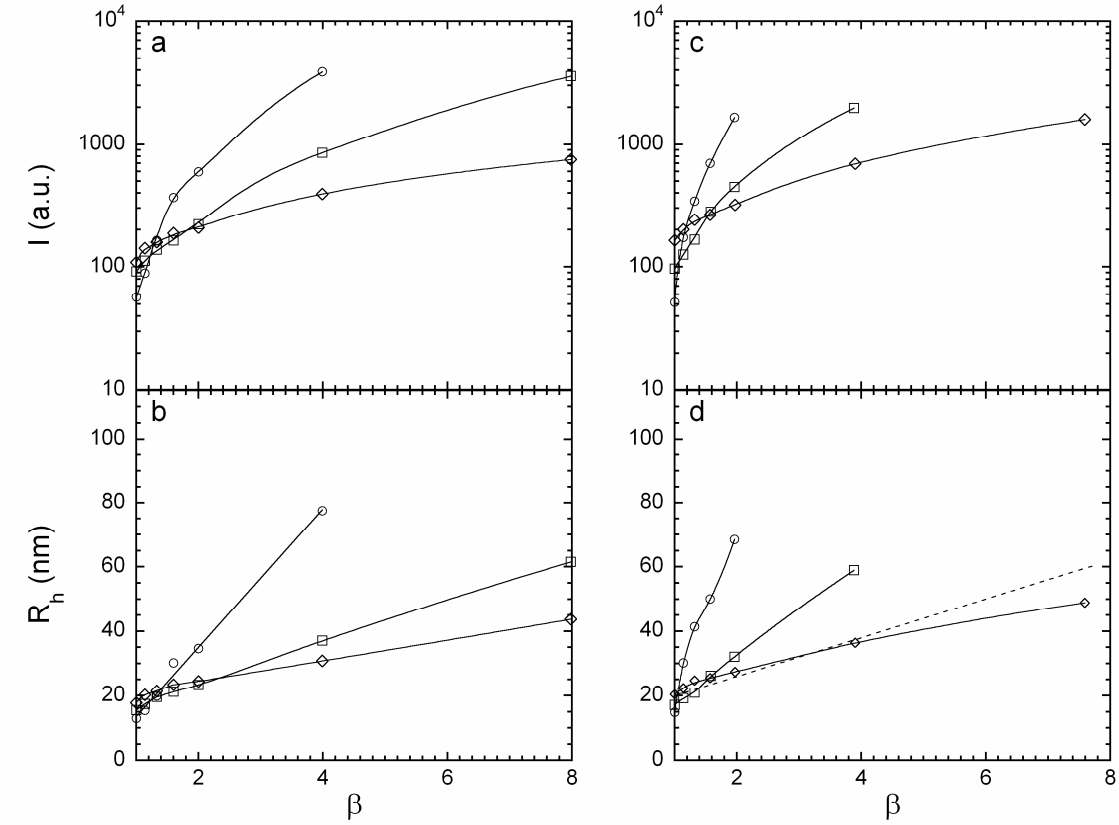

Figure 4.5: Light scattering intensity I and R_h vs. β of C3-μEs composed of PAA_{140}, $PDMAEMA_{150}$ and PAA_xPAAm_y, a,b) at f_+ = 0.50, x-y = 26-100 (○), 26-200 (□) or 26-405 (◊), c,d) at f_+ = 0.45, x-y = 39-97 (○), 39-191 (□) or 39-381 (◊). Solvent is a phosphate buffer with an ionic strength of 10 mM, pH 7.1. Lines are to guide the eye. Dashed line in d) is as described in the main text.

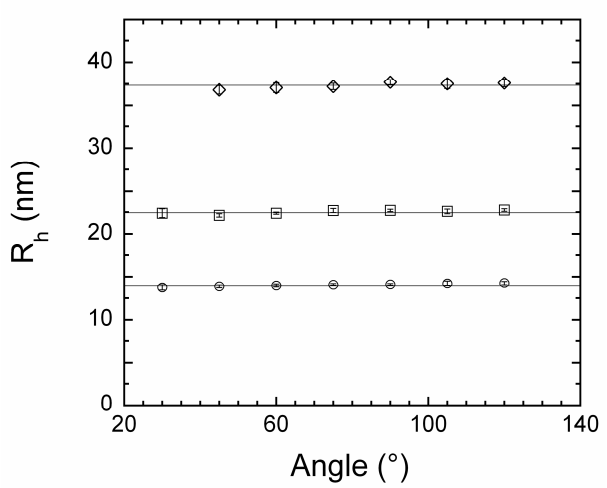

Figure 4.6: Angular dependence of R_h for C3-μEs composed of PAA_{140}, $PDMAEMA_{150}$, and $PAA_{26}PAAm_{200}$ as measured with light scattering. β = 1 (○), 2 (□), or 4 (◊), all at f_+ = 0.50 and prepared in a phosphate buffer with an ionic strength of 10 mM, pH 7.1. Average and standard deviation are shown. Lines are to guide the eye.

A growth in R_h with increasing β which is in line with expectations (geometrical packing model and literature[18], for C3-μEs with $PAA_{39}PAAm_{381}$) is shown as a dashed line in Fig. 4.5d. A R_{corona} of 14 nm and a R^0_{core} of 6 nm are assumed, as these are values close to those estimated previously for a highly similar system[18] – namely C3Ms composed of $PDMAEMA_{150}$ and $PAA_{42}PAAm_{417}$. For low β the prediction underestimates the growth and for high β the growth is overestimated. This shows that the radii obtained with increasing β are close to those expected, and that the system is probably in the stable state. Also, it shows that the model does not have enough detail to quantitatively predict the growth, as the experimental C3-μE growth curves (excluding the ones for the shortest neutral blocks discussed previously, Fig. 4.5) generally deviate from the simple linearity in R_h expected from our model. At low fractions of added polyelectrolytes ($1< \beta <1.5$) there seems to be a faster increase in R_h with β, than at higher β. The non-linear increase of R_h with β could be because of a non-linear increase in polydispersity, or changes in shape. Varying the angle in dynamic light scattering with increasing β, however, gives no dependence of R_h on the detection angle (Fig. 4.6), ruling out polydispersity changes and showing that the particles are spherical[38]. CONTIN analysis of all measurements in phosphate buffer give similar polydispersities. Generally, u_2/I^2 (as determined from cumulant analysis)[28], is fairly low (approximately 0.2) indicating that the size distribution is fairly narrow. We therefore think that changes in shape and polydispersity play only a minor role. Changes in the area a neutral block occupies at the

core corona interface, a_{db}^{-}, is another potential reason for non-linear growth. a_{db}^{-} might increase with increasing β as the radius of curvature of the core decreases with increasing size[39-41]. This effect should be most pronounced for the C3-μEs with the largest neutral block, as these have the smallest R_{core}^{0}. Indeed, the slope of the first and second part of the data (Fig. 4.4 and 4.5) differ most for the C3-μEs with the longest neutral blocks.

Interestingly, self-consistent field (SCF) calculations show non-linear behaviour (see last section), which can be attributed to a gradual transition from more star-like micelles at low β to crew-cut micelles at high β. The C3-μEs with $PAA_{39}PAAm_{191}$ seem to behave more simply; a linear fit to all data points seems to be reasonable, resulting in R_{corona} = 5 and R_{core}^{0} = 13. Here, the transition from more star-like to crew-cut is probably absent because the changes in the curvature of the core with increasing β are small.

If β is increased beyond a critical value precipitation occurs. For the C3-μEs with PAA_xPAAm_y with $y \approx 100$ precipitation occurs if β is increased from 2 to 4 and for those with $y \approx 200$ if β is increased from 4 to 8. It seems that if the ratio of the total number AA/AAm groups approaches one, the PAAm is no longer present in high enough amounts to prevent phase separation. Previously a ratio of 0.33 has been found for similar systems[12], but in that case the polyelectrolyte was part of the diblock and not free as it was here. The precipitation upon increase in β is similar to emulsification failure, which takes place with micro-emulsions if the surfactant oil-ratio becomes to low to solubilise the oil and macroscopic droplets, or even a bulk phase, appear.

Finally, C3-μEs at different values of β can be compared to C3Ms with different lengths of the charged block. Going from 26 to 39 as polyelectrolyte block length (Fig. 4.3) is similar to increasing β from 1 to 1.5 (Fig. 4.5). Comparing the increase in R_h shows, that the increase is systematically larger for the C3-μEs (about a factor of 2, note that the differences in R_h are small – 1-5 nm). The difference in conformational entropy between C3-μEs and C3Ms for a system of the same composition (in terms of the ratio of neutral and charged groups) may be responsible for the observed differences in size.

Electrophoresis

In principle both C3Ms and C3-μEs at stoichiometric ratio of the charged components, are expected to be electrically neutral particles. However, accumulation of charges may occur when the complex coacervate core is swollen with extra oppositely charged polyelectrolytes,

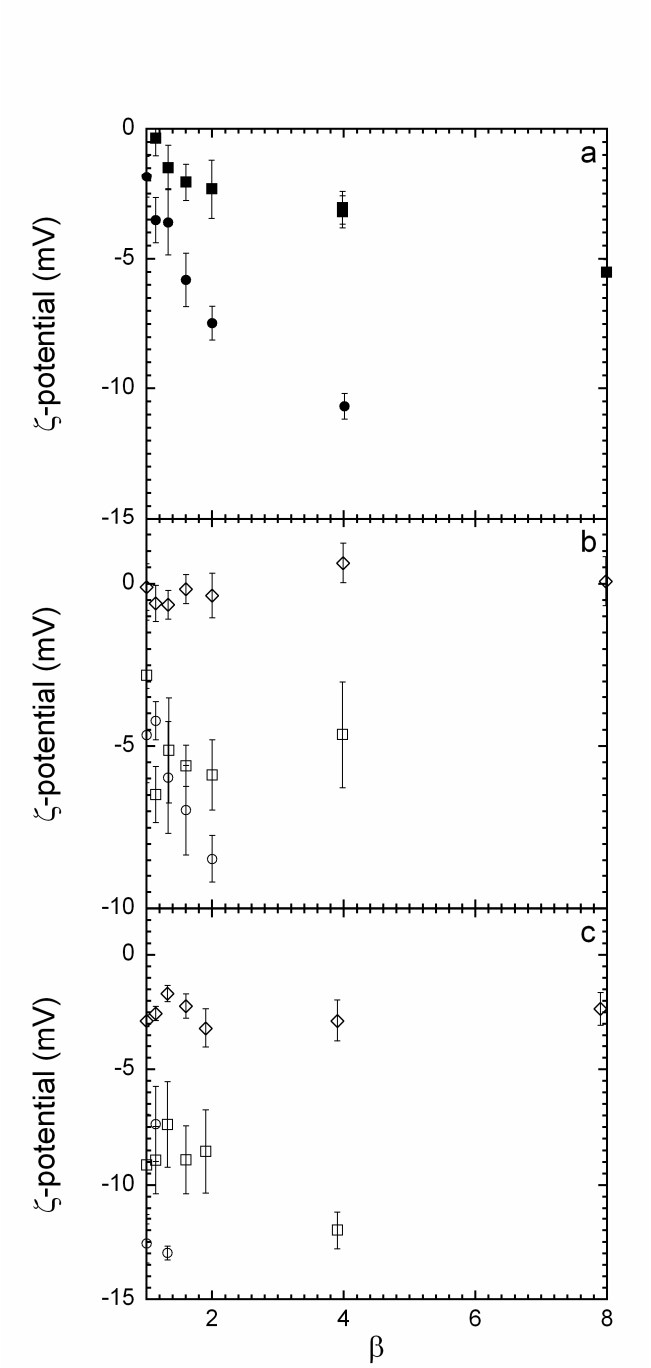

Figure 4.7: Zeta potential vs. β of non-relaxed C3Ms and C3-µEs composed of PAA_{140}, $PDMAEMA_{150}$ and a) $PAA_{26}PAAm_{200}$ (●) or $PAA_{39}PAAm_{381}$ (■), at f_+ =0.50 and 0.45 respectively, in 10 mM $NaNO_3$, pH 7.1, b) $PAA_{26}PAAm_{100}$ (○), $PAA_{26}PAAm_{200}$ (□) or $PAA_{26}PAAm_{405}$ (◊), all at f_+ = 0.50, in a phosphate buffer with an ionic strength of 10 mM, pH 7.1, c) $PAA_{39}PAAm_{97}$ (○), $PAA_{39}PAAm_{191}$ (□) or $PAA_{39}PAAm_{381}$ (◊), all at f_+ = 0.45, in a phosphate buffer with an ionic strength of 10 mM, pH 7.1.

especially if they are not added in stoichiometric amounts. A way to help determine if this happens for non-relaxed C3-μEs and relaxed C3-μEs is by measuring the electrophoretic mobility. If the core has excess charge, it is very likely to show up as a ζ-potential; the neutral PAAm of the corona will reduce the 'bare' value due to screening.

For non-relaxed C3-μEs the ζ-potential is negative (Fig. 4.7a) and the absolute value increases with increasing β and decreasing neutral block length. C3-μEs with short and medium length neutral blocks ($PAAm_y$, y = 91, 100, 191, or 200) show a more negative potential with shorter neutral blocks (Fig. 4.7). For long neutral blocks ($PAAm_y$, y = 381 or 405), the ζ-potential is close to 0 and remains constant with increasing β (Fig. 4.7); the long neutral blocks almost completely screen the small excess charge of the complex coacervate core.

The fact that the ζ-potential for most of the non-relaxed C3-μEs and relaxed C3-μEs is negative might be interpreted as evidence for being at a f_+ which is below the PMC. However, C3Ms with $PAA_{39}PAAm_{97}$ or C3-μEs with $PAA_{39}PAAm_{191}$, prepared at f_+ = 0.50 in phosphate buffer with an ionic strength of 10 mM, pH 7.1, have a ζ-potential of -10 mV, not significantly different from those at f_+ = 0.45. The ζ-potential of C3-μEs with $PAA_{39}PAAm_{191}$ only becomes $\geq$ 0 around f_+ = 0.55, which is just outside the micellar region (the light scattering intensity has dropped a factor of 100 compared to the maximum intensity in the micellar peak, data not shown), where soluble complexes are the majority complex in solution[29]. Also, the added mixture of PAA and PDMAEMA has a ζ-potential which is near 0, so it seems that the negative ζ-potential is a property of C3-μEs, both in $NaNO_3$ and phosphate buffer solution.

Self-consistent field calculations

More insight into the reasons why the geometric model gives only a rough description of the experimental data can be obtained with self-consistent field (SCF) calculations, as more detailed considerations are used in such calculations. We consider block copolymers A_NB_M (N = 100, M = 800, which in block length ratio correspond to the $PAA_{26}PAAm_{200}$ block copolymer) that form a complex with homopolymers C_{3N} due to an attractive Flory-Huggins (FH) parameter between A and C: $\chi_{AC} = -2$; this provides the driving force for the formation of micelles. In addition, we have A_{3N} homopolymers in the system, which serve to swell the core of the micelles, and there is a monomeric solvent W. Note that we do not explicitly

consider the charges of the polymers in the system. All FH parameters other than χ_{AC} are set to 0.5, which implies that all individual components are water soluble and only the combination of A and C in the system gives rise to micellisation (the B block is the corona forming block). Two-component micelles can form when A_NB_M and C_{3N} are mixed in proper proportions in excess W. In the core, which still contains a lot of W, the ratio A/C is close to 1:1 to optimize the attractive contacts (Fig. 4.9). As is common in a SCF analysis we focus on micelles near the critical micellar composition (CMC), which we here pragmatically define as micelles with a grand potential of 10 k_BT (system is dilute in micelles). The micellar size is measured by monitoring the average position of the free end of the copolymer. Let the volume fraction distribution of the free end (of the B-block) in a lattice model be given by the radial volume fraction distribution *g(r)*, then a measure for the micelle size R_m may be found from

$$R_m = \frac{4\pi\sum_r r^3\left(g(r)-g^b\right)}{4\pi\sum_r r^2\left(g(r)-g^b\right)} = \frac{4\pi\sum_r r^3\left(g(r)-g^b\right)}{N_{agg}} \qquad (4.3)$$

where N_{agg} is the number of copolymers in the spherical micelle, r = 0 is the center of the micelle and the summations run over all positive coordinates up to infinity. Here, all linear lengths are normalized by a segment length b (also size of a lattice site) and g^b is the volume fraction of copolymer ends (B-block) in the bulk (far from the micelle).

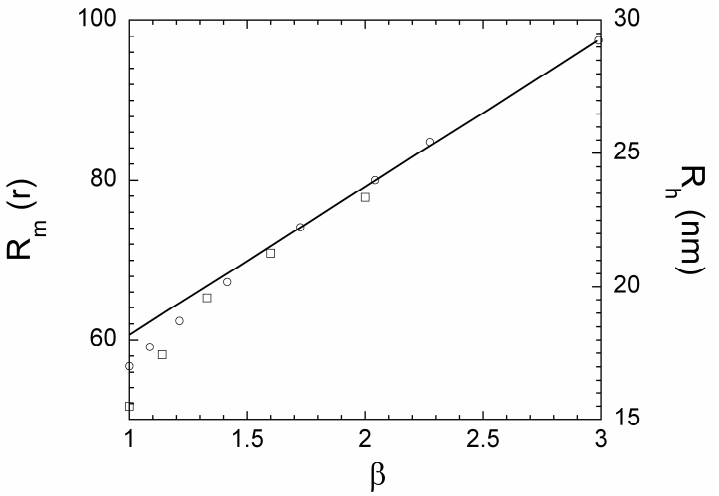

Figure 4.8: Comparison of changes in the size of the micelle (first moment of the end-point of the copolymer) as a function of β. R_m, from SCF calculations (○) and R_h from experiment (□). Line to more clearly visualise the deviations from linearity.

The geometric packing model predicts a straight line for the micelle size R_m as a function of β. The SCF model (data points, Fig. 4.8) clearly deviates from the linear behaviour. The growth of the micelle size with increasing β levels off when more homopolymers are in the micelle. This is qualitatively in agreement with the experimental data. Quantitatively, the point where the deviation is no longer visible is the same as well, namely around β = 1.5 (Fig. 4.8).

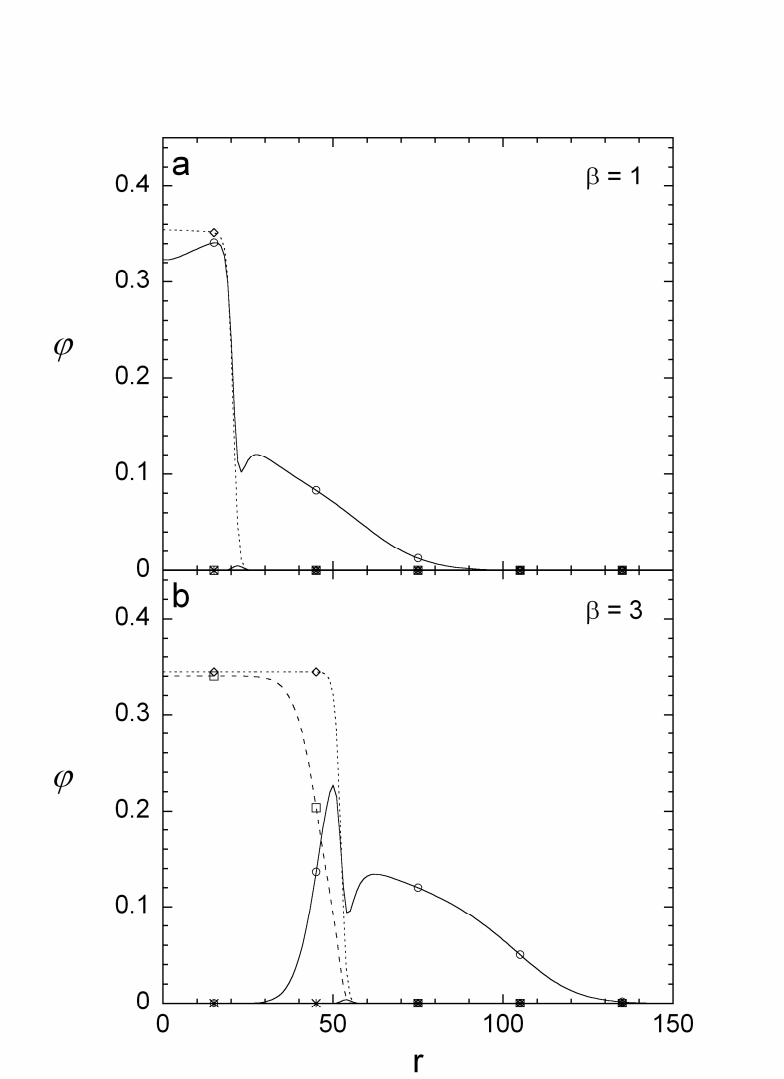

Figure 4.9: Volume fraction, φ, profiles of the various polymers from the calculations. ○ with full line is the diblock copolymer (composed of A-segments in the core and the B block forming the corona). □ is the A_{3N} polymer, ◊ the C_{3N} polymer, × with a full line (only visible as a small bump) gives the position and width of the core-corona interface. a) β = 1 and b) β = 3. Micelles have a grand potential of 10 kT.

One advantage of doing the molecular modeling is the option to inspect the predicted radial volume fraction (φ) profiles of the corresponding micelles. Comparing the profiles for a micelle in the absence of A_{3N} homopolymer (Fig. 4.9a) and one with a significant loading of the micelles with this homopolymer (Fig. 4.9b), we see an increase of the size of the core, being approximately 22b for a non-swollen micelle and close to 55b for a swollen micelle with β = 3. The size of the corona is not very different in the two micelles. The non-swollen micelle is much closer to a star (small core, large corona) and the swollen micelle is closer to a crew-cut micelle (large core, small corona)[41]. Thus, the observed non-linear behaviour correlates with the cross-over from star-like to crew-cut micelles, which occurs upon increasing β. One can calculate the effective head group area for the micelles with β = 1 and 3, giving 49b^2 and 54b^2, respectively. The effective area per molecule is higher for the swollen, crew-cut, than for the non-swollen, star-like, micelles. As the geometric model assumed that the effective area per molecule does not depend on β, we conclude that the non-linear growth both found in SCF modeling as well as in experiments may be caused by small but systematic changes in the effective area per diblock molecule.

Conclusions

Nanoparticles of various sizes can be prepared from a charged-neutral diblock copolymer and various amounts of a cationic and an anionic homopolyelectrolyte. A simple geometrical model is proposed to interpret experimental results on C3Ms composed of PAA_xPAAm_y and $PDMAEMA_{150}$ with added negative and positive polyelectrolytes (PAA_{140} and $PDMAEMA_{150}$). The model helps in distinguishing between highly aggregated metastable states (called non-relaxed C3-μEs and found when the samples are made in 10 mM $NaNO_3$) and the stable states (minimum free energy, called C3-μEs and found when samples are made in a phosphate buffer with an ionic strength of 10 mM, pH 7.1).

It is shown that with increasing added negatively and positively charged polyelectrolytes, β, the particle size and light scattering intensity increase. For C3-μEs with long enough neutral blocks non-linear growth with increasing β is observed, in contrast to the linear growth predicted by the geometrical packing model. SCF calculations strongly suggest this non-linear growth is probably due to an increase in the area occupied by the neutral block at the core corona interface, which is due to a transition from more star-like to crew-cut-like micelles, with increasing β.

We conclude that the C3-μEs we have formed here are indeed micro-emulsions, as the complex coacervate core is solubilised by the stabilizing agent (the neutral block, PAAm), the nanoparticles formed in phosphate buffer seem to be in the stable state (lowest free energy), and emulsification failure occurs upon increasing β beyond a ratio of AA/AAm of about 1.

Electrophoretic mobility measurements show that the non-relaxed C3Ms and C3-μEs are negatively charged where the formed complexes have a maximum in scattering and R_h. The ζ-potential of C3-μEs with long neutral blocks ($PAAm_y$, y = 381 or 405) is near 0, as the longer block form a thicker corona which screens the charge to a higher degree.

Appendix: Geometrical packing model for C3-μEs

C3Ms and C3-μEs consists of a complex coacervate core with a radius R_{core}, a volume V_{core}, and an area A_{core}, and a corona formed by a brush layer of the neutral tails having a thickness R_{corona}. The volume of the core follows directly from the total volume of the positive and negatively chargeable monomers in the complex coacervate core and its water content (A4.1). The area of the core-corona interface is proportional to the number of diblocks in the particle (A4.2).

$$V_{core} = \frac{4}{3}\pi R_{core}^3 = \left(n_{db}^- v^- p_{db}^- + n_{hp}^- v^- p_{hp}^- + n_{hp}^+ v^+ p_{hp}^+\right)/\varphi \qquad \text{(A4.1)}$$

$$A_{core} = 4\pi R_{core}^2 = n_{db}^- a_{db}^- \qquad \text{(A4.2)}$$

with n the number of the negative diblock copolymer molecules (db), or negative and positive homopolyelectrolytes (hp), v is the monomer volume, p the degree of polymerisation, and φ the overall volume fraction of the polyelectrolytes in the core. The polymer brush occupies an area a_{db}^- at the core-corona interface, which is determined by the balance of the osmotic pressure in the brush and the interfacial tension at the core/corona interface.

At the PMC the core is electroneutral, and for C3Ms composed of a diblock copolymer and two species homopolyelectrolytes, this gives the constraint,

$$\alpha^- n_{db}^- p_{db}^- + \alpha^- n_{hp}^- p_{hp}^- = \alpha^+ n_{hp}^+ p_{hp}^+ \qquad \text{(A4.3)}$$

where the α's are the degrees of dissociation of the corresponding monomers.

Equations A4.1-A4.3 can be rewritten as,

$$R_{total} = R_{corona} + R_{core}^0\left(\frac{N_{db}^- + N_{hp}^-}{N_{db}^-}\right) = R_{corona} + R_{core}^0\beta \qquad \text{(A4.4)}$$

and $N_{hp}^{-} = n_{hp}^{-} p_{hp}^{-}$ and $N_{db}^{-} = n_{db}^{-} p_{db}^{-}$, are the total number of monomers in the anionic homopolyelectrolytes (hp) and the anionic polyelectrolytes of the diblocks (db), respectively.

$$R_{core}^{0} = \frac{3 p_{db}^{-} \left(\nu^{-} \alpha^{+} + \nu^{+} \alpha^{-} \right)}{a_{db}^{-} \alpha^{+} \varphi} \qquad \text{(A4.5)}$$

It is assumed that ν^{-}, ν^{+}, α^{-} and α^{+} are independent of the composition and the position in the complex. In first approximation a_{db}^{-} is assumed to be constant, but it is likely that it depends on the curvature. From (A4.4) it follows, that the radius R_{total} is proportional to β, the ratio of the total number of charged monomers to those of the block copolymers. An interesting property of (A4.4) is that R_{core}^{0} can be determined experimentally from the slope of the curve of R_{total} against β.

Literature

(1) Degennes, P. G.; Taupin, C. *Journal of Physical Chemistry* **1982**, *86*, 2294.
(2) Bungenberg de Jong, H. G. In *Colloid Science*; Kruyt, H. R., Ed.; Elsevier: Amsterdam, 1949; Vol. II.
(3) Cohen Stuart, M. A.; Besseling, N. A. M.; Fokkink, R. G. *Langmuir* **1998**, *14*, 6846.
(4) Gohy, J.-F.; Varshney, S. K.; Jerome, R. *Macromolecules* **2001**, *34*, 3361.
(5) Harada, A.; Kataoka, K. *Macromolecules* **1995**, *28*, 5294.
(6) Kabanov, A. V.; Bronich, T. K.; Kabanov, V. A.; Yu, K.; Eisenberg, A. *Macromolecules* **1996**, *29*, 6797.
(7) van Vlerken, L. E.; Vyas, T. K.; Amiji, M. M. *Pharmaceutical Research* **2007**, *24*, 1405.
(8) Harada, A.; Kataoka, K. *Progress in Polymer Science* **2006**, *31*, 949.
(9) Gaucher, G.; Dufresne, M. H.; Sant, V. P.; Kang, N.; Maysinger, D.; Leroux, J. C. *Journal of Controlled Release* **2005**, *109*, 169.
(10) Euliss, L. E.; DuPont, J. A.; Gratton, S.; DeSimone, J. *Chemical Society Reviews* **2006**, *35*, 1095.
(11) Gohy, J.-F.; Antoun, S.; Jerome, R. *Macromolecules* **2001**, *34*, 7435.
(12) van der Burgh, S.; de Keizer, A.; Cohen Stuart, M. A. *Langmuir* **2004**, *20*, 1073.
(13) Harada, A.; Kataoka, K. *Macromolecules* **2003**, *36*, 4995.
(14) Park, J. S.; Akiyama, Y.; Yamasaki, Y.; Kataoka, K. *Langmuir* **2007**, *23*, 138.
(15) Hofs, B.; de Keizer, A.; Cohen Stuart, M. A. *Journal of Physical Chemistry B* **2007**, *111*, 5621.
(16) Hurter, P. N.; Scheutjens, J.; Hatton, T. A. *Macromolecules* **1993**, *26*, 5592.
(17) Nagarajan, R.; Ganesh, K. *Macromolecules* **1989**, *22*, 4312.
(18) Hofs, B.; Voets, I. K.; de Keizer, A.; Cohen Stuart, M. A. *Physical Chemistry Chemical Physics* **2006**, *8*, 4242.
(19) Leermakers, F. A. M.; Scheutjens, J. *Journal of Physical Chemistry* **1989**, *93*, 7417.
(20) Scheutjens, J.; Fleer, G. J. *Journal of Physical Chemistry* **1979**, *83*, 1619.
(21) Scheutjens, J.; Fleer, G. J. *Journal of Physical Chemistry* **1980**, *84*, 178.
(22) Shusharina, N. P.; Linse, P.; Khokhlov, A. R. *Macromolecules* **2000**, *33*, 3892.
(23) Voets, I. K. Opposites attract?! On the electrostatically driven co-assembly of polymers in aqueous solution. PhD Thesis, Wageningen University, 2008.
(24) Hall, D. G.; Pethica, B. A. In *Non-ionic surfactants*; Schick, M. J., Ed.; Marcel Dekker: New York, 1967.
(25) Stenzel, M. H.; Davis, T. P. *Journal of Polymer Science Part A-Polymer Chemistry* **2002**, *40*, 4498.
(26) Millard, P. E.; Barner, L.; Stenzel, M. H.; Davis, T. P.; Barner-Kowollik, C.; Muller, A. H. E. *Macromolecular Rapid Communications* **2006**, *27*, 821.
(27) Millard, P.-E.; Reinhardt, J.; Barner, L.; Buchmeiser, M. R.; Stenzel, M. H.; Davis, T. P.; Barner- Kowollik, C.; Müller, A. H. E. *In preparation*.
(28) Koppel, D. E. *Journal of Chemical Physics* **1972**, *57*, 4814.
(29) van der Burgh, S. Complex Coacervate Core Micelles in Solution and at Interfaces. PhD-thesis, Wageningen Universiteit, 2004.
(30) Voets, I. K.; van der Burgh, S.; Farago, B.; Fokkink, R.; Kovacevic, D.; Hellweg, T.; de Keizer, A.; Cohen Stuart, M. A. *Macromolecules* **2007**, *40*, 8476.

(31) Bakeev, K. N.; Izumrudov, V. A.; Kuchanov, S. I.; Zezin, A. B.; Kabanov, V. A. *Macromolecules* **1992**, *25*, 4249.
(32) Okubo, T.; Hongyo, K.; Enokida, A. *Journal of the Chemical Society-Faraday Transactions I* **1984**, *80*, 2087.
(33) Izumrudov, V. A.; Bronich, T. K.; Zezin, A. B.; Kabanov, V. A. *Journal of Polymer Science Part C-Polymer Letters* **1985**, *23*, 439.
(34) Kovacevic, D.; van der Burgh, S.; de Keizer, A.; Cohen Stuart, M. A. *Langmuir* **2002**, *18*, 5607.
(35) Kovacevic, D.; van der Burgh, S.; de Keizer, A.; Cohen Stuart, M. A. *Journal of Physical Chemistry B* **2003**, *107*, 7998.
(36) Voets, I. K.; de Vries, R.; Fokkink, R.; Sprakel, J.; May, R.; de Keizer, A.; Cohen Stuart, M. A. *Journal of Physical Chemistry B* **2008**, *Submitted*.
(37) Tsuchida, E.; Abe, K.; Honma, M. *Macromolecules* **1976**, *9*, 112.
(38) Xu, R. L.; Winnik, M. A.; Hallett, F. R.; Riess, G.; Croucher, M. D. *Macromolecules* **1991**, *24*, 87.
(39) Birshtein, T. M.; Amoskov, V. M. *Polymer Science, Ser. C* **2000**, *42*, 2286.
(40) Borisov, O. V.; Zhulina, E. B. *Macromolecules* **2002**, *35*, 4472.
(41) Wijmans, C. M.; Zhulina, E. B. *Macromolecules* **1993**, *26*, 7214.

Chapter Five

Reduction of protein adsorption to a solid surface by a coating composed of polymeric micelles with a glass-like core

Abstract

Adsorption studies by optical reflectometry show that complex coacervate core micelles (C3Ms) composed of poly([4-(2-amino-ethylthio)-butylene] hydrochloride)$_{49}$-*block*-poly(ethylene oxide)$_{212}$ and poly([4-(2-carboxy-ethylthio)-butylene] sodium salt)$_{47}$-*block*-poly(ethylene oxide)$_{212}$ adsorb in equal amounts to both silica and cross-linked 1,2-polybutadiene (PB). The C3Ms have an almost glass-like core and atomic force microscopy of a dried layer of adsorbed C3Ms shows densely packed flattened spheres on silica, which very probably are adsorbed C3Ms.

Experiments were performed with different types of surfaces, solvents, and proteins; bare silica and cross-linked 1,2-PB, $NaNO_3$ and phosphate buffer, and lysozyme, bovine serum albumin, β-lactoglobulin, and fibrinogen. On the hydrophilic surface the coating reduces protein adsorption > 90 % in 0.1 M phosphate buffer, whereas the reduction on the coated hydrophobic surface is much lower. Reduction is better in phosphate buffer than in $NaNO_3$, except for the positively charged lysozyme, where the effect is reversed.

Published in slightly modified form as: Hofs, B., Brzozowska, A., de Keizer, A., Norde, W., and Cohen Stuart M.A., Journal of Colloid and Interface Science, 2008, 325, 2, 309

Introduction

Proteins are well known to adsorb onto many solid surfaces[1]. Protein adsorption to bare solid surfaces is governed by various factors, which can be subdivided into properties of the surface (wettability and charge), the proteins (their charge, tendency to unfold or 'hardness', and exposed hydrophobicity), and the medium (pH, ionic strength, type of salt)[1,2]. The ability of polymeric layers, especially polymer brush layers consisting of neutral hydrophilic polymers, to prevent or reduce the adsorption of proteins has been thoroughly investigated and is of high interest[2-10], e.g. to prevent biofouling of the membranes of sensors[11] or contact lenses. Different strategies have been used to create polymer brush layers on surfaces, such as grafting from or to the surface[6], adsorption of molecularly dissolved polymers[8], Langmuir-Blodgett deposition[12], and deposition of particles (micelles[13], or other nanoparticles). Using micelles as a surface coating has the advantage that both the micelles (which form by self-assembly) and the coated surface (adsorption from solution) are easily prepared.

Recently, a relatively new class of micelles, complex coacervate core micelles (C3Ms)[14], was reported to form a coating which reduces protein adsorption[13,15]. C3Ms are formed by the electrostatic attraction between a diblock copolymer with a water-soluble neutral block and a charged block, and an oppositely charged homopolymer or diblock copolymer. C3Ms composed of poly(acrylic acid)$_{42}$-*block*-poly(acryl amide)$_{417}$ ($PAA_{42}PAAm_{417}$) and the oppositely charged poly(N,N-dimethylaminoethyl methacrylate) (PDMAEMA) have a PAAm corona and a core composed of the oppositely charged polyelectrolytes. They were found to adsorb in equal amounts to both SiO_2 and polystyrene surfaces. As PAAm is known not to adsorb to SiO_2[16] it was concluded that it is probably the core that adsorbs in both cases, leaving the neutral water-soluble PAAm blocks to form a polymer brush, which was shown to completely prevent the adsorption of lysozyme (LSZ)[13].

The ability of a coating of a different kind of C3Ms, composed of two diblock copolymers, poly([4-(2-amino-ethylthio)-butylene] hydrochloride)$_{49}$-*block*-poly(ethylene oxide)$_{212}$ ($PAETB_{49}PEO_{212}$) and poly([4-(2-carboxy-ethylthio)-butylene] sodium salt)$_{47}$-*block*-PEO_{212} ($PCETB_{47}PEO_{212}$), to suppress protein adsorption has been investigated as well[15]. The formation of C3Ms from these diblock copolymers is a complicated process. Initially, a dilute complex is formed by complexation between the two oppositely charged polyelectrolyte blocks, but subsequently the complex coacervate core contracts, expelling water, and becomes hydrophobic and more glass-like; the rate of this process can be increased by heating[17]. Such behaviour is likely because of the hydrophobic backbones of the

polyelectrolyte blocks of the two diblock copolymers. These C3Ms were allowed to adsorb onto SiO_2 and onto a polyelectrolyte multilayer (PEM), and the structure of the C3M layer on the PEM was investigated with neutron and X-ray reflectivity measurements. It was concluded that the C3Ms unfold upon adsorption, that the core of the C3Ms is adsorbed to the polyelectrolyte multilayer, and that the neutral blocks form a layer on top. LSZ adsorption onto the coated surfaces was reduced by about 80 %.

Protein adsorption in the presence of an adsorbed polymer brush can be either to the substrate (primary adsorption), to the periphery of the polymer brush (secondary adsorption), or into the polymer brush (ternary adsorption)[3]. The density of the polymer brush determines the steric repulsion generated by the brush, which prevents the proteins from adsorbing into the brush or onto the substrate. Usually the more easily accessible grafting density, σ, expressed as number of chains per nm^2, is used as a measure for the density. The number of monomer groups per nm^2, $n = \sigma N$, (where N is the number of monomers per polymer chain) can also be used as a measure of the amount of polymer present and thus for the effectiveness in reducing protein adsorption[8]. For graft copolymers consisting of short PEO blocks (1-5 kDa) grafted to polylysine, adsorbed from solution onto Nb_2O_5, the number of EO groups per nm^2 (n_{EO}) could be increased to up to about 30 nm^{-2}. These layers are very effective in preventing protein adsorption[8]. Of course, besides the polymer density, the protein size is important as well: for smaller proteins higher polymer densities are needed to prevent protein adsorption. Large proteins may perhaps adsorb due to van der Waals forces, onto the periphery of the polymer brush[1,18-21].

In this chapter we extend our study to the protein repellency of layers obtained after adsorption of C3Ms composed of $PAETB_{49}PEO_{212}$ and $PCETB_{47}PEO_{212}$. We investigate the effect of three variables: (i) The kind of protein; four different proteins were used to test the protein repellency of the adsorbed layer, namely lysozyme (LSZ), bovine serum albumin (BSA), β-lactoglobulin (β-LG), and fibrinogen (FIB)[2,22]. These proteins have different isoelectric points, (exposed) hydrophobicity[23], structural stability, and size (Table 5.1). (ii) The type of substrate, either SiO_2 (hydrophilic) or cross-linked 1,2-poly(butadiene), 1,2-PB, (hydrophobic). (iii) The type and concentration of salt; two different salts ($NaNO_3$ and phosphate buffer) and ionic strengths, 10 and 100 mM, were used. $NaNO_3$ was chosen as it is a salt with a low tendency for having specific interactions with the substrates, proteins or polyelectrolytes. Phosphate buffer was chosen as it is a commonly used solvent for proteins;

phosphate ions (especially HPO_4^{2-}) are known to interact somewhat with SiO_2[24] and strongly with cationic groups.

Protein	Dimensions (nm^3)	MW (kDa)	Isoelectric point	used dn/dc
LSZ	3*3*4.5[a]	14.7	11[a]	0.19
BSA	9*9*7[b]	66	4.5[a]	0.19
β-LG	4*4*4[c]	18.4	5.3[d]	0.19
FIB	5*5*47[e]	340	5.9[f]	0.19

Table 5.1: Protein properties.

[a] From [25], [b] from [26], [c] from [27], [d] from [28], [e] from [29], [f] from [30].

As a fourth variable it would be interesting to consider the type of the C3Ms, as the adsorption of C3Ms with either a liquid-like or more glass-like core may result in different morphologies of the adsorbed layer and, hence, different polymer brush densities. Generally, polymeric micelles with a hydrophobic core tend to adsorb as whole micelles[31]. This gives rise to two possible adsorption states for C3Ms with a more glass-like core: on one hand as micelles adsorbed via their core (making flattened micelles) or on the other hand via their corona[32-34]. For C3Ms with a liquid-like core, a different structure may be observed, e.g. the complex coacervate core forming a homogeneous film on the substrate, with the neutral polymers sticking out from the complex coacervate layer into solution. As the structure of the adsorbed layer may be expected to influence the protein repellency, we consider this factor in a forthcoming paper[35].

Materials and methods

Materials

Poly([4-(2-amino-ethylthio)-butylene] hydrochloride)$_{49}$-*block*-poly(ethylene oxide)$_{212}$ ($PAETB_{49}PEO_{212}$, M_n = 16.6 kg/mol), PDI 1.1 and poly([4-(2-carboxy-ethylthio)-butylene] sodium salt)$_{47}$-*block*-PEO_{212} ($PCETB_{47}PEO_{212}$, M_n = 17.8 kg/mol), PDI 1.1, were prepared by modification with a mercaptan of poly(butadiene)$_{65}$-*block*-PEO_{212} - which has been prepared by sequential anionic polymerization of 1,3-butadiene and ethylene oxide - and were a kind gift from Helmut Schlaad (MPI Golm). The synthesis and analysis of these polymers have been described in detail elsewhere[36]. Structures of the polymers are shown in figure 5.1. 1,2-

Poly(butadiene) (1,2-PB, M_n = 50.0 kg/mol, 1,2-content 85%), PDI 1.06, was purchased from Polymer Source Inc. (Montreal, Canada).

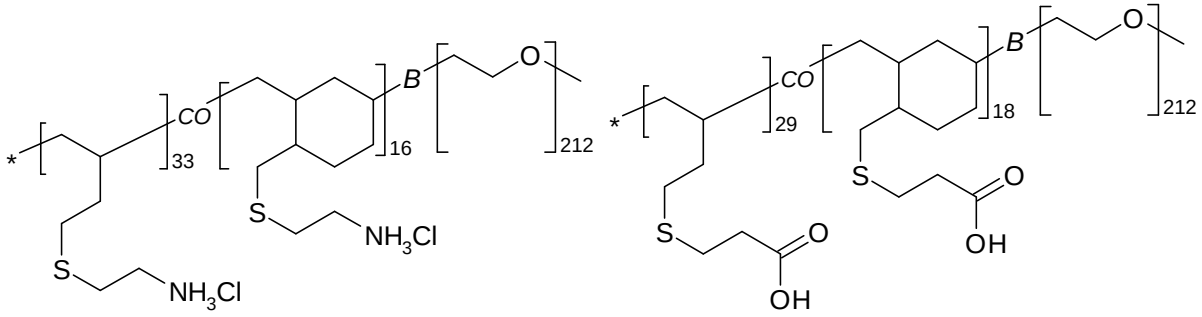

Figure 5.1: Structures of $PAETB_{49}PEO_{212}$ (left) and $PCETB_{47}PEO_{212}$ (right). Numbers besides the brackets denote the degree of polymerization.

Proteins used are LSZ (Sigma, 95% protein, from chicken egg white, L6876-5G, lot nr. 093K1455), BSA (Sigma, 98-99% protein, 84F-0103), β-LG (Sigma, 90% protein, from bovine milk, L0130-5G, lot nr. 033K7003), and FIB (Sigma, 58% protein, from human plasma, F4883-1G, lot nr. 035K7585).

All salts were of analytical grade and used as received. Aqueous solutions of polymers were prepared by dissolution of known amounts of polymer into de-ionized water (Milli-Q) to which known amounts of either $NaNO_3$, or Na_2HPO_4 and NaH_2PO_4 had been added. All salt concentrations are given as ionic strength, rather than as molar concentration. The phosphate buffer with an ionic strength of 10 mM, pH 7.7 has about 4 mM of phosphate ions. The pH was adjusted, if necessary, with 0.1 M NaOH or 0.1 M HNO_3.

Preparation of C3Ms

A stock solution of C3Ms was prepared by mixing of a 1 g/l $PAETB_{49}PEO_{212}$ solution and a 1 g/l $PCETB_{47}PEO_{212}$ solution, both with the desired ionic strength, such that the total number of positively and negatively chargeable groups was equal. After mixing of these two solutions relatively large C3Ms are obtained. This solution of large C3Ms was subsequently heated to 80 ºC, left to equilibrate at this temperature for approximately 15 minutes, and finally cooled down to room temperature. Upon heating, the large C3Ms expel solvent and decrease in size, resulting into smaller C3Ms with a hydrophobic, more glass-like core[17]. The final hydrodynamic radius, R_h, as determined with dynamic light scattering, is 17 ± 2 nm

(average ± standard deviation). The stock solution of 1 g/l of these C3Ms was usually diluted tenfold with solvent and this diluted solution was used in all reflectometry experiments.

For C3Ms in 90 mM PO_4-buffer, pH 7.7, the preparation procedure was different. As we were unable to molecularly dissolve $PAETB_{49}PEO_{212}$ in 100 mM PO_4-buffer of pH 7.7, separate 1 g/l solutions of both polymers in 10 mM PO_4-buffer of pH 7.7 were prepared. These were then mixed, heated, and finally diluted to 0.1 g/l total polymer concentration with 100 mM PO_4-buffer, pH 7.7.

Tapping mode atomic force microscopy (AFM)

Tapping mode AFM measurements were carried out with a Nanoscope III, Multimode Scanning Force Microscope (Digital Instruments, USA), with Nanoscope software version 6.11r1. The obtained raw topography images were flattened and a 1st order plane fit was applied. For determination of the surface roughness R_q ($R_q \equiv \sqrt{\frac{\sum Z_i^2}{N}}$, where Z_i is the deviation from the mean for point i, and N the number of points), 7 small sub-areas of 1*1 μm^2 were measured, for which the average and standard deviation were determined.

Surface preparation

SiO_2 surfaces were prepared by heating a silicon wafer (150 mm, 655-695 μm thickness, 100 orientation, WaferNet Inc., CA, USA) at 1000 ºC, until a SiO_2 layer with a thickness in the range 60-100 nm, as determined with a SENTECH Instruments SE 400 (SENTECH Instruments GmbH, Germany) ellipsometer (with as refractive index for SiO_2 1.46), was obtained. Strips of 4.5*1 cm^2 were cut and cleaned by ultrasonication (15 mins) in ethanol and subsequently washed with copious amounts of de-ionized water and blown dry with N_2 gas.

Cross-linked 1,2-PB surfaces were obtained with the following procedure. First, a silicon wafer was cut into strips (4.5*1 cm^2) which were subsequently cleaned in ethanol as described above. Then, the strips were put in a plasma-cleaner for 2-4 minutes. The strips were attached to a spinning table with double-sided adhesive tape. The strip was covered drop wise with 1,2-PB solution (in toluene, filtered with a 0.2 μm PTFE filter) and spin-coated at 2000 RPM for 30 s. To cross-link the 1,2-PB, the strips were put into a vacuum oven at 150 °C during 72 hours. The attachment and cross-linking of the layer was checked by rinsing a strip with chloroform; if no rinsing off was observed, the sample was considered to be cross-

linked. The total thickness of the PB film was determined in air by means of ellipsometry (refractive index of PB used for the layer: 1.52). The thickness of the PB layer can be varied by varying the concentration of the 1,2-PB solution; using a 13 g/l 1,2-PB solution results in a layer thickness of about 75 nm, whilst using 17 g/l 1,2-PB results in 100 nm thickness.

The hydrophobic cross-linked 1,2-PB layer was inspected with both a light microscope (Olympus BX60 with an Olympus DP70 camera) and by AFM (Fig. 5.2). In the light microscope image a negligible number of small defects can sometimes be observed in an otherwise smooth, featureless film. Usually >97% of the surface is defect-free. In AFM, the surface roughness, R_q, of the cross-linked 1,2-PB layer is 0.40 ± 0.05 nm (the R_q of the underlying SiO_2 layer is 0.08 ± 0.01 nm).

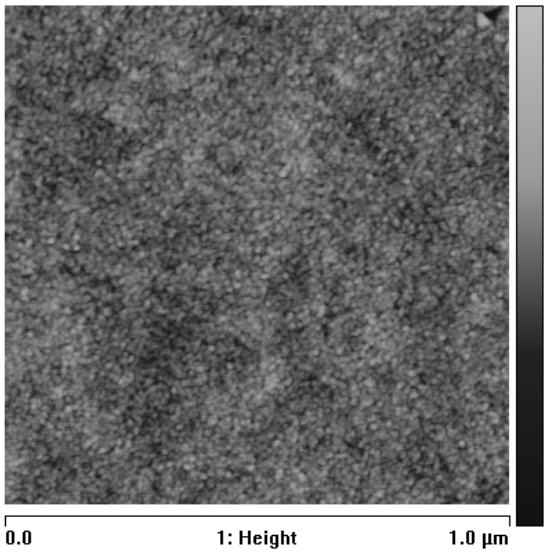

Figure 5.2: Tapping mode AFM image of the bare cross-linked 1,2-PB surface. The gradient on the right hand side represents 20 nm of height difference.

Adsorption of C3Ms onto the SiO_2 and cross-linked 1,2-PB surface was achieved by exposing the substrate to a solution containing 1 g/l of the C3Ms for at least 30 minutes, far more than is needed to reach a steady state. The substrate with adsorbed C3Ms was then rinsed with de-ionized water, blown dry with N_2 gas, and imaged with tapping mode AFM. The advancing contact angle (of deionized water) on the bare and coated substrates was determined with a Krüss DSA100, Krüss GmbH, Germany, with software DSA v1.90.0.14, by creating and measuring 4 or 5 single droplets of about 4 µl. For the bare cross-linked 1,2-PB the advancing contact angle was 88 ± 1º, which shows that the surface is hydrophobic, as

expected. The advancing contact angle of bare SiO_2, cleaned by ultrasonication in ethanol, was 37 ± 3º.

Reflectometry

The optical reflectometer used to study the adsorption of C3Ms and proteins has been described in detail elsewhere[37]. The experimental setup includes a He/Ne laser producing linearly polarized light with a wavelength of 632.8 nm and an impinging-jet flow cell. A PC with a Keithley DAXON1 12 bits voltmeter card (or better) with home-made software was used to collect the data. The adsorbed mass per unit area, Γ (mg/m^2), can be calculated from the recorded signal, ΔS, where $\Delta S = S - S_0$, where S is the output signal, and S_0 the baseline signal, with

$$\Gamma = Q_f \frac{\Delta S}{S_0} \qquad (5.1)$$

Here, Q_f is the quality factor, which depends on the substrate used (Table 5.2). Q_f was calculated with dedicated software (Prof. Huygens v 1.2a, Dullware Software). The dn/dc of PEO is 0.136 ml/g[38] and the C3Ms consist of about 60 wt% of PEO. The core of the C3Ms probably has a higher dn/dc. The dn/dc of proteins is around 0.19 ml/g[39,40]. As we can only detect overall adsorbed mass, desorption of coating components that occurs simultaneously with protein adsorption cannot be distinguished. Therefore we have chosen to ignore, for the calculations of Q_f, any optical differences between the refractive index increments of the C3Ms and the proteins; we used a single dn/dc value of 0.19 ml/g.

Surface	thickness (nm)	n	Q_f	R_q (nm) AVERAGE±STDEV	Θ (°)
cross-linked 1,2-PB	75	1.52	43	0.60±0.02	88±1
SiO_2	70	1.46	27	0.08±0.01	37±3

Table 5.2: Overview of substrates; thickness, refractive index, n, quality factor Q_f, roughness, R_q, as determined with AFM, and advancing contact angle (H_2O), Θ.

The protein repellency was determined with the optical reflectometer in a sequential adsorption experiment. Solutions were flushed through the cell as follows: solvent (to obtain a

baseline), C3M solution, solvent, protein solution, and finally solvent again. Typically, the C3Ms solutions and protein solution were flushed through the cell for 10 minutes. During the second and third solvent step any reversibly adsorbed C3Ms or proteins are removed. For each experiment, fresh SiO_2 or cross-linked 1,2-PB surfaces were used.

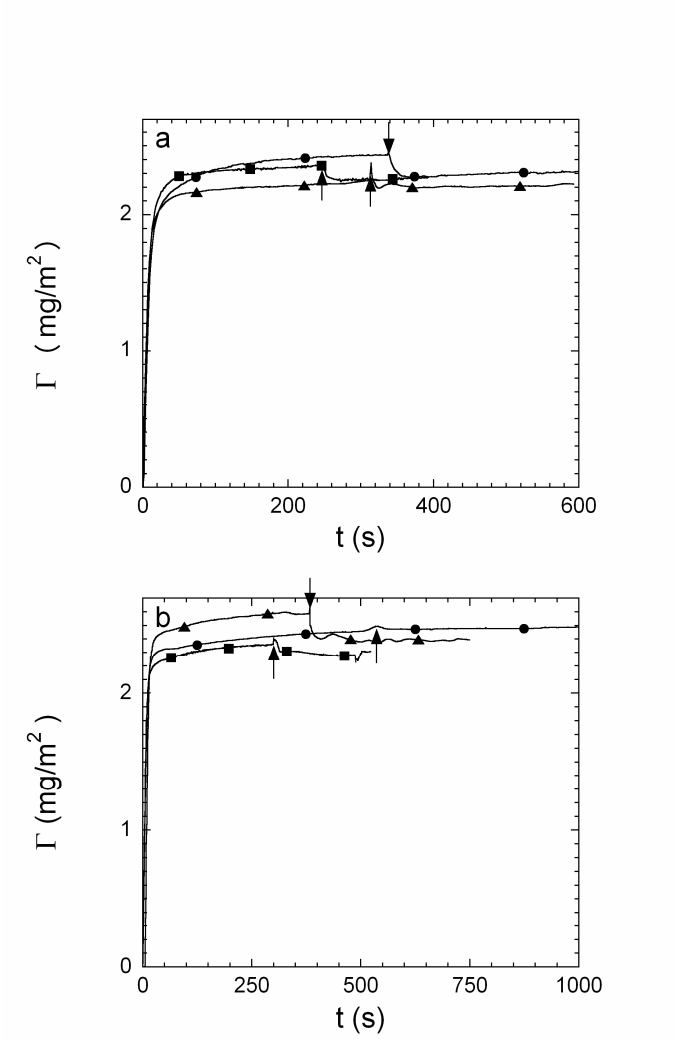

Figure 5.3: Adsorption of 0.1 g/l C3Ms to a) SiO_2 and b) cross-linked 1,2-PB. Solvent from which adsorption took place is 10 mM $NaNO_3$ (●), 10 mM PO_4-buffer, pH 7.7 (■) or 90 mM PO_4-buffer, pH 7.7 (▲).The arrows indicate when we switched from C3M solution to solvent.

Results and discussion

Adsorption of C3Ms

The adsorption of C3Ms onto SiO_2 and cross-linked 1,2-PB was measured in time with optical reflectometry (Fig. 5.3). The adsorption process is fast in all cases; within 60 seconds the rate of adsorption slows down to almost zero. The C3Ms adsorb readily to both surfaces

and in almost equal amounts (2.4 mg/m^2), independent of the nature of the surface, ionic strength, or type of salt. Adsorption of the single components of the C3Ms ($PAETB_{49}PEO_{212}$ and $PCETB_{47}PEO_{212}$) to SiO_2 and cross-linked 1,2-PB is in the range of 0.2-0.4 mg/m^2 (data not shown), much lower than that of C3Ms. After rinsing with solvent the total desorption of the adsorbed C3Ms is only about 5% of the total adsorbed amount, i.e. the C3Ms are predominantly irreversibly attached to the surfaces. The contact angles of the bare and C3M-coated SiO_2 are 37 ± 3º and 41 ± 1º, respectively. As these are almost identical to that of a PEO brush (contact angle about 40º)[41], we cannot conclude from the contact angle measurements whether a homogeneous PEO brush layer has been formed by adsorption of C3Ms to SiO_2 or not. For the bare hydrophobic cross-linked 1,2-PB the advancing contact angle is 88 ± 1º and upon coating with C3Ms it drops to 69 ± 1º. For the coated cross-linked 1,2-PB the contact angle is significantly higher than for a PEO brush. It suggests that after drying, the adsorbed C3Ms do not fully cover the surface with a PEO brush. However, one should be aware that a small deviation from complete coverage already results in a strong increase in the observed effect due to the effect of surface heterogeneity or surface roughness on the advancing contact angle. Whether this incomplete coverage is also present in the wet-state is questionable, as the PEO chains should swell considerably when water is added.

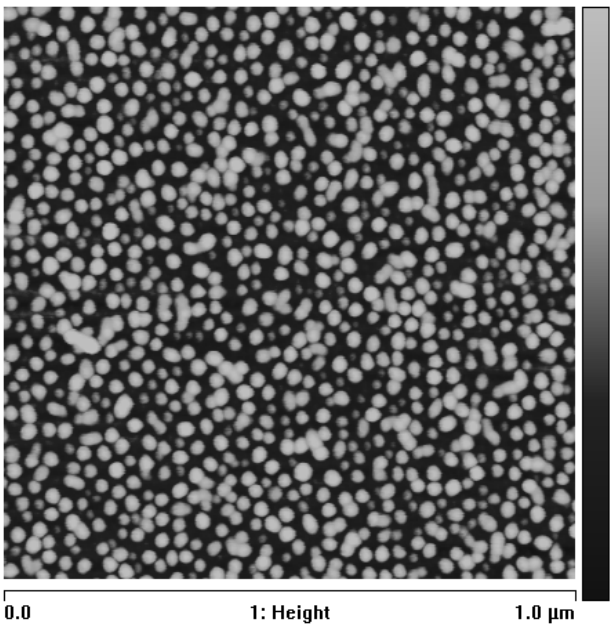

Figure 5.4: Tapping mode AFM in air of C3Ms adsorbed from 10 mM PO_4-buffer, pH 7.7, to SiO_2. The gradient on the right hand side represents 20 nm of height difference.

AFM images of C3Ms adsorbed from 10 mM phosphate buffer to both silica and cross-linked 1,2-PB were taken in air (dry state). On the surface of SiO_2 densely packed flattened spheres with a surface coverage of about 50% (close to the jamming limit of 54.7 % for random sequential adsorption of hard spheres to a flat surface[42]) were found (Fig. 5.4). The centres of the observed flattened spheres lie 30 ± 5 nm apart, and have a height of 7 ± 2 nm. The hydrodynamic radius (as determined with dynamic light scattering) of the C3Ms in solution is 17 nm. Thus the diameter of the dried adsorbed C3Ms is nearly equal to that in aqueous solution, suggesting that C3Ms attach to the surface as separate intact particles. In the AFM experiments the C3Ms appear flattened, likely due to drying as the solvent contained in the C3Ms evaporates. Calculating the mass of polymer present in a single adsorbed C3M (from the area that one flattened sphere occupies as determined by AFM, and from the adsorbed amount as determined by reflectometry), yields a mass of $1.2*10^3$ kg/mol, which compares well to the mass of a single C3M in solution which is $0.8*10^3$ kg/mol, corresponding to about 47 diblock copolymers[43]. This indicates that the C3Ms are probably adsorbed to SiO_2 as intact C3Ms. It seems unlikely that during drying the adsorbed layer breaks up into particles comparable in size to the C3Ms in bulk solution.

An AFM image taken in air after adsorption of C3Ms to cross-linked 1,2-PB (Fig. 5.5) also shows spherical shapes with approximately the same size as the C3Ms adsorbed on SiO_2, but with a somewhat higher polydispersity. The surface roughness of the cross-linked 1,2-PB surface is higher than that of SiO_2, which makes interpretation more difficult. Nevertheless, surface coverage is high and it is clear that the fine structure visible in the AFM image of the bare cross-linked 1,2-PB surface (Fig. 5.2) is replaced upon coating with C3Ms by a more coarse structure, of which the spherical shapes probably are adsorbed single C3Ms, as is the case for adsorption to SiO_2.

With ellipsometry (assuming a refractive index of 1.50 for the dry layer of adsorbed C3Ms), a layer of approximately 4 nm thickness was found to be adsorbed to both surfaces (in air), which is about half the value of the maximum height found with AFM for C3Ms on SiO_2 (adsorbed from 10 mM PO_4-buffer, measured in air). Considering that for analysis of ellipsometry data a homogeneous layer is assumed and that AFM shows about 50 % surface coverage, the agreement is very good.

Since the adsorbed amount of the micelles (about 2.4 mg/m^2, Fig. 5.5) and the number of neutral chains per unit weight is known (via the molar mass of the diblock copolymers), one can calculate that σ = 0.07 nm^{-2}, and n_{EO} = 15 nm^{-2} (assuming the adsorbed layer is a

bilayer with the complex coacervate attached to the surface and the PEO sticking out into solution). A polymer brush with this density is expected to reduce protein adsorption significantly[8].

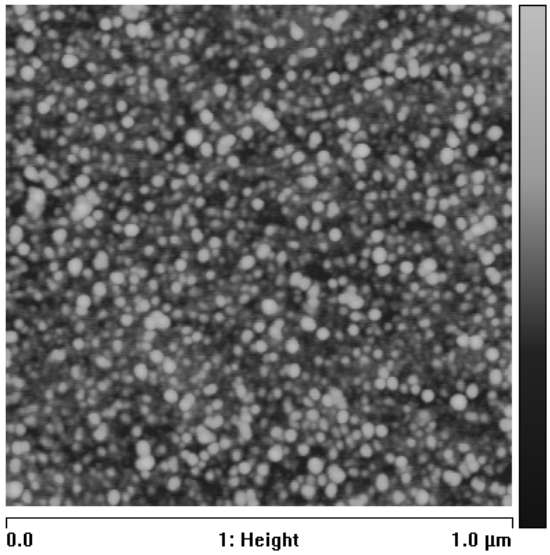

Figure 5.5: Tapping mode AFM in air of C3Ms adsorbed from 10 mM PO_4-buffer, pH 7.7, to cross-linked 1,2-PB. The gradient on the right hand side represents 20 nm of height difference.

Recently, neutron reflectometry experiments were conducted on the same C3Ms as used here, adsorbed to a polyelectrolyte multilayer (PEM). It was concluded that the C3Ms adsorb from 1 mM $NaNO_3$ to poly(styrene sulfonate) terminated PEM with the PEO sticking out into solution and the complex coacervate adsorbed to the PEM[15,44]. The used reflectivity techniques (X-ray, neutron) allow for determination of the density profile, perpendicular to the surface, and the profile is averaged over a certain area. Since in-plane (parallel to the surface) structure is not detected, it is not possible to distinguish between a layer composed of adsorbed single C3Ms and a (bi)layer composed of a PEO brush layer on top of a layer composed of the more glass-like core material at the surface. Combining all data (AFM images, reflectometry, ellipsometry, and related measurements in literature) and the known literature on adsorption of polymeric micelles (for polymeric micelles, when both micelles and free polymers are present, it is the micelles that are adsorbed[32-34]), we conclude that our C3Ms adsorb as flattened single micelles. As they have an almost glass-like core[17] and a relatively high surface tension (as the core is hydrophobic), they do not rearrange into a bilayer structure.

Adsorption of proteins onto the bare surfaces

Prior to studying the protein repellency of C3M coatings, the adsorption of four proteins – i.e. LSZ, BSA, β-LG and FIB – onto bare SiO_2 and cross-linked 1,2-PB surfaces was determined. The reflectometer cell was flushed with a 0.1 g/l protein solution during ten minutes and thereafter with solvent during two minutes. Four different solvent conditions were chosen, i.e. 10 and 100 mM $NaNO_3$, and 10 and 90 mM phosphate buffer. The results are summarized in Table 5.3. The values just before (between brackets) and after flushing with solvent are given. The adsorbed amount of protein has a weak tendency to keep on increasing after 10 minutes (typically about 10%). Protein adsorption is dependent on protein concentrations[40]: We have chosen a fixed concentration and adsorption time as we are interested in the relative effect of the coating on the protein adsorption onto the surfaces. The reported adsorbed amounts on bare surfaces (Table 5.3) are similar to those reported in literature for similar systems and conditions[2,22,45].

Protein	Γ (mg/m^2)							
	10 mM $NaNO_3$		100 mM $NaNO_3$		10 mM phosphate buffer		90 mM phosphate buffer	
	SiO_2	PB	SiO_2	PB	SiO_2	PB	SiO_2	PB
LSZ	(0.63) 0.58	(1.6) 1.4	(0.95) 0.65	(1.0) 0.95	(1.7) 1.3	(2.0) 1.5	(1.4) 0.95	(1.2) 1.0
BSA	(1.4) 1.3	(0.77) 0.71			(0.87) 0.72	(0.71) 0.71	(1.1) 1.0	(0.71) 0.71
β-LG	(0.63) 0.52	(0.87) 0.87	(0.69) 0.60	(0.87) 0.60	(0.55) 0.44	(1.0) 0.87	(0.95) 0.74	(0.69) 0.68
FIB	(2.7) 2.7	(3.7) 3.6			(2.8) 2.6	(4.1) 4.0	(3.2) 3.2	(2.6) 2.6

Table 5.3: Protein adsorption to bare SiO_2 and cross-linked 1,2-PB. All adsorbed amounts, Γ, calculated with dn/dc is 0.19. Solvent from which the proteins were adsorbed is indicated. pH of $NaNO_3$ solutions was adjusted to between 7 and 8. Per salt species and concentration, maximum adsorption before (between brackets) and after rinsing with solvent are given.

Protein adsorption is a very complicated process, as it is the result of interactions between proteins, solvent (and the electrolytes in the solvent) and the surface. Some

interesting qualitative trends can be observed in the data in Table 5.3. Differences for protein adsorption onto the hydrophilic and hydrophobic surface are most pronounced at low ionic strength; apparently, the increased electrostatic screening at high ionic strength reduces the differences. Both in 10 mM $NaNO_3$ and 10 mM phosphate buffer adsorbed amounts of proteins are substantially higher on the hydrophobic surface than on the hydrophilic one, except for BSA. The value for BSA is relatively high on SiO_2, given that both surface and protein are negatively charged. The origin of this specific effect is not clear, but is has been argued that BSA – which unfolds relatively easily (a 'soft'protein) – would be rather susceptible to exposed hydrophobicity[1,2]. The positively charged LSZ adsorbs in higher amounts to SiO_2 from 10 mM phosphate buffer than from 10 mM $NaNO_3$ (Table 5.3). This can be attributed to HPO_4^{2-} ions, which are expected to bind to the positively charged LSZ more strongly than NO_3^-, therewith lowering the charge on the LSZ, which in turn allows a denser packing on the surface. At low ionic strength there is almost no effect of changing the type of electrolyte in the solvent for the hydrophobic PB surface, but for the hydrophilic SiO_2 the effect depends on the protein; an increase in adsorbed amount for LSZ, a decrease for BSA, and almost no effect for β-LG and FIB when replacing $NaNO_3$ by phosphate buffer. These observations show that the effects of surface and solvent on protein adsorption are indeed very complicated; more measurements would be required to unravel these interactions, but this is beyond the scope of this work.

Protein adsorption onto C3M-coated surfaces

After having established the adsorption characteristics of LSZ, BSA, β-LG, and FIB onto the bare SiO_2 and cross-linked 1,2-PB surfaces, we determined how a pre-adsorbed layer of C3Ms on these surfaces affects the adsorption behaviour of the proteins. Adsorbed values were determined under the same conditions as for the bare surfaces. A reflectometry experiment is shown in Fig. 5.6. In this experiment the order of solutions flown through the cell is: (1) solvent (to obtain a baseline, not shown), (2) C3M solution, (3) solvent, (4) LSZ solution, and (5) solvent. The solution of C3Ms was supplied to the surface for well over 2 hours, the initial adsorption is fast and after 60 seconds the adsorption is at 92% of the plateau value. Therefore, in a typical experiment we supplied the C3M solution for only 10 minutes. Rinsing with solvent (10 mM $NaNO_3$) leads to a small desorption. Introducing LSZ results in a considerable additional adsorption, but switching back to solvent washes most of the adsorbed LSZ away, indicating that most of it is only weakly bound.

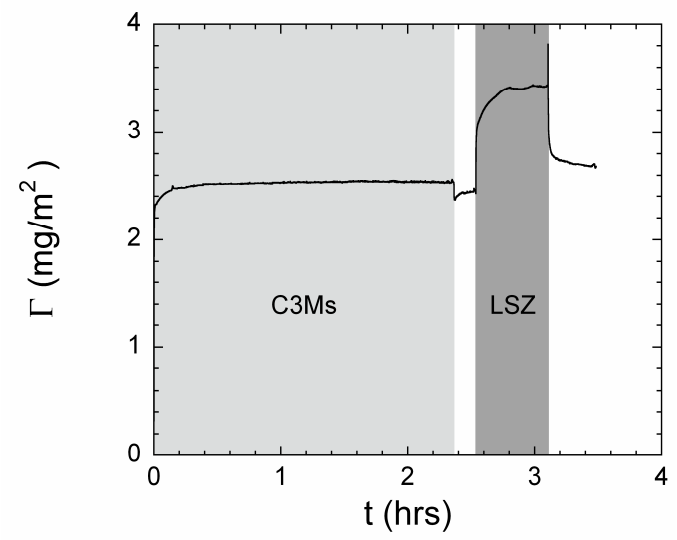

Figure 5.6: Adsorption of LSZ to C3M-coated cross-linked 1,2-PB, solvent is 10 mM $NaNO_3$, pH 7.7. White is solvent, light gray is adsorption of C3Ms and dark grey is adsorption of LSZ.

The adsorption of the proteins to the coated surfaces is more complicated than the adsorption to the bare surfaces, as several additional interactions (protein – coating, solvent – coating, and surface – coating) are involved. Nevertheless, interesting trends emerge, which will be discussed below. In Table 5.4 we show the adsorbed amounts of LSZ, BSA, β-LG and FIB to C3M-coated SiO_2 and to coated cross-linked 1,2-PB, both before and after rinsing with solvent. Generally, the adsorption of proteins is reduced significantly (> 80 %) by the coating (Table 5.4), with the following discernible trends: (i) Protein adsorption to the coated cross-linked 1,2-PB is reduced to a lower extent than to coated SiO_2. This is probably because of the relatively high hydrophobicity of the coated cross-linked 1,2-PB (as indicated by contact angle measurements), which is still 'sensed' by the protein due to inhomogeneous coverage of the surfaces. (ii) The adsorption behaviour of LSZ on one hand, and BSA, β-LG and FIB on the other, to the two types of coated surfaces is reversed by changing the solvent. In 10 mM $NaNO_3$ LSZ adsorbs in lower amounts than the negatively charged proteins, whereas in 10 mM phosphate buffer LSZ adsorbs in higher amounts. Increasing the ionic strength leads to an increase in protein adsorption to coated SiO_2, except for LSZ. LSZ does not adsorb onto coated SiO_2 from 10 mM $NaNO_3$ (a result which has also been found for coating with another type of C3Ms)[13], while significant adsorption occurs from 100 mM $NaNO_3$. For the other proteins, BSA, β-LG and FIB, adsorption is lowest from 10 mM phosphate buffer (Table 5.4); increasing the phosphate buffer ionic strength from 10 to 90 mM increases adsorption to

coated cross-linked 1,2-PB. (iii) Rinsing with solvent generally causes only little desorption (about 0.1 mg/m^2 or less). Again, LSZ is an exception; at low ionic strength rinsing with solvent strongly decreases the adsorbed amount, showing that a large fraction of the adsorbed LSZ is only weakly bound. (iv) Preventing adsorption of β-LG appears most difficult as the achieved reduction is least and shows further complications. Supplying β-LG from 100 mM $NaNO_3$ to coated SiO_2 even leads to a net loss of total adsorbed mass (desorption); this means an amount of coating is partially removed or replaced by the protein, such that more coating is desorbed than protein adsorbed. This effect has only been observed for β-LG, but coating desorption could very well play a (minor) role for the other proteins as well.

Protein	Γ (mg/m^2)							
	10 mM $NaNO_3$		100 mM $NaNO_3$		10 mM phosphate buffer		90 mM phosphate buffer	
	SiO_2	PB	SiO_2	PB	SiO_2	PB	SiO_2	PB
LSZ	(0.00) 0.00 100%	(1.0) 0.24 83%	(0.09) 0.05 93%	(0.34) 0.20 80%	(1.3) 0.51 61%	(0.87) 0.51 66%	(0.25) 0.09 92%	(0.63) 0.54 47%
BSA	(0.28) 0.25 84%	(0.55) 0.47 34%			(0.03) 0.01 99%	(0.05) 0.03 95%	(0.02) 0.01 99%	(0.23) 0.16 78%
β-LG	(0.32) 0.24 54%	(0.54) 0.47 46%	(-0.19) -0.17 *	(0.25) 0.15 75%	(0.04) 0.00 100%	(0.28) 0.21 76%	(0.09) 0.05 94%	(0.39) 0.39 42%
FIB	(0.36) 0.33 88%	(0.87) 0.71 80%			(0.06) 0.03 99%	(0.21) 0.18 95%	(0.09) 0.04 99%	(0.95) 0.87 67%

Table 5.4: Protein adsorption to the C3M-coated SiO_2 and cross-linked 1,2-PB. All adsorbed amounts, Γ, in mg/m^2 calculated with dn/dc = 0.19. Solvent from which the proteins were adsorbed is indicated. pH of $NaNO_3$ solutions was adjusted to between 7 and 8. Per salt species and concentration, maximum adsorption before (between brackets) and after rinsing with solvent are given and the reduction of protein adsorption compared to the bare surface in % is given. * Protein partially displaces the layer.

From the gathered data it turns out that the effectiveness of the C3M coating in reducing protein adsorption depends on more than just n_{EO}. In previous experiments similar densities of n_{EO}[8] reduced protein adsorption by about 94 %. In this study, two times longer PEO blocks are used. Possibly, these may need higher n_{EO} densities in order to reach the same efficiency. The EO units of longer PEO blocks can be located farther away from the surface, lowering the height of the steric barrier (as the polymer density is lower) while increasing the range over which the barrier is effective. With a more dilute, more extended polymer brush, protein adsorption into the polymer brush can be enhanced as well. Furthermore, it is likely that our coating is inhomogeneous on the 10 nm scale, as indicated by AFM images in air, which show that there is a clear particulate structure. If there is structure on the nano-scale level, it is likely that there are PEO density inhomogeneities, leading to 'weak spots' at which protein adsorption will be locally possible. A similar phenomenon has been reported in a comparison of protein adsorption to surfaces grafted with PEO stars and linear PEO[46].

Conclusions

The adsorption of C3Ms to SiO_2 and cross-linked 1,2-PB was determined with both reflectometry and ellipsometry. AFM imaging in air shows that the C3Ms are adsorbed intact as flattened spheres, which is consistent with the highly viscous, almost glass-like core that these C3Ms have[17]. The C3Ms are most likely adsorbed via their PEO chains.

Proteins adsorb readily to both SiO_2 and cross-linked 1,2-PB. The positively charged lysozyme shows increased adsorption to both surfaces when phosphates are present. Increasing the ionic strength of the phosphate buffer from 10 to 90 mM reduces the observed effects, which are therefore likely due to electrostatics.

Protein adsorption is generally reduced by the presence of the coating. More precisely, protein adsorption to the C3M-coated hydrophobic cross-linked 1,2-PB is higher than to the C3M-coated hydrophilic SiO_2. Adsorption of negatively charged proteins to coated surfaces is reduced to a greater extent if the solvent is phosphate buffer, but adsorption of the positively charged lysozyme from phosphate buffer to the coated surfaces is reduced less, as compared to adsorption from a $NaNO_3$ solution. By judiciously choosing the surface, coating it with C3Ms, and choosing the type of salt and ionic strength, it is possible to reduce adsorption of LSZ, BSA, β-LG and FIB to values in the range 0.01 - 0.09 mg/m^2.

That protein adsorption is not fully suppressed is probably due to the local structure of the coating, which has nano-sized ‘holes’ that presumably allow attachment of proteins to the substrate.

Literature

(1) Norde, W. *Advances in Colloid and Interface Science* **1986**, *25*, 267.
(2) Malmsten, M. *Journal of Colloid and Interface Science* **1998**, *207*, 186.
(3) Currie, E. P. K.; Norde, W.; Cohen Stuart, M. A. *Advances in Colloid and Interface Science* **2003**, *100*, 205.
(4) Ratner, B. D.; Bryant, S. J. *Annual Review of Biomedical Engineering* **2004**, *6*, 41.
(5) Senaratne, W.; Andruzzi, L.; Ober, C. K. *Biomacromolecules* **2005**, *6*, 2427.
(6) Kato, K.; Uchida, E.; Kang, E. T.; Uyama, Y.; Ikada, Y. *Progress in Polymer Science* **2003**, *28*, 209.
(7) Malmsten, M.; Emoto, K.; Van Alstine, J. M. *Journal of Colloid and Interface Science* **1998**, *202*, 507.
(8) Pasche, S.; De Paul, S. M.; Voros, J.; Spencer, N. D.; Textor, M. *Langmuir* **2003**, *19*, 9216.
(9) Pasche, S.; Textor, M.; Meagher, L.; Spencer, N. D.; Griesser, H. J. *Langmuir* **2005**, *21*, 6508.
(10) Pasche, S.; Voros, J.; Griesser, H. J.; Spencer, N. D.; Textor, M. *Journal of Physical Chemistry B* **2005**, *109*, 17545.
(11) Wisniewski, N.; Reichert, M. *Colloids and Surfaces B-Biointerfaces* **2000**, *18*, 197.
(12) Currie, E. P. K.; Sieval, A. B.; Avena, M.; Zuilhof, H.; Sudholter, E. J. R.; Cohen Stuart, M. A. *Langmuir* **1999**, *15*, 7116.
(13) van der Burgh, S.; Fokkink, R.; de Keizer, A.; Cohen Stuart, M. A. *Colloids and Surfaces A: Physicochemical and Engineering Aspects* **2004**, *242*, 167.
(14) Cohen Stuart, M. A.; Hofs, B.; Voets, I. K.; de Keizer, A. *Current Opinion in Colloid & Interface Science* **2005**, *10*, 30.
(15) Voets, I. K.; de Vos, W. M.; Hofs, B.; de Keizer, A.; Conhen Stuart, M. A.; Steitz, R.; Lott, D. *J. Phys. Chem. B* **2008**, *112*, 6937.
(16) Bijsterbosch, H. D.; Cohen Stuart, M. A.; Fleer, G. J. *Macromolecules* **1998**, *31*, 8981.
(17) Voets, I. K.; de Keizer, A.; Cohen Stuart, M. A.; Justynska, J.; Schlaad, H. *Macromolecules* **2007**, *40*, 2158.
(18) Jeon, S. I.; Andrade, J. D. *Journal of Colloid and Interface Science* **1991**, *142*, 159.
(19) Jeon, S. I.; Lee, J. H.; Andrade, J. D.; de Gennes, P. G. *Journal of Colloid and Interface Science* **1991**, *142*, 149.
(20) Leckband, D.; Sheth, S.; Halperin, A. *Journal of Biomaterials Science-Polymer Edition* **1999**, *10*, 1125.
(21) Szleifer, I. *Biophysical Journal* **1997**, *72*, 595.
(22) Norde, W.; Favier, J. P. *Colloids and Surfaces* **1992**, *64*, 87.
(23) Wierenga, P. A. Basics of macroscopic properties of adsorbed protein layers, formed at air-water interfaces, based on molecular parameters. PhD Thesis, Wageningen University, 2005.
(24) Murashov, V. V.; Leszczynski, J. *Journal of Physical Chemistry A* **1999**, *103*, 1228.
(25) Claesson, P. M.; Blomberg, E.; Froberg, J. C.; Nylander, T.; Arnebrant, T. *Advances in Colloid and Interface Science* **1995**, *57*, 161.
(26) Carter, D. C.; Ho, J. X. Structure of Serum-Albumin. In *Advances in Protein Chemistry, Vol 45*, 1994; Vol. 45; pp 153.

(27) Wong, D. W. S.; Camirand, W. M.; Pavlath, A. E. *Critical Reviews in Food Science and Nutrition* **1996**, *36*, 807.
(28) Marsh, R. J.; Jones, R. A. L.; Sferrazza, M. *Colloids and Surfaces B-Biointerfaces* **2002**, *23*, 31.
(29) Weisel, J. W.; Stauffacher, C. V.; Bullitt, E.; Cohen, C. *Science* **1985**, *230*, 1388.
(30) Abe, T.; Sheppard, E.; Wright, I. S. *Journal of Physical Chemistry* **1955**, *59*, 266.
(31) Munch, M. R.; Gast, A. P. *Macromolecules* **1990**, *23*, 2313.
(32) Hamley, I. W.; Connell, S. D.; Collins, S. *Macromolecules* **2004**, *37*, 5337.
(33) Li, S. L.; Palmer, A. F. *Macromolecules* **2005**, *38*, 5686.
(34) Ligoure, C. *Macromolecules* **1991**, *24*, 2968.
(35) Brzozowska, A.; Hofs, B.; de Keizer, A.; Norde, W.; Cohen Stuart, M. A. *Submitted*.
(36) Justynska, J.; Hordyjewicz, Z.; Schlaad, H. *Polymer* **2005**, *46*, 12057.
(37) Dijt, J. C.; Cohen Stuart, M. A.; Hofman, J. E.; Fleer, G. J. *Colloids and Surfaces* **1990**, *51*, 141.
(38) Molyneux, P. *Water-soluble synthetic polymers: properties and behavior*; CRC Press, Boca Raton, Florida, US, 1983/84; Vol. I en II.
(39) Perlmann, G. E.; Longsworth, L. G. *Journal of the American Chemical Society* **1948**, *70*, 2719.
(40) van der Veen, M.; Norde, W.; Cohen Stuart, M. A. *Colloids and Surfaces B-Biointerfaces* **2004**, *35*, 33.
(41) Cohen Stuart, M. A.; de Vos, W. M.; Leermakers, F. A. M. *Langmuir* **2006**, *22*, 1722.
(42) Schaaf, P.; Talbot, J. *Journal of Chemical Physics* **1989**, *91*, 4401.
(43) Voets, I. K. Opposites attract?! On the electrostatically driven co-assembly of polymers in aqueous solution. PhD Thesis, Wageningen University, 2008.
(44) Voets, I. K.; de Vos, W. M.; Hofs, B.; de Keizer, A.; Cohen Stuart, M. A.; Steitz, R.; Lott, D. *Journal of Physical Chemistry B* **2008**.
(45) Santore, M. M.; Wertz, C. F. *Langmuir* **2005**, *21*, 10172.
(46) Sofia, S. J.; Premnath, V.; Merrill, E. W. *Macromolecules* **1998**, *31*, 5059.

Chapter Six

General discussion

Introduction

This thesis deals with a special class of polymer nanoparticles (micelles and other complexes) composed of charged polymers. Quite generally, micelles are obtained for molecular systems in which parts with a low solubility are chemically connected to parts with a good solubility. The fact that these antagonistic properties are forced to remain spatially close leads to the characteristic structure of a solvophobic core surrounded by a solvophilic shell or corona. Conventional micelles composed of small amphiphiles (surfactants) are fairly well understood; their size and aggregation number is controlled by a thermodynamic equilibrium, and perturbations out of this equilibrium relax fast. When the amphiphilic molecules are long polymers, however, the relaxation rates increase; polymers in a poor solvent often relax very slowly or not at all. Such a frozen state is commonly referred to as a polymer glass; it precludes that the state of lowest free energy is reached so that the morphology is largely kinetically controlled.

Research on complex coacervate core micelles (C3Ms) was started relatively recently and has focused on the formation of C3Ms, with only little attention being given to the kinetics and reversibility[1-3]. The present thesis deals with these issues. In particular, we investigated how their structures and properties are influenced by the way they are prepared, how their size can be varied, and how they can be used to coat surfaces in order to achieve protein-repellent surfaces. We now discuss what we have learned and what questions remain.

Comparison between C3Ms and amphiphilic polymeric micelles

The basic principles underlying formation of C3Ms and polymeric micelles composed of amphiphilic diblock copolymers are very similar, but there are also notable differences between the two systems. In the case of C3Ms, it is the obligatory co-assembly between oppositely charged polyelectrolytes that is the first step in the micellization pathway (Fig. 6.1). This leads to the formation of a complex or cluster of a certain size, which depends on the concentration and length of the used polyelectrolytes. If the cluster is small, rearrangement into micelles is more easy than for large clusters. For amphiphilic diblock copolymers there are two possible first steps in the micellization pathway. The first is similar to that of the first step in case of C3Ms; upon decreasing the solvent quality for one of the two blocks, the amphiphilic blocks can assembly into a cluster (again, either large or small). Alternatively, intramolecular compaction of the hydrophobic block of the amphiphilic polymer can occur (in aqueous solutions) prior to self-assembly (Fig. 6.1). Which of these

two pathways is taken depends on the concentration of the amphiphilic polymers; at high concentrations self-assembly into clusters is more likely than at low concentrations, where intramolecular compaction is the most likely first step. Both systems may become 'frozen' in a metastable cluster-state; than the energy barrier which needs to be overcome in order for the clusters to rearrange into micelles is so high that the formation of micelles is prevented.

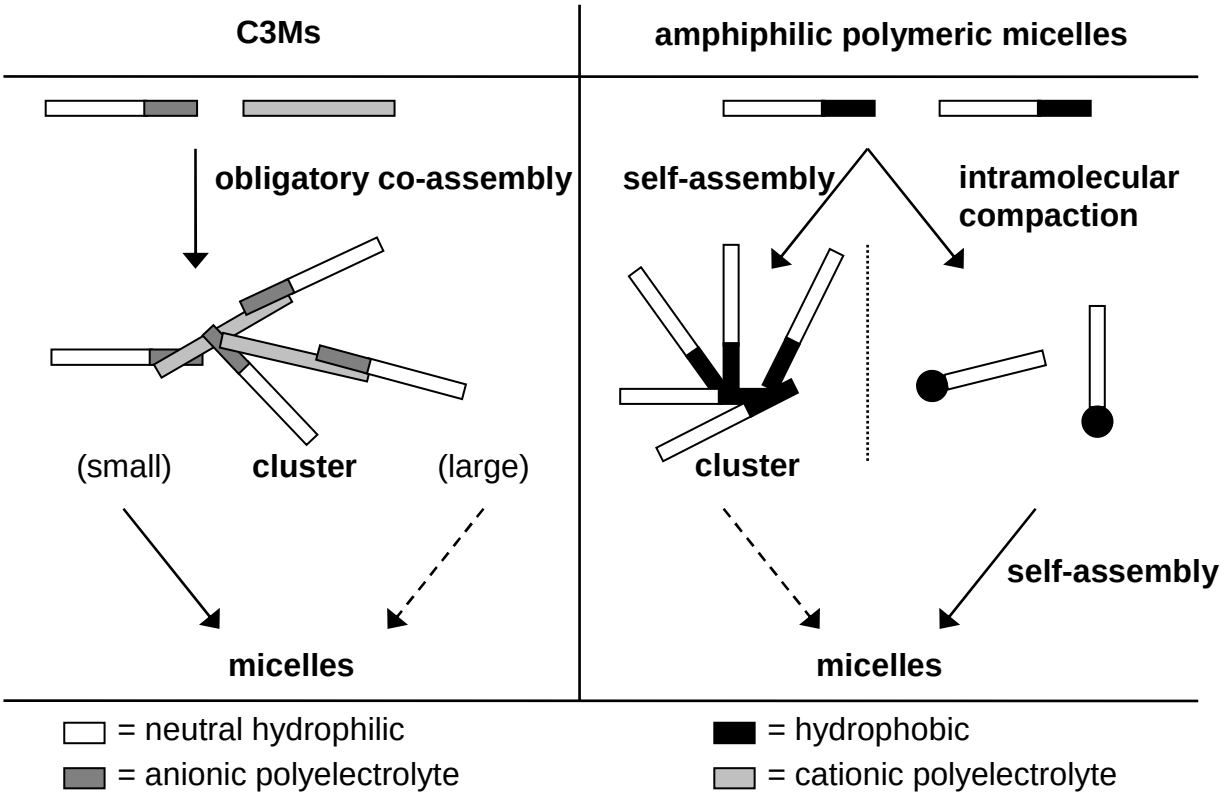

Figure 6.1: Schematic of the micellization pathways of C3Ms and amphiphilic polymeric micelles. On the top the polymers are molecularly dissolved. The first step is (obligatory) co-assembly in the case of C3Ms, and self-assembly or intramolecular compaction in case of amphiphilic polymeric micelles. If assembly occurs, a cluster is formed. Small clusters may rearrange into micelles faster than large clusters (indicated by full and dashed arrow, respectively). If intramolecular compaction occurs, self-assembly into micelles may follow. The legend is shown at the bottom of the scheme.

On the unstable, metastable, and stable state

Generally, little attention has been paid to whether C3Ms are in the thermodynamically stable, metastable, or even unstable state. An unstable state is clearly established when the complexes continually rearrange (e.g. change size) on the timescale of the experiments. The difference between a metastable state and the stable state is more difficult to determine

experimentally, as in both cases the complexes do not rearrange on this timescale. However, when the same state is reached independently of the preparation procedure, one can be fairly sure that the obtained complexes are the stable state. In the case of C3Ms with a polyelectrolyte with a hydrophobic backbone (and a neutral block; $PAETB_{49}PEO_{212}$), it is quite easy to obtain, instead of C3Ms (with a complex coacervate core and a neutral corona), a highly aggregated metastable state, which we denoted as highly aggregated polyelectrolyte complexes (HAPECs, chapter 3). Table 6.1 shows that with different preparation procedures, differently sized aggregates are obtained: for the combination of $PAETB_{49}PEO_{212}$ and PAA_{2000} (f_- = 0.5, pH 7), direct mixing or a f_- titration leads to HAPECs with R_h > 100 nm, whilst a pH cycle gives rise to C3Ms with a R_h of only 25 nm. In a pH cycle the initially obtained HAPEC is first completely dissociated by increasing the pH to an extreme value (in this case 11). The dissociation is only achieved if at least one of the polyelectrolyte species involved in the complex loses nearly all of its charge. Secondly, the complex has to be formed again, in a controlled way, which can be achieved by slowly changing the pH. The charge on the uncharged polyelectrolyte increases and C3Ms are formed again. As in this case fairly similar states are reached with a pH cycle upon reaching pH 7 (either going upwards in pH or downwards; two different paths, see also Chapter 3, Fig. 3.6) we conclude that these C3Ms are probably close to the stable state. However, the pH cycle is not always needed in order to reach the stable state: for C3Ms composed of $PDMAEMA_{150}$ and $PAA_{26}PAAm_{405}$ there is no observable difference in light scattering intensity and R_h between samples obtained after direct mixing and after a pH cycle. These C3Ms are therefore believed to be in the stable state. Compared to such a C3M system, C3Ms with a polyelectrolyte having a hydrophobic backbone have an increased chance of ending up in a metastable state.

Furthermore, for C3Ms with $PAETB_{49}PEO_{212}$ the difference between the stable state (which is probably the one obtained via a pH cycle) and the metastable state (obtained by direct mixing of solutions with matched pH, or f_- titration) may be small if one uses a short oppositely charged polyelectrolyte. The C3Ms obtained by mixing solutions of $PAETB_{49}PEO_{212}$ and PAA_{140} (f_- = 0.50, 10 mM $NaNO_3$, chapter 3) have a R_h of about 25 nm (Table 6.1). This is a reasonable value for micelles composed of these polymers which fits well with the expected core-corona structure. However, a pH cycle (Table 6.1) leads to C3Ms with a R_h of only 15 nm. It seems that the C3Ms with the higher radius are slightly more highly aggregated species (HAPECs), which are not in the stable state, but rather in a metastable state (as the R_h does not change with time). For complexation between PAA_{2000}

and $PAETB_{49}PEO_{212}$, the difference in particle size between the metastable state (obtained with direct mixing, matched pH`s, or f_- titration) and the stable state is much larger; about 100 vs. 25 nm, respectively. Thus, the difference observed increases with increasing length of the complexing homopolyelectrolyte, probably as upon initial complexation larger networks are formed.

PAA_x, x =	f_-	DM, matched pH`s		DM, non-matched pH`s, t = 0 days	f_- titration	pH cycle
		t = 0 days	t = 2 days			
2000	0.3	70	50	-	65	-
	0.5	100	100	>100	120	25
	0.7	150	25	-	40	-
140	0.5	-	-	>100	25	15

Table 6.1: Overview of obtained R_h for C3Ms and HAPECs composed of $PAETB_{49}PEO_{212}$ and PAA_x. DM = direct mixing of two solutions containing the oppositely charged polymers; both in the case of matched pH`s or non-matched pH`s this leads to very large aggregates in a metstable or unstable state. In a f_- titration one polymer species is slowly added to the other. In a pH cycle the pH is slowly changed from 3 to 11 to 3 by the addition of acid/base. Polymer concentration was around 1 g/l and background solvent was 10 mM $NaNO_3$ (prior to the preparation procedure) in all cases.

Introducing an extra polyelectrolyte species in order to increase the volume of the core of the C3Ms (to create C3-μEs) also enhances the likelihood of obtaining metastable states (chapter 4). For the three-component ($PDMAEMA_{150}$, PAA_{140}, and $PAA_{26}PAAm_{405}$) system in $NaNO_3$ solutions, even the pH cycle (previously shown to be a good method to get at least close to the stable state) gives highly path-dependent results (Fig. 6.2). The reason for this is probably the bimodal molecular weight distribution in the PAA species (there being both PAA_{26} and PAA_{140}). The affinities of these two species of PAA for the oppositely charged PDMAEMA are different, with PAA_{140} having the largest affinity, as is evident by the larger pH range of complexation observed for the C3-μE system compared to the C3M system (Fig. 6.2). As a result, slowly changing the pH of the three component solutions from 11 back to 7 will initially result in complexation between the two homopolyelectrolytes. At a somewhat lower pH, the diblock copolymer will also start to participate in the complexation with PDMAEMA. A highly aggregated complex is produced (much bigger than the stable state

particles found in phosphate buffer, where the C3-μEs have a R_h of 25 nm), because first a PEC is grown onto which the stabilizing diblocks attach at a lower pH. Even more highly aggregated complexes appear when the three component complexes are built up by increasing pH from 3 to 7.

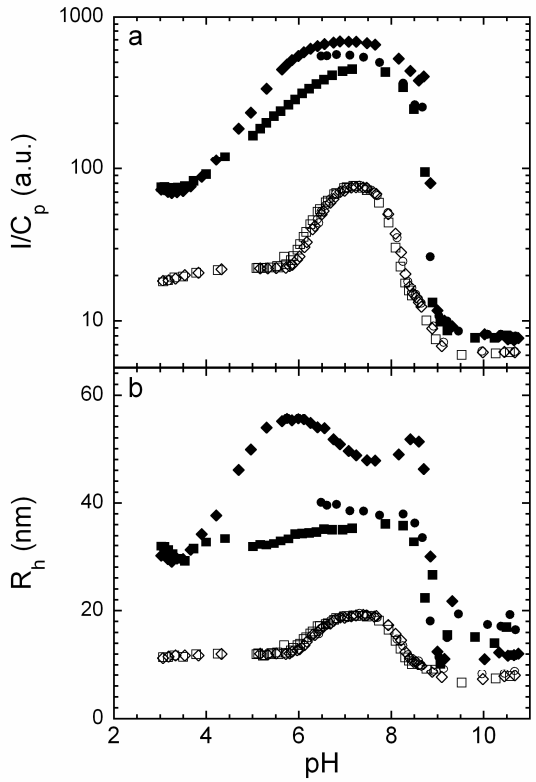

Figure 6.2: pH cycle; (○,●) pH up to 11, (□,■) pH down to 3, (◊,♦) pH up to 11. Open symbols for the solution/C3Ms with $PAA_{26}PAAm_{405}$ and $PDMAEMA_{150}$, closed symbols for the solution/C3-μEs with $PAA_{26}PAAm_{405}$, PAA_{140} and $PDMAEMA_{150}$, β = 2. Solvent is 10 mM $NaNO_3$, f_+ = 0.50. a) Light scattering intensity, I, divided by total polymer concentration, C_p. b) Hydrodynamic radius, R_h, as a function of pH.

These examples show that often there are experimental difficulties in obtaining C3Ms in the stable (i.e. lowest free energy) state. These difficulties are similar to the difficulties encountered upon preparing amphiphilic polymeric micelles in the stable state. The difficulties in both cases stem from the fact that the solubility of the core forming material in water is low. However, by taking different routes, especially those in which more time to reach equilibrium is given during complexation, e.g. by slowly increasing the complexation strength (as is for instance done by slowly dialysing to a selective solvent in the case of

amphiphilic polymeric micelles, or by a pH cycle or salt reduction by dialysis in case of C3Ms), it is sometimes possible to obtain aggregates whose composition and shape are virtually indistinguishable from the stable state. All this shows that, in the language of colloid science, C3Ms can be seen as intermediate between hydrophilic (reversible) association colloids and micelles from amphiphilic diblock copolymers.

Rearrangements

When, upon direct mixing a random primary complex between the polyelectrolytes has been formed, most of the associated energy and entropy changes (coming from Coulombic interactions between the oppositely charged polyelectrolytes and release of counter-ions, respectively) have already occurred. Theoretically, the micellar size is calculated from the balance between the tendency to contract due to the interfacial tension (between the core and the solvent) and the tendency to swell due to osmotic pressure generated by the neutral blocks. From this balance, a free energy profile is obtained which features an equilibrium between unimers and micelles with sizes distributed around an optimal value. There is a modest gain in translational entropy if there are more and smaller micelles, however, this will also lead to a larger interfacial area between core and solvent and this is a stronger effect. Thus the driving force for rearrangements towards more and smaller micelles may be low.

The mechanisms which can lead to rearrangements of our C3Ms around $f_+ = 0.50$ are the following: (i) dissociation, diffusion and association of a single polymer (i.e. one polyelectrolyte detaches from the complex coacervate core of a particular C3M and then complexes with a different one[4]), (ii) reptation, where one polyelectrolyte slides along an oppositely charged one, thus rearranging the structure, and (iii) merging of two C3Ms followed by splitting up[4]. The first and especially third option are presumably very slow processes as the neutral corona acts as a powerful steric barrier which has to be overcome in order for rearrangements to take place. The second, reptation, acts only intra-C3M. The slow speed of the rearrangement processes, as well as the low driving force and the tendency to initially form a random complex, are the main reasons why systems are easily trapped in a metastable state.

The speed of the rearrangements in polyelectrolyte complexes comprising a diblock copolymer with a charged and a neutral block depends on the following factors (chapter 3):

(i) Salt, the addition of which has been shown in one case[1] to enhance the rate of rearrangements by a factor of 10^4, supposedly by increasing the critical micellar concentration (CMC) and/or reptation speed.

(ii) The total number and size of the neutral blocks in the diblock copolymer, since a larger fraction of neutral chains increases the energy barrier controlling the merging of two C3Ms and the entry of a single polymer into a C3M.

(iii) The chemistry of the polyelectrolytes: more hydrophobic backbones give stronger cohesion and slower rates of rearrangements.

(iv) Excess charge, which can either increase or decrease rearrangement rates. Around $f_- = 0.5$ there is little or no excess charge and hence the complexes are more stable, whereas deviating from $f_- = 0.5$ increases the net charge of the complexes and thus increases the rearrangement rate by increasing the CMC. Alternatively, excess charge leads to electrical double layer repulsion, and decreases the chance of two C3Ms merging and thus the rearrangement rate. Measurements (chapter 3) suggest that the former effect is dominant.

Most C3Ms, HAPECs, and both non-relaxed C3-μEs and C3-μEs at $f_+ = 0.50$ that we investigated show no change in the R_h with time once they are formed. Also, for non-relaxed C3-μEs, heating nor ultrasonication have an effect on the R_h. This indicates that the aggregates, once formed, do not rearrange intermicellarly, i.e. by mass transfer between the micelles. Intermicellar rearrangement after formation takes place only away from $f_+ = 0.50$ (chapter 3), or upon applying a pH cycle (which rearranges the complex from the inside out, by changing the charge balance leading to dissociation, followed by reassociation of the oppositely charged weak polyelectrolytes). Also, changing the charge balance by adding extra polyelectrolyte will lead to rearrangements.

Mixing two populations of C3Ms can also give more insight into rearrangements. For example, upon mixing (1:1) a solution of C3Ms (composed of $PAA_{26}PAAm_{200}$ and $PDMAEMA_{150}$, $f_+ = 0.50$, phosphate buffer with an ionic strength of 40 mM, $\beta = 1$) with C3-μEs (composed of same + PAA_{140}, $f_+ = 0.50$, same solvent, $\beta = 4$) one could either obtain a bidisperse solution with both species present (if no rearrangements take place), or if rearrangements are fast, one could obtain the average stable state for the new composition ($\beta = 2.5$). For the C3Ms at $\beta = 1$, $R_h = 15$ nm and the light scattering intensity $I = 60$. For the C3-μEs, $R_h = 38$ nm and $I = 820$. In the first scenario (no rearrangements) one should find a $\langle R_h \rangle$ slightly smaller than 38 nm (as this is the weight average which is determined with light scattering), with an average $\langle I \rangle$ of 440. In the second scenario (fast rearrangements) one should find C3-μEs (interpolated from results in chapter 4) with $R_h = 25$ nm and $I = 250$. The experiment, however, gives a solution containing particles with $R_h = 39$ nm and $I = 620$. This

scattering intensity is even higher than the one expected if the two solutions just mix without any changes in aggregation number, indicating that some kind of aggregation takes place. This shows that these kind of systems do somehow rearrange upon mixing of two different populations, but not in the direction of a monodisperse system. Perhaps Ostwald ripening (where big particles grow at the expense of small ones, a common phenomenon when dealing with e.g. emulsions) occurs, but more research is needed before we can draw any conclusions. Most importantly, even at the relatively high salt concentration used for this experiment (40 mM ionic strength phosphate buffer; critical salt concentration is about 0.1 M) the complexes formed show intermediate behaviour: they do not rearrange to the stable state, nor are they completely kinetically frozen.

Another, aggressive, way of manipulating these complexes is by applying a strong DC electric field, as is done in Kerr effect measurements (also called electro-optic birefringence measurements). In these, a very short DC pulse is generated and applied over an aqueous solution and the changes in birefringence as a function of the strength of the electric field that is applied are recorded. We performed a series of these Kerr effect measurements on aqueous solutions (1 mM $NaNO_3$) containing C3Ms, and found that, as a side-effect of the applied DC pulses (field strength about 2×10^5 V m^{-1} and pulse length about 1×10^{-5} s), the R_h of C3Ms composed of $PAETB_{49}PEO_{212}$ and PAA_{42} increases from 20 to 38 nm, while the light scattering intensity only increases 2.5 fold. For C3Ms from $PAA_{42}PAAm_{417}$ and $PDMAEMA_{150}$, R_h only slightly increases (25 to 27 nm). Clearly in the former case the C3Ms do not rearrange back to the stable state after an applied DC field has changed their size and aggregation number, showing such rearrangements are very slow or absent – that the particles are in effect kinetically frozen. Also, the field strength required to produce a measurable effect is high, showing that a high force is needed in order to induce rearrangement of C3Ms in a solution with a low salt concentration.

Control of size

The research performed in both chapter 2 and 4 shows that the size of C3Ms (or C3-μEs) can be controlled. The C3-μEs made in chapter 4 have hydrodynamic radii varying from about 15 to 100 nm and the preparation procedure is easy. The control of size is potentially useful, for instance for drug-delivery purposes where control of the size of the nanoparticles can increase the delivery of these by passive targeting[5]. Furthermore, the ease at which new types of C3-μEs, using various diblock copolymers with different neutral blocks, can be made is useful, as the outer shell is a second variable that partly determines the efficiency of

nanoparticles used in drug-delivery[5]. Because both the size and the corona structure can be controlled in the case of C3-μEs, this would allow in principle (with careful screening) to find the most efficient formulation. However, the use of C3-μEs for drug-delivery has several drawbacks which have to be addressed. One is the possible toxicity of the charged components (mainly the cationic) of the C3-μEs. Another is the finite although low CMC; upon administering a solution of the particles to a patient, their concentration will drop rapidly and then the particles might dissociate, loosing their advantageous properties. Both problems might be decreased by cross-linking the oppositely charged polyelectrolytes after formation of the C3-μEs.

Micelles as surface coating

One area of possible application of C3Ms is as coatings on surfaces in order to prevent protein adsorption[6]. In principle, a polymer brush on a surface is capable of preventing protein adsorption. However, a certain brush density is needed for maximum effectiveness (no protein adsorption)[7,8]. If the brush layer is not homogeneous in the plane of the surface, proteins may adsorb in areas where the polymer density is low, as we have seen in chapter 5. AFM images indicated that the adsorption of C3Ms with more glass-like cores to SiO_2 and to cross-linked 1,2-PB occurs in the form of intact C3Ms, which gives rise to surfaces carrying randomly distributed C3Ms. Proteins were shown to adsorb to the coated surfaces to various degrees, presumably at locations where the polymer density was lower ('in between' the adsorbed C3Ms). Micelles composed of amphiphilic diblock copolymers have the same disadvantage as the mentioned C3Ms, that is, that they tend to adsorb as micelles, or in the case of non-adsorbing water soluble chains, as hemispheres. Decreasing the size of the adsorbing micelles would not only decrease the size of the 'holes', but also the driving force for adsorption and the distance over which the steric barrier – which acts to prevent protein adsorption to the surface – acts. For the smallest micelles, those composed of surfactants, it is known that the adsorbed layer is usually washed off by rinsing with solvent[9]; such a layer is not suitable as a protein-repellant coating.

C3Ms consisting of polyelectrolytes having less hydrophobic backbones have the disadvantage that their density is lower. Upon adsorption onto a surface, the polymer density achieved is relatively low, compared to the polymer densities reachable with other methods. Even so, they can be effective in preventing adsorption of a single type of protein[6]. However, a coating of a certain type of C3Ms is unable to prevent adsorption of a variety of proteins[10], presumably because the polymer density reached is simply not high enough. Hence, steric

hindrance alone is not enough; the contribution of at least one additional factor (e.g. charge) is needed to fully prevent adsorption of a protein.

Another question which has to be addressed is for how long (time) a given polymer brush on a substrate is effective. One problem of using PEO (commonly used for making polymer brushes) is its (bio)degradability[11,12]. As it is expected to degrade with the passage of time, a polymer brush with PEO is not very suitable for long-term usage. Damage to the layer has to be prevented as well (or repaired very quickly), so the layer has to be scratch-resistant (or, alternatively, self-healing). More research is currently being performed, and it is much needed.

Further research

In order to form C3Ms in the stable state, the same trick that is applied to obtain micelles from amphiphilic polymers would work; that is, dissolve the diblock copolymers and polyelectrolytes in a water-miscible, non-selective solvent (i.e. a solution with a salt concentration above the critical one) and then change the solvent quality in order to induce complexation (i.e. by dialysis against water). Upon decreasing the salt concentration, the attractive interaction between the oppositely charged polyelectrolytes is slowly increased. As weak interactions most likely result in complexes in thermodynamic equilibrium, it is also more likely that the complexes will be close to the stable state as the interaction is slowly increased in strength. However, the same things that cause difficulties for amphiphilic diblock copolymers (polydispersity of the used polymers, freezing-in of the structure at a certain ratio of non-selective/selective solvent or for C3Ms, salt concentration) could also play a role here. Polydispersity of the polyelectrolytes (especially the shortest species) is the main problem and therefore it would be best to eliminate this factor. This may perhaps be accomplished by using human-designed, nature-made polymers (for a review on these genetically engineered protein-based polymers, see[13]) instead of chemically synthesized polymers. The effect of polydispersity on the formation of C3Ms is also interesting to study: especially polydispersity of the homopolyelectrolyte and the polyelectrolyte block of the diblock copolymer. Polydispersity in the neutral block will probably have only small effects on the formation of C3Ms.

The rearrangement processes of C3Ms are poorly understood. A study into the relative importance of the different rearrangement mechanisms with respect to a variation of salt concentration would be interesting. As the salt concentration is increased towards the critical salt concentration (above which no C3Ms are formed) the shift in CMC might result in faster

rearrangements as the dissociated state becomes more common. Also, the role of the neutral blocks forming the neutral corona should be investigated. With shorter neutral blocks the rearrangements should be faster as well as the steric barrier, generated by the density and height of the corona, that has to be overcome by a single polymer chain is expected to be lower for shorter neutral blocks. Combining such a study with the effect of mixing different populations of C3Ms (with either unlabeled C3Ms or C3Ms labelled with fluorescent groups, e.g. an acceptor and donor pair) should lead to a significant increase in our understanding of how these systems behave and which parameters govern their rearrangement rate.

Literature

(1) Cohen Stuart, M. A.; Besseling, N. A. M.; Fokkink, R. G. *Langmuir* **1998**, *14*, 6846.
(2) Voets, I. K.; de Keizer, A.; Cohen Stuart, M. A.; Justynska, J.; Schlaad, H. *Macromolecules* **2007**, *40*, 2158.
(3) Holappa, S.; Kantonen, L.; Andersson, T.; Winnik, F.; Tenhu, H. *Langmuir* **2005**, *21*, 11431.
(4) Halperin, A.; Alexander, S. *Macromolecules* **1989**, *22*, 2403.
(5) Brigger, I.; Dubernet, C.; Couvreur, P. *Advanced Drug Delivery Reviews* **2002**, *54*, 631.
(6) van der Burgh, S.; Fokkink, R.; de Keizer, A.; Cohen Stuart, M. A. *Colloids and Surfaces A: Physicochemical and Engineering Aspects* **2004**, *242*, 167.
(7) Currie, E. P. K.; Norde, W.; Cohen Stuart, M. A. *Advances in Colloid and Interface Science* **2003**, *100*, 205.
(8) Pasche, S.; De Paul, S. M.; Voros, J.; Spencer, N. D.; Textor, M. *Langmuir* **2003**, *19*, 9216.
(9) Zhang, R.; Somasundaran, P. *Advances in Colloid and Interface Science* **2006**, *123*, 213.
(10) Brzozowska, A. M.; Hofs, B.; de Keizer, A.; Fokkink, R.; Cohen Stuart, M. A.; Norde, W. *In preparation* **2008**.
(11) Pepic, D.; Zagar, E.; Zigon, M.; Krzan, A.; Kunaver, M.; Djonla, J. *European Polymer Journal* **2008**, *44*, 904.
(12) Kumagai, Y.; Doi, Y. *Polymer Degradation and Stability* **1992**, *35*, 87.
(13) Haider, M.; Megeed, Z.; Ghandehari, H. *Journal of Controlled Release* **2004**, *95*, 1.

Summary

The research described in this thesis concerns the formation, solution properties, and adsorption of polyelectrolyte complexes composed of at least one diblock copolymer with a neutral and a charged block and either an oppositely charged homopolyelectrolyte or a diblock copolymer, with a neutral block and an oppositely charged polyelectrolyte block. Upon mixing the aqueous solutions of different polymers, the oppositely charged polyelectrolytes associate, forming a polyelectrolyte complex. If the resulting complex is liquid-like we call it a complex coacervate. If the neutral blocks are large enough with respect to the charged ones and the oppositely charged components are mixed at a 1:1 charge ratio (charge stoichiometric ratio), they stop the growth of the polyelectrolyte complex in such a way that complex coacervate core micelles (C3Ms) are formed. This is usually a spherical particle, which has a core comprised of the oppositely charged polyelectrolytes, surrounded by a corona of neutral polymer chains. Away from the stoichiometric mixing ratio, smaller complexes are formed, which are called soluble complex particles (SCPs). The micelles are the main focus of this thesis, but the formation of the soluble complex particles is also investigated. The salt concentration, pH, and the chemical structure of the polyelectrolytes are important variables in the formation of these polyelectrolyte complexes.

In *chapter 2* C3Ms were made from multiple polymer species; a diblock copolymer with a polyelectrolyte block and a neutral block, poly(acrylic acid)-block-poly(acryl amide), an oppositely charged polyelectrolyte, poly(N,N-dimethyl aminoethylamide), and a second diblock copolymer species with a charged block and a neutral block, poly(N,N-dimethyl aminoethylamide)-block-poly(glyceryl methacrylate). The polyelectrolyte block of the second diblock copolymer species had charged blocks that were oppositely charged to that of the first diblock copolymer species and whose neutral block was different from that of the first diblock copolymer. The effect of systematically varying the ratio of the homopolyelectrolyte and second diblock copolymer (based on the number of chargeable groups), while keeping the mixing fraction f_+ (that is the number of positively chargeable groups, divided by the total number of chargeable groups) constant, was studied with light scattering. It was shown that the size of the resulting C3Ms decreased with increasing percentage of the second diblock copolymer. Without the second diblock copolymers the C3Ms have a hydrodynamic radius of 25 nm, whilst with only second diblock copolymer they have a radius of only 16 nm. Using a simple geometrical model and the light scattering intensities, the aggregation numbers were estimated to be in the range of 20-70 polymers.

In *chapter 3* the formation of both SCPs and C3Ms was studied. The used diblock copolymer, poly([4-(2-aminoethylthio)-butylene] hydrochloride)-block-poly(ethylene oxide), has a polyelectrolyte part with a rather hydrophobic backbone which slows down the formation and subsequent rearrangements to a pace where it could be easily followed with light scattering. It was mixed with the oppositely charged poly(acrylic acid) at different f_+. Using light scattering and cryogenic transmission electron microscopy, it was shown that the complexes formed at $f_+ = 0.3$ are initially very large (> 140 nm) and network like (as there is relatively little neutral polymer to stop the growth of the complexes), and rearrange relatively quickly, compared to the complexes formed at $f_+ = 0.5$ and 0.7 (80 nm), towards small micellar complexes. The very large transient complexes formed at $f_+ = 0.3$ are called highly aggregated polyelectrolyte complexes (HAPECs). The complexes formed at $f_+ = 0.5$ are apparently most stable; that is, their size remains the same in time. It was concluded that there are at least three factors which influence the rearrangement rate of polyelectrolyte complexes; (1) high neutral blocks content, (2) excess charge, and (3) the chemistry of the polyelectrolytes. Increasing the salt concentration has previously been determined to speed up the rate of rearrangements as well. Furthermore, the radius of the complexes at $f_+ = 0.5$ (80nm) is too large for the complexes to have the typical core-corona structure. Apparently, these large complexes are HAPECs as well. However, with different preparation procedures micelles can be obtained; if the HAPECs are forced to disassemble by changing the pH to an extreme value (either 11 or 3) and are subsequently re-assembled by changing the pH back to normal (7), the resulting C3Ms have a radius of about 15 nm. This is probably the state of minimum free energy, the stable state, whereas the highly aggregated complexes are in a metastable state (as they do not spontaneously rearrange in time).

In *chapter 4* complex coacervate core micro-emulsions (C3-μEs) were obtained by mixing solutions of anionic polyelectrolytes (poly(acrylic acid)) and diblock copolymers with an anionic polyelectrolyte block and a neutral block (poly(acrylic acid)-block-poly(acryl amide)) with solutions of a cationic polyelectrolyte (poly(N,N-dimethyl aminoethylamide)). By varying the fraction of the anionic polyelectrolyte and anionic diblock copolymer species, while keeping f_+ constant, C3-μEs with radii varying from about 15 to 100 nm were prepared. Basically, these are C3Ms in which the core is swollen with extra complex, composed of oppositely charged homopolyelectrolytes. The core of C3-μEs could be swollen up to an anionic polyelectrolyte/neutral groups ratio of about one. At higher core forming polyelectrolyte content the PAAm is no longer present in high enough amounts to prevent

precipitation. The solvent was shown to have a pronounced effect upon the size of the obtained complexes; in $NaNO_3$ larger complexes were obtained which are in a metastable state. In phosphate buffer (a salt known to weaken the attractive forces between the used polyelectrolytes), smaller complexes were obtained, which are probably in the stable state. The geometrical model introduced in *chapter 2* was extended and predicted a linear growth of the C3-μEs. The experimentally observed growth was however, non-linear, probably due to a transition of the neutral polymers in the corona from more star-like to more crew-cut behaviour (shown by self consistent field calculations).

In *chapter 5* the ability of a layer of adsorbed C3Ms with a more glass-like core (composed of poly([4-(2-aminoethylthio)-butylene] hydrochloride)-block-poly(ethylene oxide) and poly([4-(2-carboxy-ethylthio)-butylene] sodium salt)-block-poly(ethylene oxide)), to prevent protein adsorption to either silica or cross-linked 1,2 polybutadiene was investigated. With atomic force microscopy it was shown that the layer consists of closely packed adsorbed complex coacervate core micelles. Protein adsorption to the coated surfaces was generally reduced by > 80 %, and showed the following trends: (i) Protein adsorption to the coated polybutadiene was reduced to a lower extent than to coated silica. (ii) The adsorption behaviour of the protein lysozyme on one hand, and bovine serum albumin, β-lactoglobulin, and fibrinogen on the other, onto the two types of coated surfaces was reversed by solvent ($NaNO_3$ or phosphate buffer). (iii) The difference in adsorbed amount before and after rinsing with solvent was generally low (about 0.1 mg/m^2 or less). Lysozyme is an exception as at low ionic strength, rinsing with solvent causes a large decrease in the adsorbed amount. (iv) Preventing adsorption of β-lactoglobulin adsorption appears most difficult as the achieved reduction was least and shows further complications. Adsorption of β-lactoglobulin from 100 mM $NaNO_3$ to coated silica lead to a net desorption; this means that the coating is partially removed or replaced by the protein.

This thesis shows that many polyelectrolyte complexes formed by mixing of aqueous solutions of oppositely charged polyelectrolytes and charged-block-neutral diblock copolymers are not in the stable state. It seems that most C3Ms, once formed at stoichiometric charge ratio, are kinetically frozen, as they do not rearrange much, even upon mixing of two populations. However, they do respond to changes in the charge balance, although they do not necessarily rearrange to the state of lowest free energy. This behaviour seems to stem from the strength of the forces and the height of the energy barriers involved. For instance, most of the associated energy and entropy gain associated with the formation of C3Ms (coming from

Coulombic interactions and counter-ion release) occurs in the initial formation of the polyelectrolyte complexes. Therefore, mixing C3-μEs with C3Ms (both composed of basically the same polymers) does not lead to large rearrangements as the driving force is small and the barrier is high; single polymers need to dissociate, diffuse, penetrate the neutral corona, and associate again. The small driving force which tries to minimize the interfacial area between the core and the solvent stems from the low interfacial tension of these systems (the complex coacervate core contains mostly water). This force is partly counteracted by the entropy that can be gained by increasing the number of particles and by the osmotic pressure generated by the neutral blocks that form a corona. Changes in the charge balance, however, (e.g. via a pH change) act quickly within a single micelle and are not hindered by a steric barrier. For single polyelectrolytes the association with a C3M results in a rather high energy gain; this combined with the fact that no dissociation is required makes these changes relatively quick as well, compared to the very slow inter-micellar rearrangements. Thus, the time scales on which SCPs and C3Ms rearrange spans a very wide range.

Samenvatting

Het onderzoek beschreven in dit proefschrift betreft de vorming van kolloïden uit tegengesteld geladen polymeren. Kolloïden zijn kleine deeltjes die in een oplossing zweven; de vetbolletjes en eiwit aggregaten in melk zijn voorbeelden van kolloïden. De grootte van kolloïdale deeltjes (ruwweg 0,00000001 tot 0,00001 meter – 10 nanometer, nm, tot 10 micrometer, μm) staat ongeveer in dezelfde verhouding tot de mens (2 meter) als dezelfde mens tot de omtrek van de aarde (40.000.000 meter). Polymeren bestaan uit kleine eenheden, genaamd monomeren (grootte ongeveer 1 nm), die aan elkaar vast zitten en samen een polymeer vormen. De hier gebruikte polymeren hebben een lineaire structuur; d.w.z. dat de monomeren aan elkaar zitten zoals bv. de wagons van een goederentrein. De verschillende monomeren van de gebruikte polymeren hebben verschillende eigenschappen; sommige zijn positief (+) geladen, andere negatief (-), en een derde soort is neutraal (N). Naast simpele polymeren die maar uit één soort monomeren bestaan; --------, ++++++ (dit zijn beiden polyelectrolieten), of NNNNNNNN, hebben we zogenaamde di(=twee)blok co-polymeren gebruikt. Deze bestaan uit twee soorten monomeren, bv. + en N en zien er ongeveer zo uit; ++++++NNNNNNNN. Als je een waterige oplossing van negatief geladen polymeer en een oplossing van diblok copolymeer met een positief geladen blok en een neutraal blok mengt, zullen de tegengesteld geladen blokken dicht bij elkaar gaan zitten, oftewel complexeren. Het gevormde polyelectrolietcomplex (PEC) is echter niet goed oplosbaar in water. Het PEC zal groeien (complexeren met andere kleine PECs) om het contactoppervlak met water te minimaliseren. De groei van dit PEC kan worden gestopt door de waterminnende neutrale blokken; als dit gebeurd dan is er een kolloïd van tegengestelde polymeren ontstaan (voor een schematisch plaatje hiervan, zie Fig. 1.5). Als de deeltjes, zoals in Fig. 1.5, een kern hebben die bestaat uit een PEC en een mantel daaromheen die bestaat uit de neutrale waterminnende polymeerblokken, dan heet het kolloïd een ‘complex coacervaat kern micel’ (C3M).

Er zijn een aantal variabelen van belang voor de vorming van C3Ms en PECs. De zoutconcentratie van de waterige oplossing kan zo hoog worden gemaakt dat er geen PECs gevormd worden, of dat ze uit elkaar vallen. De chemische structuur van de polyelectrolieten speelt een rol; bij zwakke polyelectrolieten is de lading pH afhankelijk. De verhouding tussen de lengte van het geladen en neutrale blok van het diblok copolymeer, en ook de mengverhouding van de tegengesteld geladen polymeren beïnvloed de vorming van de kolloïden. Deze mengverhouding is in dit proefschrift uitgedrukt als de mengfractie, f_+, dit is

het aantal positief oplaadbare monomeren gedeeld door het totaal aantal oplaadbare monomeren.

De meest gebruikte techniek (in dit proefschrift) is lichtverstrooiing. Hierbij laat je een lichtstraal van een laser door een oplossing met kolloïden gaan. Het licht wordt door de kolloïden, en ook het water, verstrooid. De fluctuaties in het verstrooide licht worden gevolgd en met deze informatie wordt de deeltjesgrootte, de hydrodynamische straal, R_h, bepaald (de snelheid van de fluctuaties is afhankelijk van hoe snel de deeltjes bewegen en grotere deeltjes bewegen langzamer). Grotere deeltjes verstrooien veel meer licht dan kleine, en zo 'zie' je voornamelijk de kolloïden.

In *hoofdstuk 2* staat beschreven wat er gebeurd als je een aantal dingen varieert. Als één van de twee tegengesteld geladen polymeren in overmaat aanwezig is krijg je kleinere kolloïden (genaamd 'oplosbaar complex deeltjes' (SCPs)) dan als ze één op één ($f_+ = 0.50$) worden gemengd (Fig. 2.3b); dit omdat ladingsopbouw de groei van de deeltjes tegengaat. Als je C3Ms maakt van een diblok copolymeer met een geladen en een neutraal waterminnend blok en een tegengesteld geladen polyelectroliet, zijn de C3Ms groter dan als je een gedeelte (of alle) van de polyelectrolieten vervangt door een diblok copolymeer met een blok met dezelfde lading en een neutraal waterminnend blok (Fig. 2.5); dit omdat de neutrale blokken de groei van de kolloïden tegengaan. Door een simpel geometrisch model van de C3Ms te combineren met de lichtverstooiingsdata werd er geschat uit hoeveel polymeren de C3Ms ongeveer bestaan; 20-70.

In *hoofdstuk 3* is de vorming van C3Ms en SCPs bestudeerd. We gebruikten hiervoor een kort (±150 monomeren lang) of lang (2000 monomeren lang) negatief geladen polyelectroliet, in combinatie met een diblok copolymeer met een positef geladen blok met een waterhatende ruggegraat en een neutraal waterminnend blok. Deze waterhatende ruggegraat zorgt ervoor dat de herschikking van de gevormde kolloïden langzamer gaat. Bij menging van de oplossingen van de tegengesteld geladen polymeren worden er 'grote geaggregeerde polyelectrolietcomplexen' (HAPECs) gevormd; deze deeltjes hebben niet de kern-mantel structuur van een C3M (Fig. 1.5), maar meer een netwerk structuur (Fig. 3.9a). Als de mengfractie $f_+ = 0.3$, worden de gevormde HAPECs kleiner met het verloop van tijd; na een dag zijn ze ongeveer tien keer zo klein (Fig. 3.3b). Bij $f_+ = 0.5$ zijn er geen veranderingen in de grootte van de HAPECs waargenomen (ze zitten in een ingevroren toestand), en bij $f_+ = 0.7$ is er geen waarneembare verandering met het korte polyelectroliet, maar een langzame met het lange.. We concluderen dat neutrale blokken in de weg zitten en

de snelheid van herschikking verlagen, terwijl ladingsopbouw de herschikkingsnelheid versnelt. Om van deze polymeren kolloïden met de kern-mantel structuur van C3Ms te maken, moet je ze, na vorming, uit elkaar laten vallen door de pH te verhogen om ze daarna door de pH langzaam terug te veranderen weer te laten complexeren (Fig. 5b).

In *hoofdstuk 4* hebben we C3Ms gemaakt waarvan in de kern extra PEC zit. Het extra kernmateriaal bestaat uit tegengesteld geladen polyelectrolieten. De mantel uit de waterminnende neutrale polymeren. De grootte van de gevormde kolloïden hangt niet alleen af van de hoeveelheid extra kernvormend materiaal dat wordt aangeboden, maar ook van welk zout je gebruikt: als je een oplossing met natrium nitraat gebruikt worden ze groter dan als je een fosfaatbuffer gebruikt (Schema 4.1, Fig. 4.4 en 4.5). Het verschil tussen de beide gevallen wordt veroorzaakt doordat de meerwaardige fosfaationen de binding tussen de gebruikte tegengesteld geladen polyelectrolieten verzwakken. De grotere gezwollen deeltjes die worden gevormd in de oplossing met natrium nitraat noemen we niet-ontspannen ‘complex coacervaat kern micro-emulsies’ (C3μ-Es); deze zitten in een ingevroren toestand. De kleinere die gevormd worden in fosfaatbuffer noemen we C3μ-Es. Het geometrische model dat is geïntroduceerd in hoofdstuk 2 werd uitgebreid om ook op C3μ-Es van toepassing te zijn en voorspelde een lineaire groei. De geobserveerde experimentele afwijkingen van de voorspelde groei, komen waarschijnlijk van de overgang van een kleine naar een grote kern (met een respectievelijk grote en kleine kromming op het oppervlak van de kern); de neutrale waterminnende ketens gedragen zich hierdoor anders.

In *hoofdstuk 5* worden C3Ms gebruikt als oppervlakte-deklaag. De gebruikte C3Ms bestaan uit diblok copolymeren met een geladen en neutraal blok, waarvan de geladen blokken tegengesteld geladen zijn en beiden een waterhatende ruggegraat hebben. De gebruikte C3Ms hebben dan ook een relatief waterhatende kern. Ze adsorberen in ongeveer even grote hoeveelheid op het waterminnende oppervlak silica, en het waterhatende poly-butadieen. Met behulp van de ‘atomaire kracht microscoop’ (AFM) werd gezien dat de C3Ms zijn geadsorbeerd als C3Ms (Fig. 5.4). De adsorptie van eiwit op de bedekte oppervlakken was gemiddeld ongeveer 80% minder dan op de kale oppervlakken (Tabel 5.4).

Dit proefschrift laat zien dat veel polyelectrolietcomplexen die gevormd worden door menging van oplossingen van tegengesteld polyelectrolieten en geladen-blok-neutraal diblok copolymeren in ingevroren toestand terechtkomen. De gevormde kolloïden zijn dan relatief grote aggregaten (HAPECs of ‘niet ontspannen C3μ-Es’). Om C3Ms te vormen, die kleiner zijn en de karakteristieke kern-mantel structuur hebben, moet soms een speciale route

genomen, of speciaal zout gebruikt, worden die dit invriezen vermijdt en/of ongedaan maakt. Als C3Ms eenmaal gevormd zijn, herschikken ze zich bijna niet; behalve als de ladingsbalans wordt verstoord of de zoutconcentratie drastisch wordt verhoogd. Dit komt omdat de meeste energie die gewonnen kan worden door de complexeren van de tegengesteld geladen polymeren al vrij komt bij de eerste complexvorming. De drijvende kracht (resterende energie die gewonnen kan worden) voor herschikking is laag.

Commonly used abbrevations

1,2-PB	1,2-polybutadiene
BIC	block ionomer complex
β-LG	β-lactoglobulin
BSA	bovine serum albumin
C3M	complex coacervate core micelle
C3-μEs	complex coacervate core micro-emulsions
CEAC	critical excess anionic charge
CECC	critical excess cationic charge
CMC	critical micellar concentration
C_p	polymer concentration
db	diblock copolymer
D-C3Ms	double diblock C3Ms
DLS	dynamic light scattering
FIB	fibrinogen
HAPEC	highly aggregated polyelectrolyte complex
hp	homopolyelectrolyte
I	light scattering intensity
IPEC	inter-polyelectrolyte complex
LS-T	light scattering titration
LSZ	lysozyme
NPEC	non-stoichiometric polyelectrolyte complex
PAA	poly(acrylic acid)
PAAm	poly(acrylamide)
PAETB	poly([4-(2-amino-ethylthio)-butylene] hydrochloride)
PCETB	poly([4-(2-carboxy-ethylthio)-butylene] sodium salt)
PDMAEMA	poly(N,N-dimethyl aminoethyl methacylate)
PDI	polydispersity index
P4EVP	poly(N-ethyl-4-vinylpyridinium bromide)
PEC	polyelectrolyte complex
PEM	polyelectrolyte multilayer
PEO	poly(ethylene oxide)
PGMA	poly(glyceryl methacrylate)
PIC	poly-ion complex
PMAA	poly(methacrylic acid)
PMC	preferred micellar composition
R_h	hydrodynamic radius
S-C3Ms	single diblock C3Ms
SCP	soluble complex particle

Dankwoord

Dit proefschrift is zeker niet de enige ontwikkeling die ik in de afgelopen vier jaar heb doorgemaakt. Vele andere ontwikkelingen kwamen erdoor, en er omheen tot stand. Graag wil ik iedereen die mij in deze tijd kende bedanken, want zonder jullie, was dit proefschrift hoogstwaarschijnlijk anders – eenieder en alles heeft invloed op je.

Mijn directe begeleider Arie, en wat minder directe begeleider Martien, wil ik graag bedanken voor hun werk, de (nuttige) discussies en geduld, vooral tijdens de afsluitende periode, die werd gekenmerkt door een Bas met Pfeiffer. Ik kan iedereen de combinatie van Pfeiffer en wetenschappelijk schrijven afraden.

De club badmintonners; vele uren alternatieve inspanning (als in alternatief voor het promotiewerk) werden dankzij de (studenten)badmintonclub de Lobbers mogelijk gemaakt en vele uren ontspanning waren daar, vanwege de sociale sfeer van de club, als twee handen op een buik. Vooral de vaste barhangers, sparring partners, mede Rijncup-organisatoren, mee-eters, weekendgangers, enkeljarige, en meerjarige teamgenoten (Susan, Matthijs, Marcella en Peter B.); bedankt.

Dank ook aan een andere ontspanningsgroep; vele jaren rollenspellen met Henk, Jappe, Raoul, Peter W. en Marieke, waarin de meeste tijd werd besteed aan allerhande grappen, grollen en algemeen geklaag over maatschappij, mensen, computers en wetenschap, zijn uitstekend bevallen. Ik hoop dat de groep ondanks de semi-simultane verhuizing van een aantal van hen nog een tijdje door kan gaan.

De ultieme plek voor ontspanning was gewoon thuis. In de Hollandseweg 218, liefkozend ‘Het Huis met het Lijk in de Open Haard’ gedoopt, was er altijd tijd voor lezen, spelen (bord, kaart en computer), babbelen, muziek beluisteren of domweg hangen. Dank voor deze veilige rusthaven, dank aan de andere bewoners daarvan, met wie het eigenlijk altijd goed toeven was (Anoeska, Anja, Guido V., Remko).

Mijn directe familie (paps, mams, broers, zusje en aanhang) wordt bedankt voor het mij mijn gang laten gaan en de interesse in de vage dingen waar ik mee bezig was: ik hoop dat de Nederlandstalige samenvatting voor jullie een goed en redelijk duidelijk beeld geeft van waar ik mij de afgelopen jaren mee heb bezig gehouden.

Collega`s zijn op een of andere manier toch mensen met wie je veel omgaat, zeker in onze groep, de familie FYSKO. Allemaal bedankt voor de gezellige sfeer, praatjes, borrels (FICS), AIO-uitjes, fietstochten (vooral de ‘Pak de Poema’ tocht), de thee en de lol in en om

de busjes tijdens de PhD-trip naar Zweden en Denemarken. In het bijzonder wil ik de volgende mensen bedanken: Bart ‘distraction gaming’ Postmus, Guido ‘project’ Sala, Saskia ‘geit’ Lindhoud, Wiebe ‘Brugman’ de Vos, Petya ‘3 uur’ Iakovlev, Ilja ‘duizendpoot’ Voets, Agata ‘sarcasme’ Brzozowska, Remco ‘licht en geluid’ Fokkink, Josie ‘moederkloek’ Zeevat, Joris ‘Josti’ Sprakel, en als laatste maar zeker niet minste, Paulina ‘krolik’ Skrzeszewska.

Bas

(\ /)
(. .)
c(")(")

List of publications

- Brzozowska, A.M.; Hofs, B.; de Keizer, A.; Fokkink, R.; Cohen Stuart, M.A.; Norde, W., 2008, *Reduction of protein adsorption on silica and polystyrene surfaces by reversible adsorbed complex coacervate core micelles*, submitted
- Hofs, B.; Brzozowska, A.; de Keizer, A.; Norde, W.; Cohen Stuart M.A., 2008, *Reduction of protein adsorption to a solid surface by a coating of polymeric micelles with a glass-like core*, Journal of Colloid and Interface Science, 325, 2, 309-315
- Hofs, B.; van der Burgh, S.; de Keizer, A.; Leermakers, F.A.M.; Cohen Stuart, M.A., 2008, *Complex coacervate core micro-emulsions*, Soft Matter, 4, 7, 1473-1482
- Voets, I.K.; de Vos, W.M.; Hofs, B.; de Keizer, A.; Cohen Stuart, M.A.; Steitz, R.; Lott, D., 2008, *Internal structure of a thin film of mixed polymeric micelles on a solid/liquid interface*, Journal of Physical Chemistry B, 112, 23, 6937-6945
- Hofs, B.; de Keizer, A.; Cohen Stuart, M.A., 2007, *On the stability of (highly aggregated) polyelectrolyte complexes containing a charged-block-neutral diblock copolymer*, Journal of Physical Chemistry B, 111, 20, 5621-5627
- Hofs, B.; Voets, I.K.; de Keizer, A.; Cohen Stuart, M.A., 2006, *Comparison of complex coacervate core micelles from two diblock copolymers or a single diblock copolymer with a polyelectrolyte*, Physical Chemistry Chemical Physics, 8, 36, 4242-4251
- Cohen Stuart, M.A.; Hofs, B.; Voets, I.K.; de Keizer, A., 2005, *Assembly of polyelectrolyte-containing block copolymers in aqueous media*, Current Opinion in Colloid and Interface Science, 10, 1-2, 30-36
- Koster, G.; VanDuijn, M.; Hofs, B.; Dogterom, M., 2003, *Membrane tube formation from giant vesicles by dynamic association of motor proteins*, Proceedings of the National Academy of Sciences, 100, 26, 15583-15588

Levensloop

Peter Sebastiaan Hofs (“we noemen hem Bas”) werd geboren op 28 augustus van het jaar 1980 in het Veluwse dorp Voorthuizen. Daar groeide hij op en op het Johannes Fontanus College te Barneveld behaalde hij in 1998 zijn VWO diploma. Vervolgens ging Bas aan de Wageningen Universiteit Moleculaire Wetenschappen studeren. Van september 2002 tot maart 2003 werkte Bas bij de leerstoelgroep Fysische chemie en kolloïdkunde aan een afstudeervak over de kolloïdale stabiliteit van lipide blaasjes (vesicles). Daarna bracht hij in 2003 een aantal maanden door als stage op het FOM (Fundamenteel Onderzoek naar Materie) instituut AMOLF (voor Atoom en MOLecuul Fysica) te Amsterdam, met het trekken van buisjes uit grote lipide blaasjes (giant vesicles) met behulp van een optisch pincet. In maart 2004 begon hij bij de leerstoelgroep Fysische chemie en kolloïdkunde aan het in dit boekje omschreven promotieonderzoek. Vanaf 1 januari 2009 is Bas werkzaam bij het KWR (Kiwa Water Research) te Nieuwegein als onderzoeker in de waterzuivering.

Educational activities

Courses / conferences	Organizer / place	Year
Winterschool Han-Sur-Lesse	(UU and WU)	2004
RICCI school of neutron scattering	(Sardinia, I)	2004
SONS meeting	(Berlin, D)	2004
Ostwald colloquium	(Berlin, D)	2004
POLYAMPHI meeting	(Berlin, D)	2004
Winterschool Han-Sur-Lesse	(UU and WU)	2005
RPK-B polymeerfysica	(PTN)	2005
Symposium Macro-Ion complexation	(WUR, PCC)	2005
Student conference Biezenmortel	(WUR, PCC)	2005
Schiermonnikoog conference	(WUR, PCC)	2005
POLYAMPHI meeting	(Arcachon, F)	2005
POLYAMPHI summer school	(Chodova Plana, CZ)	2005
Structure and dynamics of self-organized macromolecular systems	(Prague, CZ)	2006
SONS networking workshop	(Prague, CZ)	2006
Dutch Polymer Days	(DPI)	2007
Student conference Ven	(Ven, S)	2007
ECIS conference	(Geneva, CH)	2007
POLYAMPHI summer school	(WUR, PCC)	2007

Other activities

PCC meetings	(WUR, PCC)	2004-2008
Colloquia	(WUR, PCC)	2004-2008
BASF excursion	(Ludwigshafen, D)	2006
PhD trip Sweden/Denmark	(WUR, PCC)	2007

UU = Utrecht University
WU = Wageningen University
WUR = Wageningen University and Research centre
PCC = Physical Chemistry and Colloid science
PTN = Polymeer Technologie Nederland
DPI = Dutch Polymer Institute